UNIVERSITÀ DI PISA

Scuola di dottorato in Ingegneria "Leonardo da Vinci"

Corso di Dottorato di Ricerca in

TELERILEVAMENTO

Tesi di Dottorato di Ricerca

"Space time adaptive processing in multichannel passive radar"

Autore

Christian Moscardini

_____

Relatori

Prof. Fabrizio Berizzi

_____

Prof. Marco Martorella

_____

SSD ING-INF/03

Abstract

Nowdays, passive bistatic radar (PBR) systems have become a subject of intensive research, owing essentially to its unique features, such as low probability of interception, small size and low cost. Passive radar is a concept where illuminators of opportunity are used. In a bistatic passive radar the main challenges are: estimating the reference signal which is required for detection, mitigating the direct signal, multipath and clutter echoes on the surveillance channel and finally achieving a sufficient SINR to detect targets.

This thesis is concerned with the definition and application of adaptive signal processing techniques to a multichannel passive radar receiver. Adaptive signal processing techniques are well known for active pulse radars. A PBR system operates in a continuous mode, therefore the received signal is not avalaible in the classical array elements-slow time-range domain such as in active pulse radar. A major component of this research focuses on demonstrating the applicability of traditional adaptive algorithms, developed in the active radar contest, with passive radar.

Firstly a new detailed formulation of the sub optimum “batches algorithm”, used to evaluate the cross correlation function, is proposed. Then innovative 1D temporal adaptive processing techniques are defined extending the matched filter concept to an adaptive matched filter formulation. Afterwards a new spatial adaptive technique, based on the application of the adaptive digital beamforming after the matched filter, is investigated. Finally both 1D spatial and temporal adaptive techniques are extended to 2D space-time adaptive processing techniques. Specifically we demonstrate the applicability of STAP processing to a passive bistatic radar and we show how the classical STAP algorithms, developed for active radar systems, can be applied to a PBR system. The new defined passive radar signal processing architectures are compared with the standard approaches and the effectiveness of the proposed techniques is demonstrated considering both simulated and real data.

Contents

List of Figures

Acronyms

AF	Ambiguity Function
ADC	Analog to Digital Converter
CAF	Cross Ambiguity Function
2D-CCF	Two Dimensional Cross Correlation Function
CFAR	Constant Fals Alarm Rate
CIP	Coherent Processing Interval
DAB	Digital Audio Broadcasting
DFT	Discrete Fourier Transform
DOA	Direction of Arrival
DPI	Direct Path Interference
DVB-T	Digital Video Broadcasting Terrestrial
ECA	Extensive Cancellation Algorithm
FMCW	Frequency Modulated Continuous Wave
FFT	Fast Fourier Transform
GMTI	Ground Moving Target Indicator
ICM	Internal Clutter Motion
IDFT	Inverse Discrete Fourier Transform
IO	Illuminator of Opportunity
LCMV	Linearly Constrained Minimum Variance
LMS	Least Mean Square
LS	Least Square
LSL	Least Square Lattice
LSMI	Loaded Sample Matrix Inverse
MVDR	Minimum Variance Distorsionless Response
NLMS	Normalized Least Mean Square

OFDM	Orthoganal frequency Division Multiplexing
PBR	Passive Bistatic Radar
PCL	Passive Coherent Location
PR	Passive Radar
PRI	Pulse Repetition Interval
RLS	Recursive Least Square
SCA	Sequential Cancellation Algorithm
SCM	Sample Covariance Matrix
SDR	Signal to Direct signal Ratio
SF	Stepped Frequency
SFN	Single frequency Network
SINR	Signal to Noise plus Interference Ratio
SLL	Side Lobe level
SMI	Sample Matrix Inverse
SRP	Synthetic Range Profile
STAP	Space Time Adaptive Processing

Chapter 1.
Introduction

1.1 Passive radar systems

In recent years there has been a growing interest in Passive Bistatic Radar (PBR) using existing transmitters as illuminators of opportunity to perform target detection, localization and tracking [Kuschel 2010], [Howland 2005]. Bistatic radar may be defined as a radar in which the transmitter and receiver are at separate locations. The very first radars were bistatic, until pulsed waveforms and T/R switches were developed [Kuschel 2010]. Bistatic radars can operate with their own dedicated transmitters, which are specially designed for bistatic operation, or with *transmitters of opportunity*, which are designed for other purposes but found suitable for bistatic operation. When the transmitter of opportunity is from a non-radar transmission, such as broadcast, communications or radio-navigation signal, the bistatic radar has been called: *Passive Radar (PR), Passive Coherent Location (PCL)*. In this thesis we use the term *Passive Bistatic Radar* (PBR) to indicate a passive bistatic radar system.

PBR systems have some significant attractions, in addition to those common to all bistatic radars. There has been considerable work on the theory behind PBR and much has been written about its potential [Baker 2005], [Griffiths 2005],

As well as being completely passive and hence potentially undetectable, they can allow the use of parts of the RF spectrum (VHF and UHF) that are not usually available for radar operation, and which may offer a counter-stealth advantage, since stealth treatments designed for microwave radar frequencies may be less effective at VHF and UHF. Broadcast transmissions at these frequencies can have substantial transmit powers and the transmitters are usually sited to give excellent coverage.

There are a great variety of signals that can be used for PBR purposes. Their performance in PBR systems will vary significantly, depending on a variety of factors: (i) power density at target (ii) coverage (both spatial and temporal), and (iii) ambiguity function shape depending both on the waveform and on the transmitter-target-receiver geometry. In particular broadcast transmitter represent some of the most attractive choices for long range surveillance application due to their excellent coverage. The most common signals used for PBR applications are FM radio and UHF television broadcasts ([Howland 2005], [Griffiths 2005], [Griffiths 1986], [Howland 1999]), as well as digital transmission such as Digital Audio Broadcasting (DAB) ([Coleman 2008], [Guner 2003]) and Digital Video Broadcasting-Terrestrial (DVB-T) ([Berger 2010], [Bongioanni 2009], [Gao 2006], [Glende 2007], [Langellotti 2010], [Poullin 2005-2010], [Kuschel 2008], [Saini 2005], [Yardley 2007]).

For analogue modulation formats, the ambiguity performance depends strongly on instantaneous modulation. Periodic modulation features, such as the sync parts of the waveform in analogue television waveforms, result in ambiguities. For VHF FM radio the ambiguity performance varies significantly, and some types of music; those with high spectral content) are better than others. For digital modulation formats, the ambiguity performance is much more constant with time, and does not depend on the programme content, since signals are more noise-like. Such signals exhibit a radar ambiguity function that has almost ideal thumb tack nature with excellent range resolution. Digital transmissions are therefore to be preferred, even though they tend to be of lower power than their analogue counterparts. A PBR receiver requires at least two signals in order to perform the matched filter receiver: a copy of the transmitted signal and the received signal from the surveillance area. Therefore the simpler PCL radar system requires two antennas: the first antenna, often called the reference antenna, is used to capture the reference signal and should point in the direction of the transmitter, the second antenna, usually called the surveillance antenna, is used to capture the signals of potential target. If an antenna array rather than single receiver antennas is used then the performance of the passive radar system may be improved. In a bistatic passive radar the main challenges are: estimating the reference signal which is required for detection, mitigating the direct signal, multipath and clutter echoes on the surveillance channel and finally achieving a large enough gain processing to detect

targets. The transmitted waveforms is not under control of the radar designer and the sidelobes of the ambiguity function can mask possible target echoes. Different techniques have been proposed to resolve these problems and they can be summarized as [Griffiths 2007]:

- ✓Spatial cancellation
- ✓Spectral/temporal cancellation

To add additional complexity, if the environment is non-stationary adaptive control of the processing is required. Adaptive signal processing techniques have been studied and developed extensively over several decades, both for radio communications and for radar applications, especially considering active pulse radar.
In this thesis we will demonstrate the applicability of classical adaptive algorithms considering a multichannel passive radar. Alternative passive radar signal processing architectures will be proposed and compared with classical and standard approaches.

1.2 Theoretical background

In this section, the main theoretical notions that will be used during the development of this thesis are described. Section 1.2.1 deals with the definition of the classical monostatic ambiguity function and the main differences with respect to a bistatic geometry are detailed. In section 1.2.2 the theoretical background of the adaptive signal processing techniques is analyzed. Finally in section 1.2.3 the main aspects of the adaptive signal processing techniques defined in the well known contest of active pulse radar are detailed.

1.2.1 Monostatic-Bistatic ambiguity function

The ambiguity function is conventionally derived assuming a monostatic radar and a slowly fluctuating point target. In [Tsao 1997] a mathematical model of this physical situation is derived and in this section we recall the principal assumptions.
Assume that the transmitted pulse is given by

$$s_T(t) = \sqrt{2}\,\mathrm{Re}\left\{\sqrt{E_t} f(t) e^{i\omega_c t}\right\} \quad 0 \le t \le T \tag{1.1}$$

where $\mathrm{Re}\{\ \}$ denotes the real part operation, $f(t)$ is the complex envelope of the transmitted pulse and ω_c is the carrier frequency.

If a point target is moving and located at some distance from the radar site, the received target echo can be modeled as

$$s_R(t) = \sqrt{2}\,\mathrm{Re}\left\{\sqrt{E_t} b f\left(t - \tau(t)\right) e^{i\omega_c t - \tau(t)}\right\} \tag{1.2}$$

where $\tau(t)$ is the time delay due to the target motion. The complex envelope of the received signal can be modeled as a time delayed version of the transmitted signal multiplied by a zero-mean complex Gaussian random variable b. This assumption is true when the number of scatterers on the target is large and none of the scatters is dominant. The term slowly fluctuating refers to fact that the variable b can be supposed stationary while the target is illuminated by the transmitted pulse.

Whit some approximations, detailed in [Tsao 1997], the target return (1.2) can be simplified as

$$s_R(t) = \sqrt{2}\,\mathrm{Re}\left\{\sqrt{E_t} b f\left(t - \tau_a\right) e^{i\left(\omega_c + \omega_{Da}\right)t}\right\} \quad \tau_a \le t \le \tau_a + T \tag{1.3}$$

where the round trip delay τ_a is defined as

$$\tau_a = \frac{2R_a}{c} \tag{1.4}$$

and the Doppler shift ω_{Da} is defined as

$$\omega_{Da} = \frac{-2V_a\omega_c}{c} \tag{1.5}$$

We recall that R_a and V_a are respectively the target position and the target radial velocity at an arbitrary instant when the target is being illuminated, while c represents the speed of light. The subscript "a" is used to indicate the actual value of the parameters associated with the target.

It is important to note that:

- the development of the conventionally monostatic ambiguity function is based on the target model defined in equation (1.3)

•while the target model is usually employed also for a bistatic radar, the relationship among the radar measurements, delay and Doppler shift, and the target parameters, distance and velocity, is not represented by equations (1.4) and (1.5)

After defining a slowly fluctuating point target model we now deals with the definition of the ambiguity function and its relation with the radar detection and parameters estimation problem.

Firstly we are interested in the detection of a slowly fluctuating point target in presence of additive noise. In particularly we want to examine a particular value of range and Doppler and decide whether or not a target is present at that point. We can formulate the binary hypothesis testing problem as

$$\begin{cases} \tilde{r}(t) = \tilde{n}(t) & H0 \\ \tilde{r}(t) = \tilde{s}_R(t) + \tilde{n}(t) & H1 \end{cases} \tag{1.6}$$

where $\tilde{n}(t)$ denotes the complex envelope of a Gaussian white noise process and $\tilde{s}_R(t)$ is the complex envelope of the target echo defined in equation (1.3). It is possible to demonstrate that the Neyman-Pearson receiver is given by

$$M_{NP}(\tau,\nu) = \left| \int_{-\infty}^{+\infty} \tilde{r}(t) f^*(t-\tau) e^{-i2\pi\nu t} dt \right|^2 \underset{H_0}{\overset{H_1}{\gtrless}} \lambda \tag{1.7}$$

where Λ denotes the test statistic and the threshold λ is selected in order to achieve a specific false alarm probability.

The above test maximizes the probability of detection under a false alarm probability constraint, assuming that a slowly fluctuating moving point target is located at the point (τ,ν) in the range-Doppler plane.

The receiver, expressed in equation (1.7), can be seen in the form of the classical matched filter receiver which is used by the vast majority of radars and communication receiver. This filter can be defined as the optimum filter that maximizes the SNR (Signal to Noise Ratio) at the filter output.

Substituting the target received signal, defined in equation (1.2), in equation (1.7) the output of the optimum receiver, after down conversion, is given by

$$M_{NP}(\tau,\nu) = E_t |b|^2 \left| \int_{-\infty}^{+\infty} f(t-\tau_a) f^*(t-\tau) e^{-i2\pi(\nu-\nu_a)t} dt \right|^2 + \tilde{n}_{out}(t) \tag{1.8}$$

In [Tsao 1993], excluding the noise term and the multiplicative factor in equation (1.8), the ambiguity function is defined as

$$\theta(\tau_H, \tau_a, \omega_{D_H}, \omega_{D_a}) \triangleq \left| \int_{-\infty}^{+\infty} f(t-\tau_a) f^*(t-\tau_H) e^{-i(\omega_{D_H}-\omega_{Da})t} dt \right|^2 \tag{1.9}$$

It should be noted that the exact definition of the ambiguity function varies throughout the literature. Often the term ambiguity function is used to refer to the quantity

$$\chi(\tau,\omega) \triangleq \int_{-\infty}^{+\infty} f(t) f^*(t-\tau) e^{-i\omega t} dt \tag{1.10}$$

In the rest of this thesis we utilizes this definition of the ambiguity function. Therefore the output of the matched filter can be expressed as

$$M_{NP}(\tau,\omega) \triangleq E_t |b|^2 \left| \chi(\tau-\tau_a, \omega-\omega_a) \right|^2 + \tilde{n}_{out}(t) \tag{1.11}$$

Equation (1.11) gives some initial insight to the significance of the ambiguity function: the result of the matched filter receiver is the ambiguity function of the transmitted signal, scaled and shifted to be centered on the range and Doppler shift corresponding to the location and velocity of the target.

We can arrive at the same expression of the ambiguity function by using the theory of parameters estimation for a slowly fluctuating point target. The complex envelope of the received signal is assumed to be

$$s_R(t) = \sqrt{E_t} b f(t-\tau_a) e^{i\omega_{Da}t} + \tilde{n}(t) \quad \tau_a \le t \le \tau_a + T \tag{1.12}$$

where (τ_a, ω_{D_a}) are the unknown nonrandom parameters that are to be estimated and $\tilde{n}(t)$ denotes the complex envelope of a Gaussian white noise process. As shown in [Tsao 1993], the likelihood function of the optimum estimator involves the same ambiguity function as given in equation (1.9).

At the end of this section we can conclude that

- the optimum receiver is strictly dependent on the ambiguity function of the transmitted signal

- to minimize the estimation of target parameters it is desirable that ambiguity function approximate an impulse located at $(\tau = 0, \omega = 0)$
- in a bistatic configuration, the relationship between range and Doppler-velocity are strictly dependent on the relative position of target, transmitter and receiver. A more appropriate formulation of the bistatic ambiguity function, depending on these mentioned parameters can be found in [Tsao 1993].

1.2.2 Adaptive signal processing

In much of the radar and signal processing literature the expression for adaptive filter is referred to an adaptive linear combiner. The main objective of an optimum filter is to maximize, in some appropriate sense, the signal response while simultaneously minimizing the response due to interference. The term adaptive means that the filter is calculated by using the received data and by estimating the interference statistical properties. The reasons for this are obvious: the strength, the Doppler frequency position and the angular location of the interference cannot known a priori. The theory relative to this argument is well developed in literature and we want to only recall the principal aspects [Van Trees 2002], [Manolakis 2005], [Guerci 2003], [Ward 1994]. These preliminary concepts will be included in subsequent chapters.

First we discuss the design of optimum linear filters that maximize the output signal-to noise power ratio and assume that the interference statistical properties are known a priori, after we extend the discussion to the adaptive filter. Such filters are widely used to detect signals in additive noise in many applications, including digital communications and radar.

Suppose that the observation data obtained by sampling the output of a single sensor at M instances, or M sensors at the same instant, are arranged in a vector $\boldsymbol{x}$.

We have mentioned these two cases because both temporal and spatial adaptive processing will be considered in subsequent chapter.

Furthermore, we assume that the available signal $\boldsymbol{x}$ consists of a desired signal $\boldsymbol{s}$ plus an additive noise plus interference signal $\boldsymbol{i}$, that is

$$\boldsymbol{x} = \boldsymbol{s} + \boldsymbol{i} \tag{1.13}$$

We suppose $\boldsymbol{s}$ to be a signal of the form $\boldsymbol{s} = \boldsymbol{s}_0\alpha$ where $\boldsymbol{s}_0$ is the completely known shape of $\boldsymbol{s}$ and α is a complex random variable.

The deterministic target model will assume a particular shape in relation to the considered application and in general it is defined as function of target parameters:

- temporal adaptive processing: $\boldsymbol{s}_0(\nu_a)$ is a function of the target frequency Doppler ν_a
- spatial adaptive processing: $\boldsymbol{s}_0(\phi_a, \vartheta_a)$ is a function of the target angular location (ϕ_a, ϑ_a)
- space-time adaptive processing: $\boldsymbol{s}_0(\nu_a, \phi_a, \vartheta_a)$ is a function of both target frequency Doppler ν_a and angular location (ϕ_a, ϑ_a).

The signal $\boldsymbol{s}$ and $\boldsymbol{i}$ are assumed to be uncorrelated with zero mean.

The output of a linear processor (combiner or FIR filter) with coefficients $\{w_k\}_1^M$ is

$$y = \boldsymbol{w}^H \boldsymbol{x} = \boldsymbol{w}^H \boldsymbol{s} + \boldsymbol{w}^H \boldsymbol{i} \tag{1.14}$$

and its power is a quadratic function of the filter coefficients

$$P_y = E\left\{|y|^2\right\} = \boldsymbol{w}^H \boldsymbol{R}_x \boldsymbol{w} \tag{1.15}$$

where $\boldsymbol{R}_x \in \mathbb{C}^{MxM}$ is the correlation matrix of the signal $\boldsymbol{x}$.

The output noise plus interference power is

$$P_i = E\left\{\left|\boldsymbol{w}^H \boldsymbol{i}\right|^2\right\} = \boldsymbol{w}^H \boldsymbol{R}_i \boldsymbol{w} \tag{1.16}$$

where $\boldsymbol{R}_i$ is the interference plus noise correlation matrix defined as

$$\boldsymbol{R}_i \triangleq E\left\{\boldsymbol{i}\boldsymbol{i}^H\right\} \quad \in \mathbb{C}^{MxM} \tag{1.17}$$

The determination of the output SINR, and hence the subsequent optimization, depends on the nature of the signal $\boldsymbol{i}$. If $\boldsymbol{i}$ is an additive white noise the interference plus noise correlation matrix is given by $\boldsymbol{R}_i = \sigma_i^2 \boldsymbol{I}$ and the filter that maximizes the output SNR, defined as

$$SNR(\boldsymbol{w}) \triangleq \frac{P_a \left|\boldsymbol{w}^H \boldsymbol{s}\right|^2}{\sigma_i^2 \boldsymbol{w}^H \boldsymbol{w}} \tag{1.18}$$

is given by

$$\boldsymbol{w} = \eta \boldsymbol{s}_0 \tag{1.19}$$

The optimum filter is a scaled replica of the known signal shape. This property resulted in the term matched filter, which is widely used in communications and radar applications. This result is the same obtained in equation (1.7) where the $\boldsymbol{s}_0(\tau_a, \nu_a)$ is a function of the target range τ_a and of the target frequency Doppler ν_a

The maximum value of the output SNR is given by

$$SNR_o \triangleq \frac{P_a \boldsymbol{s}^H \boldsymbol{s}}{\sigma_i^2} \tag{1.20}$$

We note that we can choose the constant η in any way we want in order to obtain the same maximum SNR.

If $\boldsymbol{i}$ is an additive colored noise the interference plus noise correlation matrix is given by $\boldsymbol{R}_i$ and the output SINR is given by

$$SINR(\boldsymbol{w}) \triangleq \frac{P_a \left| \boldsymbol{w}^H \boldsymbol{s} \right|^2}{\boldsymbol{w}^H \boldsymbol{R}_i \boldsymbol{w}} \tag{1.21}$$

and the optimum matched filter for color additive noise is given by

$$\boldsymbol{w} = \eta \boldsymbol{R}_i^{-1} \boldsymbol{s}_0 \tag{1.22}$$

Therefore, the optimum matched filter in additive color noise is the cascade of a whitening filter followed by a matched filter for white noise.

Using equation (1.22) in equation (1.21) the optimum SINR a the output of the optimum processor becomes

$$SNR_{opt} = P_a \boldsymbol{s}_0^H R_i^{-1} \boldsymbol{s}_0 \tag{1.23}$$

It's worth noting that since the target parameters are unknown a priori, $\boldsymbol{s}_0$ is a known function of unknown parameters, so the receiver should implement multiple detectors that form a filter bank to cover all potential target parameters.

So far we have considered the optimum filter theory that requires the knowledge of the second order statistics of the interference and cannot be implemented in practice. Therefore to solve this problem, the filter coefficients are typically estimated by adaptive algorithms. Adaptive processing refers to the case where the interference

covariance matrix is unknown and must be estimated from the observed data. A typically used block adaptive implementation is the Sample Covariance Matrix (SCM) algorithm given by

$$\hat{\boldsymbol{R}}_i = \frac{1}{N_t}\sum_{m=1}^{N_t} \boldsymbol{x}_i^{(m)} \boldsymbol{x}_i^{(m)H} \quad \boldsymbol{x}_i^{(m)} \in \Omega_{training}^{NxN_t} \tag{1.24}$$

where the vector $\boldsymbol{x}_i^{(m)}$ represents the m-th interference-plus-noise component of the signal belonged to the training data set $\Omega_{training}^{NxN_t}$.

It is to show that if the training data samples are uncorrelated and have identical correlation matrix $\boldsymbol{R}_i$, equation (1.24) is an unbiased estimate of $\boldsymbol{R}_i$. If additionally the training data samples are Gaussian and independent identically distributed than equation (1.24) corresponds to the maximum likelihood estimate of $\boldsymbol{R}_i$.

The larger the sample support, the better the estimate of the correlation matrix $\hat{\boldsymbol{R}}_i$ for stationary data.

Proceeding by substituting the sample covariance matrix into the optimum filter in equation (1.22) we obtain the known Sample Matrix Inversion beamforming [Reed 1972] as

$$\mathbf{w}_{SMI} = \eta \hat{\mathbf{R}}_i^{-1} \mathbf{s}_0 \tag{1.25}$$

In [Brennan 1973] the authors have been characterized the impact of replacing the actual correlation matrix with its sample estimate under this conditions: the training data samples are free of target signal contamination and are i.i.d. Gaussian vectors. The important obtained result states that the SMI method produces a SINR loss that is about 3 dB if $N_t = 2N$.

Although 2N i.i.d. Gaussian samples yield an SINR that is within about 3 dB of optimum, the corresponding adapted filter response may not be suitable for most situations due to filter response distortions.

To implement the optimum filter in practice, we must assume that we can estimate $\boldsymbol{R}_i(k)$ without the presence of the useful signal $\boldsymbol{s}(k)$. However, in many applications the useful signal is present all the time so that an estimate of a signal free correlation

matrix is not possible. In this case the optimum filter must be constructed with the correlation matrix $\boldsymbol{R}_x(k)$ relative to the total signal as

$$\boldsymbol{w}_1 = \eta \boldsymbol{R}_x^{-1} \boldsymbol{s}_0 \tag{1.26}$$

It is possible to demonstrate that this optimum filter produces an identical solution of the filter (1.22) in the case when it is perfectly matched to the signal of interest.

Of course we experience a loss in performance substituting an estimate of the true correlation matrix into the optimum weight expression.

We can observe that the main problems of the SMI technique are:

- the choice of the training data set $\Omega_{training}^{NxN_t}$ in order to have a good estimate of the interference-plus-noise covariance matrix. To obtain a useful estimate, the training data set has to be homogeneous over a number of training data relatively large compared to the value of K.
- in addition, the presence of the target component in the training data set could result in a partially cancellation of the desired signal and subsequent loss in performance.
- the computational load associated to the inversion of the estimated covariance matrix

The main theoretical aspects underlined in this paragraph will be used in the definition of temporal and spatial adaptive techniques that will be defined in subsequent chapters. We will see how to resolve the problem of data training selection in relation to the spatial and temporal adaptive techniques in a passive radar scenario.

1.2.3 Adaptive signal processing for pulse radar systems

In this section a brief overview of adaptive processing applied to the contest of the well known active pulsed radar scenario is presented. During the development of the adaptive techniques in a passive radar scenario we will underline the similarities and the adaptations to this theory.

In a active pulse radar system the transmitted signal is a coherent burst of pulses and can be modelled as

$$u(t) = \sum_{m=0}^{M-1} u_p(t - mT_R) \tag{1.27}$$

where $u_p(t)$ is the complex envelope of a single pulse and T_R is the pulse repetition interval (PRI).

After down conversion each pulse of the baseband signal is matched filtered separately with the receiver filter $h(t) = h_p^*(-t)$ as shown in Figure 1.1.

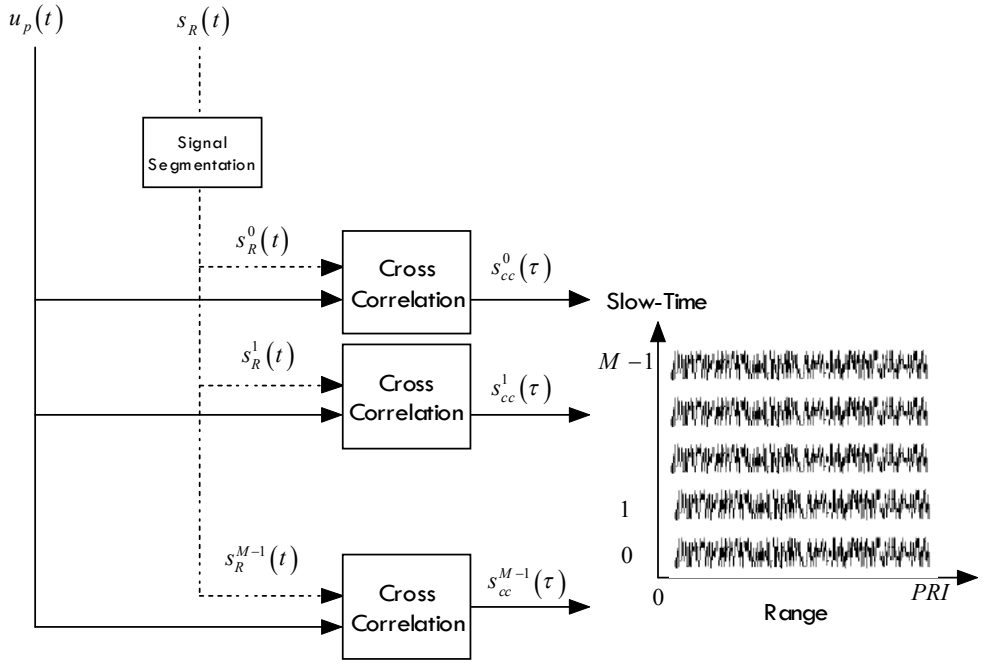

Figure 1.1 Pulse radar architecture

The m-th matched filter output $s_{cc}^m(\tau)$ is given by the cross correlation between the transmitted pulse $u_p(t)$ and the received signal collected into the m-th PRI $s_R^m(t)$

$$s_{cc}^m(\tau) = \int_0^{PRI} s_R^m(t) u_p^*(\alpha - \tau) d\alpha \tag{1.28}$$

After A/D converter, for each PRI, L range samples are collected to cover the range interval of interest. The received data for one CPI comprises LM complex baseband samples. This signal is the classical slow time-range bidimensional data.

Modeling the received signal, in the case of a single slowly fluctuating point target, as in equation (1.3)

$$s_R(t) = \sqrt{2}\,\mathrm{Re}\left\{\sqrt{E_t}\,b u(t-\tau_a) e^{i(\omega_c+\omega_{Da})t}\right\} \tag{1.29}$$

the m-th matched filter output $s_{cc}^m(\tau)$ is given by

$$s_{cc}^m(\tau) = \sqrt{E_t}\,b e^{i\omega_{Da} m T_R} \int u_p^*\left(t-\left(\tau - mT_R - \tau_a\right)\right) u_p(t) e^{i\omega_{Da} t}\,dt \tag{1.30}$$

Using equation(1.10), equation (1.30) can be modified as

$$s_{cc}^m(\tau) = \sqrt{E_t}\,b \sum_{m=0}^{M-1} e^{i\omega_{Da} m T_R}\, \chi_p(\tau - \tau_a, -\omega_{Da}) \tag{1.31}$$

where $\chi_p(\tau,\omega)$ is the ambiguity function of the single pulse.

The output of the matched filter receiver for the m-th pulse is the ambiguity function of the transmitted pulse scaled and shifted on the time delay corresponding to the location of the target and calculated at the target Doppler frequency. Comparing equation (1.31) with equation (1.11) we can observe that we have some losses related to the target Doppler shift. This fact can be explaining considering that the filter is matched to only the target delay and not to the target Doppler frequency.

Consider only the target range gate the samples from each PRI are given by

$$s_{cc}^m(\tau_a) = \sqrt{E_t}\,b e^{i\omega_{Da} m T_R}\, \chi_p(0, -\omega_{Da}) \simeq \alpha e^{i\omega_{Da} m T_R} \tag{1.32}$$

where we have assumed that the waveform is insensitive to target Doppler shift and the other terms have been groped into a single complex random amplitude α.

The slow-time snapshot for the target range cell can be written as

$$\boldsymbol{s}_{cc}(\tau_a) = \alpha \boldsymbol{v}_t(\omega_{Da}) = \alpha\left[1; e^{i\omega_{Da} T_R}; \ldots; e^{i\omega_{Da}(M-1)T_R}\right] \tag{1.33}$$

where $\boldsymbol{v}_t(\omega_{Da})$ is the so called temporal steering vector. It is a Vandermonde form because the waveform is a uniform PRF and the target velocity is supposed constant.

The theory developed in the previous section can be applied in this case defining the vector $\boldsymbol{s}_0$, shown in equation (1.13), equal to the temporal steering vector $\boldsymbol{v}_t(\omega_{Da})$. The well known adaptive temporal (Doppler-Pulse) processing techniques, i.e. Moving Target Indicator (MTI) or Adaptive Moving Target Indicator (AMTI), are based on this consideration. In chapter 3 and 4 we will see how this analysis may be extended to the passive radar scenario.

So far we have considered the receiver system composed by only a single receiver, now we extend the development to a radar antenna consisting of N elements.

The single sensor signal model defined in equation (1.31) can be modified as

$$s_{cc}^{m}\left(\tau,\boldsymbol{r}_n\right)=\sqrt{E_t}be^{i\omega_{Da}mT_R}e^{i\omega_c\frac{\left\langle\hat{\boldsymbol{k}}(\phi_a,\vartheta_a),\boldsymbol{r}_n\right\rangle}{c}}\chi_p\left(\tau-\tau_a,-\omega_{Da}\right) \tag{1.34}$$

where

$\hat{\boldsymbol{k}}\left(\phi_a,\vartheta_a\right)$ is a unit vector pointing in the $\left(\phi,\vartheta\right)$ angular direction and $\boldsymbol{r}_n$ is the n-th array element vector position.

It is assumed that the transmitted waveform is narrowband and the relative delay term is insignificant within the complex envelope.

After A/D converter the received data for one CPI comprises LMN complex baseband samples. This signal is the classical slow time-range-antenna elements multidimensional data, typically known as CPI datacube as schematically shown in Figure 1.2..

Consider only the target range gate, as shown in equation (1.32), the target samples from each PRI are given by

$$s_{cc}^{m}\left(\tau_a,\boldsymbol{r}_n\right)\simeq\alpha e^{i\omega_{Da}mT_R}e^{i\omega_c\frac{\left\langle\hat{\boldsymbol{k}}(\phi_a,\vartheta_a),\boldsymbol{r}_n\right\rangle}{c}} \tag{1.35}$$

Examination of equation (1.35) shows that one exponential term depends on the spatial index n and the other depends on the temporal index m.

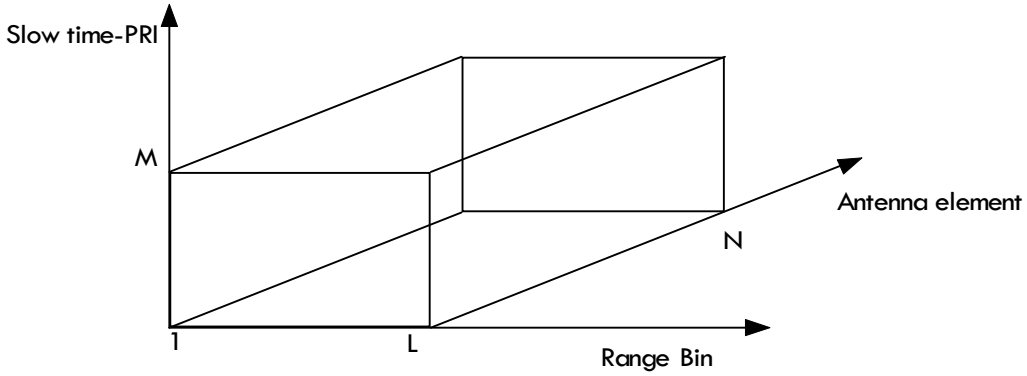

Figure 1.2 CPI datacube

The spatial snapshot for the m-th pulse and for the target range cell can be written as

$$\boldsymbol{s}_{cc}^{m}\left(\tau_a\right)=\alpha e^{i\omega_{Da}mT_R}\boldsymbol{v}_s\left(\phi_a,\vartheta_a\right)=$$
$$=\alpha e^{i\omega_{Da}mT_R}\left[e^{i\omega_c\frac{\left\langle\hat{\boldsymbol{k}}(\phi_a,\vartheta_a),\boldsymbol{r}_0\right\rangle}{c}};e^{i\omega_c\frac{\left\langle\hat{\boldsymbol{k}}(\phi_a,\vartheta_a),\boldsymbol{r}_1\right\rangle}{c}};...;e^{i\omega_c\frac{\left\langle\hat{\boldsymbol{k}}(\phi_a,\vartheta_a),\boldsymbol{r}_{N-1}\right\rangle}{c}}\right] \tag{1.36}$$

where $\boldsymbol{v}_s\left(\phi_a,\vartheta_a\right)$ is the so called spatial steering vector.

The theory developed in the previous section can be applied in this case defining the vector $\boldsymbol{s}_0$, shown in equation (1.13), equal to the spatial steering vector. The well known adaptive spatial processing techniques, also known as adaptive beamforming technique, are based on this simple consideration. In chapter 5 we will see how this analysis may be extended to the passive radar scenario..

In the case of an airborne pulse radar the 1D temporal adaptive processing and 1D spatial adaptive processing have been extended to the so called Space Time Adaptive Processing (STAP) techniques. This techniques elaborates the received signal in a joint spatiotemporal domain for advanced clutter suppression. The need for joint space and time processing arises from the inherent two-dimensional nature of the ground clutter due to the platform motion.

In this contest the adaptive filter theory can be applied thinking that the received signal can be alternatively written as

$$\boldsymbol{s}_{cc}\left(\tau_a\right)=\alpha\left[1\boldsymbol{v}_s\left(\phi_a,\vartheta_a\right);e^{i\omega_{Da}T_R}\boldsymbol{v}_s\left(\phi_a,\vartheta_a\right);...;e^{i\omega_{Da}(M-1)T_R}\boldsymbol{v}_s\left(\phi_a,\vartheta_a\right)\right]=$$
$$=\alpha\boldsymbol{v}_{t-s}\left(\omega_{Da},\phi_a,\vartheta_a\right) \tag{1.37}$$

where $\boldsymbol{v}_{t-s}\left(\omega_{Da},\phi_a,\vartheta_a\right)$ is the space-time steering vector, and defining the vector $\boldsymbol{s}_0$, shown in equation (1.13), equal to the space-time steering vector.

In chapter 6 we will see how this analysis may be extended to the passive radar scenario.

1.3 Main contributions to research

The main obvious problem of passive radars is the necessity to estimate a copy of the transmitted signal. Therefore the simpler PBR system requires two receiving channels in order to collect the reference signal and the surveillance signal and to perform the matched filter receiver. The main challenge in passive bistatic radars is to mitigate the

interference signal, such as the direct path interference and its multipath, on the surveillance channel.

The second chapter introduces a typical passive radar scenario and describes the defined signal model for both reference and surveillance channel. Moreover the chapter presents the typical signal processing chain used in a PBR system. The main blocks are represented by both the matched filter block and the interference suppression block. The scope of the last block is to mitigate and ideally to suppress the interference components received on the surveillance channel. It is worth noting that the main feature of the traditional PBR signal processing chain is the presence of the interference suppression block before the matched filter.

The matched filter processor serves two distinct purposes: to provide the necessary signal processing gain to allow detection of the target echo and to estimate the bistatic range and Doppler shift of the target. The output of the matched filter is the classical 2D cross correlation function, often called as Cross Ambiguity Function (CAF). The evaluation of the 2D cross correlation function can be computationally expensive and a large number of complex operations has to be performed which sets a strong limitation on real time processing. Sub optimum approaches can be exploited to reduce the computational cost if a small SNR degradation can be accepted.

The third chapter develops a comparative study between optimum and sub optimum methods in terms of computational load and SNR loss. A new detailed formulation of the sub optimum "batches algorithm" is proposed. The exact matched filter formulation for OFDM waveforms is derived and we reveal that this approach is similar to the batches algorithm considering the same small Doppler approximation. The analogies with the classical processing used in active pulse radar are underlined. This analysis constitutes the basis for the development and the adaptation of the classical adaptive signal processing techniques, developed for active pulse radars, to a passive radar scenario.

The cancellation of the interference signal is a crucial issue for target detection in a passive bistatic scenario. Different techniques, both in spatial and temporal domain, have been proposed to solve this problem.

The forth chapter deals with the suppression of the direct signal and clutter echoes in a single receiver passive radar scenario. A variety of temporal adaptive processing has been developed for the removal of the interference component in the surveillance channel before the matched filter. A new formulation of the adaptive matched filter based on the "batches algorithm" is derived. The main advantage of the adaptive matched filter solution is the possibility to suppress strictly static clutter potentially affected by ICM (Internal Clutter Motion). The effectiveness of the proposed solution is demonstrated considering both simulated and real data.

Simpler passive bistatic radar systems use only two antennas for the reception of both surveillance and reference signal. Using a phased array antenna it is possible to electronically steer multiple beams at the same time to collect reference and surveillance channel and improve the target localization process. Typically digital beamforming techniques are applied directly on the received signal and before the matched filter.

The fifth chapter introduces the main advantages of a multichannel passive radar system implementing digital beamforming techniques. The main drawbacks of the mentioned traditional solution are detailed and a new scheme, based on the application of digital adaptive beamforming after matched filter, is investigated. The proposed technique improves the performances in terms of clutter cancellation on the surveillance channel. Once defined a multichannel signal model the effectiveness of the proposed solution has been demonstrated on simulated data.

In presence of a moving PBR, as in moving platform active radars, the clutter spectrum exhibits an angular direction–dependent mean frequency. Target detection realized by filtering the clutter in the frequency Doppler domain is difficult with a single antenna. An improvement in clutter suppression can be achieved by using an antenna array and

two-dimensional signal processing. Space-Time adaptive processing is typically used to filter out interferences in GMTI radars in order to detect slow moving target.

The sixth chapter demonstrates the applicability of STAP processing to passive bistatic radars. In the STAP literature, it is assumed that the available signal is formed by the echoes from a pulse-Doppler radar. A PBR system operates in a continuous mode, therefore the received signal is not avalaible in the classical array elements- slow time-range domain such as in an active pulse radar. The chapter introduces how the 1D temporal and spatial adaptive techniques can be extended to the 2D STAP processing and shows how the classical STAP algorithms, developed for active radar systems, can be applied to a PBR system.

Chapter 2.
Signal processing techniques in passive radar systems

2.1 Introduction

In this chapter we introduce the signal processing techniques typically adopted in a PBR system. The principal block is represented by the matched filter. In section 2.2 we define the simpler PBR matched filter architecture by using the concepts developed in section 1.2.1. The matched filter is the optimum receiver in presence of additive white noise. A typical PBR scenario is more complex and this simpler structure presents several drawbacks. In section 2.3 the adopted model, for both reference signal and received signal and a typical passive bistatic scenario is described. The PBR environment will be presented and the main problems relative to a basic matched filter architecture will be underlined. In section 2.4 we will present an advanced signal processing architecture used in a typical PBR scenario. The main block introduced is the interference suppression block before the matched filter. The scope of this block is that to mitigate and ideally to suppress below the noise floor the several interference components received on the surveillance channel.

2.2 PBR matched filter architecture

The theory developed in section 1.2.1 explains that a PBR receiver requires at least two signals in order to perform the matched filter receiver: a copy of the transmitted signal

and the received signal from the surveillance area. The principal obvious potential problem of non-cooperative passive radar is that there is no copy of the transmitted signal at the receiver. This problem is important for every bistatic configuration but it becomes relevant for passive configuration because the transmitter is non-cooperative.
Generally these two signals are addressed as surveillance channel, for the reception from the area of interest, and reference channel, which provides a reference for correlation based matched filter. The PBR matched filter receiver is shown in Figure 2.1.

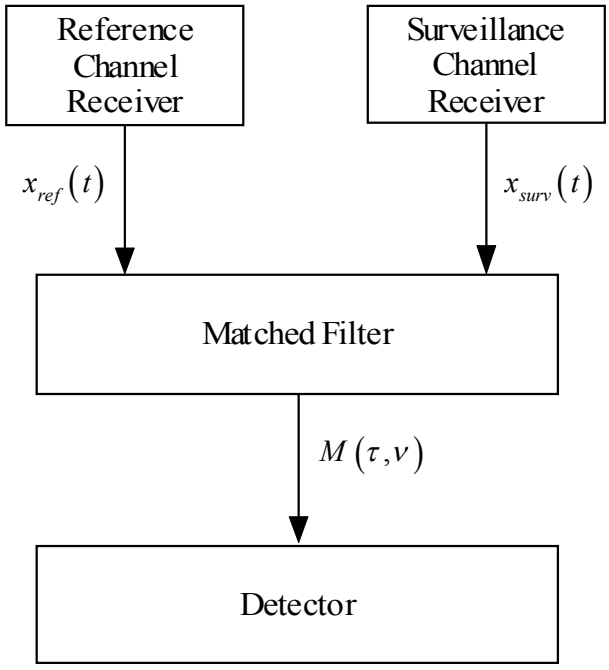

Figure 2.1 Block diagram of the PBR matched filter

The simpler PCL radar system requires two antennas: the first antenna, often called the *reference antenna,* is used to capture a direct version of the signal being utilised and should point in the direction of the transmitter, the second antenna, usually called the *surveillance antenna*, is used to capture the signals of potential target.
The output of the matched filter block is obtained as

$$M(\tau,\nu) = \int_0^{T_{CUT}} x_{surv}(t)\, x_{ref}^{*}(t-\tau)\, e^{-j2\pi\nu t}\, dt \qquad (2.1)$$

where $M(\tau,\nu)$ denotes the range–Doppler cross-correlation surface, $x_{surv}(t)$ is the echo signal and $x_{ref}(t)$ is the reference signal, delayed by an amount τ seconds and Doppler shifted by ν Hz.

The cross correlation function at the matched filter output is achieved by correlating the surveillance signal $x_{surv}(t)$ with Doppler-shifted versions of the reference signal $x_{ref}(t)$ to form a bank of filters matched to every possible Doppler frequency of interest.

The matched filter stage serves two important purposes:

- ✓the generation of sufficient signal processing gain to allow the targets to be detected above the noise floor
- ✓the estimation of the bistatic range and bistatic Doppler shift of the target echoes.

In this first section we assume an ideal scenario in which we can perfectly capture the transmitted signal and the surveillance channel is composed by only target and thermal noise component. Based on this assumption the complex envelope of the total signal received in the reference channel $x_{ref}(t)$ and in the surveillance channel $x_{surv}(t)$ are given by

$$\begin{cases} x_{ref}(t) = \alpha_{ref} x(t) + n_{ref}(t) \\ x_{surv}(t) = \beta^1_{surv} x\left(t - \tau_1^T\right) e^{i2\pi\nu_1^T t} + n_{surv}(t) \end{cases} \tag{2.2}$$

where $x(t)$ is a copy of the transmitted signal, α_{ref} is the complex amplitude relative to the reference channel, β_{surv} is the complex amplitude relative to the surveillance channel, τ_1^T is the target delay, ν_1^T is the target Doppler frequency, and $n_{ref}(t), n_{surv}(t)$ are thermal noise components.

Using equation (2.2) in equation (2.1) the output of the matched filter can be written as

$$M(\tau,\omega) \triangleq \alpha_{ref}\beta^1_{surv}\chi\left(\tau - \tau_1^T, \omega - \nu_1^T\right) + n_{out}(\tau,\omega) \tag{2.3}$$

The output of the matched filter receiver is ideally the ambiguity function of the transmitted signal, scaled and shifted to be centered on the time delay and Doppler shift corresponding to target location and velocity.

2.3 Signal modelling and interference environment in a passive bistatic radar

In this section the adopted model, for both reference signal and received signal and a typical passive bistatic scenario is described paying particular attention to the definition and representation of different contributions within the received signals. The purpose of this section is to provide a review of the interference environment and its impact on the PBR matched filter architecture described in the previous subsection.

2.3.1 Single target geometry

In this first section we analyze the simpler scenario in which we have a single target and a single illuminator of opportunity. A typical passive radar single target geometry is shown in Figure 2.2.

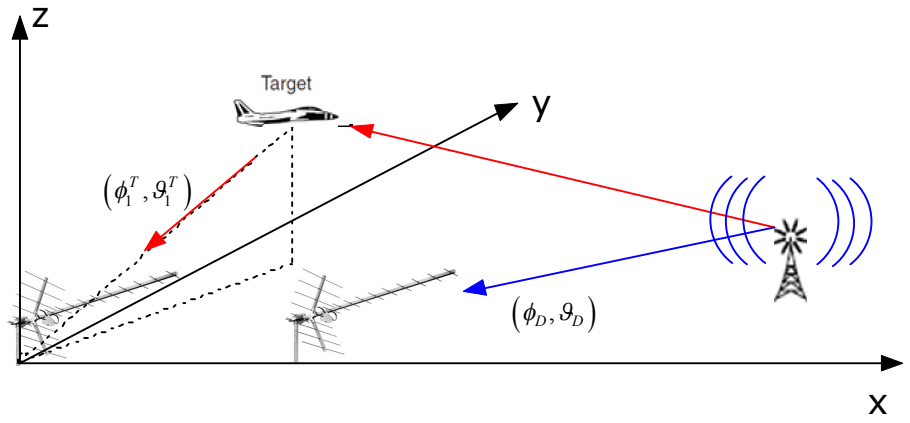

Figure 2.2 Single target scenario

The reference and surveillance antennas are assumed to be collocated with the reference antenna steered toward the illuminator of opportunity and the surveillance antenna pointed in the direction to be surveyed.

Based on this assumption the complex envelopes of the total signal received in the reference channel $x_{ref}(t)$ and in the surveillance channel $x_{surv}(t)$ are given by

$$\begin{cases} x_{ref}(t) = \alpha_{ref} x(t) + \alpha_{surv}^{1} x\left(t - \tau_1^T\right) e^{i2\pi\nu_1^T t} + n_{ref}(t) \\ x_{surv}(t) = \beta_{ref} x(t) + \beta_{surv}^{1} x\left(t - \tau_1^T\right) e^{i2\pi\nu_1^T t} + n_{surv}(t) \end{cases} \tag{2.4}$$

where $x(t)$ is a replica of the transmitted signal, α_{ref} is the complex amplitude of the direct signal received via the main-lobe of the reference antenna, $\alpha_{surv}^{1}, \tau_1^T, \nu_1^T$ are respectively the complex amplitude, the delay with respect to the direct signal and the Doppler frequency shift of the target echo received via the side-back lobes of the reference antenna, β_{ref} is the complex amplitude of the direct signal received via the side-back lobe of the surveillance antenna, $\beta_{surv}^{1}, \tau_1^T, \nu_1^T$ are respectively the complex amplitude, the delay with respect to the direct signal and the Doppler frequency shift of the target signal received via the mainlobe of the surveillance antenna, $n_{ref}(t), n_{surv}(t)$ are respectively the thermal noise contribution at the reference and surveillance antenna.

We can observe that the terms $\alpha_{surv}^{1}, \alpha_{ref}, \beta_{surv}^{1}, \beta_{ref}$ are strictly related to the received target power P_t and the received direct power P_d.

The bistatic radar equation gives the target power received in the surveillance channel as

$$P_t = \frac{ERP\lambda^2 \sigma_b G_{surv}\left(\phi_1^T, \vartheta_1^T\right)}{(4\pi)^3 \left(R_T R_R\right)^2} \tag{2.5}$$

where ERP is the effective radiated power from the illuminator of opportunity, σ_b is the target bistatic radar cross-section, $G_{surv}\left(\phi_1^T, \vartheta_1^T\right)$ is the reference antenna gain respect to the angular direction $\left(\phi_1^T, \vartheta_1^T\right)$ of the surveillance area, R_T is the transmitter to target distance, R_R is the target to receiver distance and the propagation losses have been supposed negligible.

The power received directly from the transmitter of opportunity in the surveillance channel is

$$P_d = \frac{ERP\lambda^2 G_{surv}\left(\phi_D, \vartheta_D\right)}{(4\pi)^3 (L)^2} \tag{2.6}$$

where ERP is the effective radiated power from the transmitter, $\left(\phi_D, \vartheta_D\right)$ are respectively the azimuth and elevation angles that defines the illuminator angular position, $G_{surv}\left(\phi_D, \vartheta_D\right)$ is the reference antenna gain respect to the angular direction $\left(\phi_D, \vartheta_D\right)$ of the illuminator of opportunity, L is the transmitter to receiver distance. The target signal to direct signal ratio SDR in the surveillance channel is therefore

$$SDR_{surv} = \frac{P_t}{P_d} = \frac{\sigma_b G_{surv}\left(\phi_1^T, \vartheta_1^T\right)(L)^2}{\left(R_T R_R\right)^2 G_{surv}\left(\phi_D, \vartheta_D\right)} \tag{2.7}$$

With similar considerations the SDR in the reference channel can be evaluated as

$$SDR_{ref} = \frac{P_t}{P_d} = \frac{\sigma_b G_{ref}\left(\phi_1^T, \vartheta_1^T\right)(L)^2}{\left(R_T R_R\right)^2 G_{ref}\left(\phi_D, \vartheta_D\right)} \tag{2.8}$$

where $G_{ref}\left(\phi_1^T, \vartheta_1^T\right)$ is the reference antenna gain respect to the direction of the surveillance area and $G_{ref}\left(\phi_D, \vartheta_D\right)$ is the reference antenna gain respect to the angular direction of the transmitter.

In typically scenarios the SDR can assume values between $\left[-90dB \div -70dB\right]$ as shown in the several references.

Assume the contribution of the target signal in the reference channel is negligible, equation (2.4) becomes

$$\begin{cases} x_{ref}(t) = \alpha_{ref} x(t) + n_{ref}(t) \\ x_{surv}(t) = \beta_{ref} x(t) + \beta_{surv}^1 x\left(t - \tau_1^T\right) e^{i2\pi v_1^T t} + n_{surv}(t) \end{cases} \tag{2.9}$$

Using equation (2.9) in equation (2.1) the output of the matched filter can be written as

$$M(\tau, \omega) \triangleq \alpha_{ref}\beta_{ref}\chi(0,0) + \alpha_{ref}\beta_{surv}^1 \chi\left(\tau - \tau_1^T, \omega - v_1^T\right) + n_{out}(\tau, \omega) \tag{2.10}$$

The presence of the direct signal in the surveillance channel causes any unwanted contributions at the output of the matched filter. The main contribution is confined to the zero-Doppler and zero range bin but the range and Doppler sidelobes of this autocorrelation function could remain significant.

The target to direct signal ratio at the output of the matched filter is proportional to the SDR_{surv} calculated at the input. If the sidelobe level of the ambiguity function or the

surveillance antenna are not comparable with the SDR_{surv} the target could be masked by the direct signal.

2.3.2 Multi target geometry

Considering the presence of N_T targets in the scenario, as shown in Figure 2.3, we can extend the single target model as

$$\begin{cases} x_{ref}(t) = \alpha_{ref} x(t) + \sum_{n=1}^{N_T} \alpha_{surv}^{m} x\left(t - \tau_m^T\right) e^{i2\pi v_m^T t} + n_{ref}(t) \\ x_{surv}(t) = \sum_{n=1}^{N_T} \beta_{surv}^{m} x\left(t - \tau_m^T\right) e^{i2\pi v_m^T t} + n_{surv}(t) \end{cases} \tag{2.11}$$

where $x(t)$ is a replica of the transmitted signal, α_{ref} is the complex amplitude of the direct signal received via the main-lobe of the reference antenna, $\alpha_{surv}^{m}, \tau_m^T, v_m^T$ are respectively the complex amplitude, the delay with respect to the direct signal and the Doppler frequency shift of the m-th target, $\beta_{surv}^{m}, \tau_m^T, v_m^T$ are respectively the complex amplitude of the m-th target signal received via the mainlobe of the surveillance antenna, the m-th target delay with respect to the direct signal and the m-th target Doppler frequency shift,

$n_{ref}(t), n_{surv}(t)$ are respectively the thermal noise contribution at the reference and surveillance antenna.

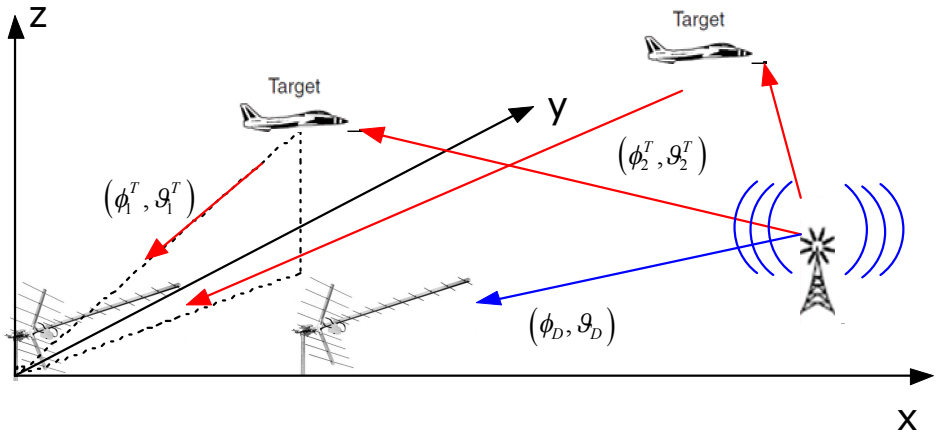

Figure 2.3 Multi target scenario

Note that the contribution of the direct signal component in the surveillance channel is not considered in this section because we have analyzed this component in the previous section. Assume the contribution of the target signal in the reference channel is negligible, equation (2.11) can be written as

$$\begin{cases} x_{ref}(t) = \alpha_{ref} x(t) + n_{ref}(t) \\ x_{surv}(t) = \sum_{m=1}^{N_T} \beta_{surv}^{m} x\left(t - \tau_m^T\right) e^{i2\pi v_m^T t} + n_{surv}(t) \end{cases} \tag{2.12}$$

Using equation (2.12) in equation (2.1) the output of the matched filter is

$$M(\tau,\omega) \triangleq \sum_{m=1}^{N_T} \alpha_{ref} \beta_{surv}^{m} \chi\left(\tau - \tau_m^T, \omega - v_m^T\right) + n_{out}(\tau,\omega) \tag{2.13}$$

As we can see from equation (2.13) the matched filter receiver is not optimum when more than one moving target echo is present in the received signal. To understand this we can think to a simplified scenario. Let us assume that only two target are present in the received signal: one strong echo originating from a nearby target and one weak echo originating from a far target. The amplitudes of the ambiguity functions relative to the two target will be related to the amplitudes of the two received signals. Therefore the ratio between the two target power, at the output of the matched filter, will be proportional to the ratio

$$\frac{\left|\beta_{surv}^{strong}\right|}{\left|\beta_{surv}^{weak}\right|} \tag{2.14}$$

In this case the detection of the first target will be performed almost perfectly while detection of the weak echo could be very difficult or impossible.

This event typically occurs when a specular reflection is observed on a large jet aircraft, or when a target passes very close to the transmitter or receiver. In this case, the range and Doppler sidelobes of this large return can be sufficient to mask the other, smaller target returns on the correlation surface. [Kulpa 2005] propose the iterative removal of such returns by estimating their position in range–Doppler, and then adaptively filtering them from the original data, before recalculating the correlation surface. The approach can be repeated for every strong return, but at the expense of non real-time operation in some instances.

2.3.3 Multipath environment

In the precedent sections we have assumed that the received signal in the reference channel and in the surveillance channel is free to multipath. In an actual application this assumption will not be fulfilled and the received signal consists of more terms originating from the reflections of the transmitted power from distributed objects.
The typical baseband complex envelope model for the multipath channel is

$$x_{rx}(t) = \alpha_0 x(t) + \sum_{n=1}^{N_C} \alpha_n e^{i\theta_n} x(t - \tau_m) + n(t) \tag{2.15}$$

where

$x_{rx}(t)$ is the received signal

$x(t)$ is a delayed replica of the transmitted signal

α_0 is the complex amplitude of the direct signal

N_C is the number of paths

$\alpha_m, \vartheta_m, \tau_m$ are respectively the amplitude, the phase and the delay with respect to the direct signal of the m-th path

$n(t)$ is the thermal noise contribution

This model is widely accepted in open literature relative to radio communication applications and it is used in all works about passive radar systems.
The received signal expressed in equation (2.15) can be seen as the sum of different contributions relative to a set of small discrete stationary scatterers. A continuous backscattering environment can be emulated by utilizing a large number of such scatters. Different criteria can be adopted to set the positions and the backscattering characteristics of the scatterers which determine the delays and amplitudes of the correspondent echoes.
A widely accepted statistical model in the radio communication community, as defined in the standard DVB-T ETSI [ETSI 2009] assume the following distributions:
the amplitude term α relative to each path is assumed to have a Rayleigh distribution

$$f(\alpha) = \frac{1}{\bar{\alpha}_i^2} \exp\left(-\frac{\alpha^2}{2\bar{\alpha}_i^2} \right) u(\alpha) \tag{2.16}$$

the phase term θ of the scattering contribution is assumed to be uniformly distributed between 0 and 2π

and the time delay is supposed to have a truncated exponential distribution

$$f(\tau)=\begin{cases}\dfrac{1}{\tau_0\left(1-e^{-\tau_M/\tau_0}\right)}e^{-\tau/\tau_0} & 0\le\tau\le\tau_M\\ 0 & otherwise\end{cases} \tag{2.17}$$

The characteristic parameters of each distribution are related to the scenario that we want to simulate, in [ETSI 2009] a typical set of these parameters is suggested. The number of independent path is typically set to $N_C=20$.

The amplitude of the direct path can be chosen by defining the level of the Rice factor

$$K_R \triangleq \frac{\alpha_0^2}{\sum_{n=1}^{N_C}\overline{\alpha}_n^2} \tag{2.18}$$

that generally assumes value between 0 dB, in urban scenarios, to 20 dB, in rural scenarios.

The defined model is valid when omnidirectional antennas are used. To analyze system performance with directional antennas it is also necessary to model the angular distribution of the multipath interference.

A geometrically based statistical model statistical for line-of-sight multipath radio channel, was first proposed in [Liberti 1996]. The model, known as the geometrically based single bounce (GBSB), assume that scatterers are ominidirectional reradiating elements uniformely distributed over a finite surface and that a single bounce occurs during the signal propagation. Distributing the scatteresr inside a finite area leads to a joint angle of arrival and time of arrival probability density function which exepresses the intrinsic relationship between the two parameters in a 2D geometry. A generalized GBSB model has been obtained in [Lauri 2007] by assuming that the scattering centers are uniformly distributed inside a volumetric region. The joint distribution of time delay, azimuth angle and elevation angle which describes the specific multipath scenario has been defined. The signal received by the surveillance antenna is modeled as the sum of the direct path plus the reflection due to independent scattering points, statistically described following the generalized GBSB model.

Specifically they can be fixed in order to simulate a totally controlled scenario or can be generated according to a statistical model.

In order to have a controlled scenario, a hybrid deterministic-statistical angular model has been defined as

$$x_{rx}(t) = \alpha_0 x(t) + \sum_{n=1}^{N_C} x(t-\tau_m) \sum_{k=1}^{N_n} G_{surv}(\phi_{n,k}, \vartheta_{n,k}) \alpha_{n,k} e^{i\theta_{n,k}} + n(t) \qquad (2.19)$$

Specifically the received signal for the n-th path is generated as the sum of N_n random independent scattering points, characterized by their angular position $(\phi_{n,k}, \vartheta_{n,k})$, and statistically described following the statistical model defined above.

The number of angular direction for the n-th path is assumed random and the angular directions are assumed uniformly distributed within a set of fixed angular sectors. The angular sectors are determined in relation to the target and illuminator of opportunity angular locations as shown in Figure 2.4.

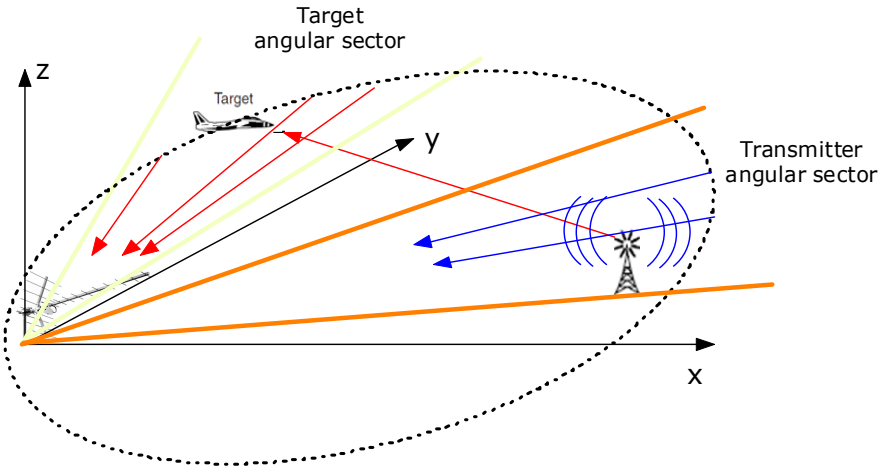

Figure 2.4 Multipath model

The amplitudes α_n^{new} associated to each path and defined as

$$\alpha_n^{new} \triangleq \sum_{k=1}^{N_n} G_{surv}(\phi_{n,k}, \vartheta_{n,k}) \alpha_{n,k} e^{i\theta_{n,k}} \qquad (2.20)$$

are chosen in order to maintain the same level of power defined by the statistical omnidirectional model, described in equation (2.15)

$$E\left\{\left|\alpha_n^{new}\right|^2\right\} = \bar{\alpha}_n^2 \tag{2.21}$$

The defined model can be further extended in order to considerate the effects of ICM (Internal Clutter Motion) induced for example by vegetation or sea clutter

$$x_{rx}(t) = \alpha_0 x(t) + \sum_{n=1}^{N_C} \alpha_n^{new} x\left(t - \tau_n\right) e^{i2\pi f_d(n)t} + n(t) \tag{2.22}$$

where $f_d(n)$ is the frequency Doppler associated to each path. The values $f_d(n)$ can be generated by using a statistical distribution or by using some model of the Doppler power spectrum, for example the Billingsley model in the case of vegetation.

The main effects of the ICM is a small extension of the received signal around zero Doppler frequency strictly related to the operating wavelength and the wind speed.

Based on the previous assumptions the complex envelope of the reference and surveillance channel is given by

$$\begin{cases} x_{ref}(t) = \alpha_0 x(t) + \sum_{n=1}^{N_C} \alpha_n^{new} e^{i2\pi f_d(n)t} x\left(t - \tau_n\right) + n_{ref}(t) \\ x_{surv}(t) = \beta_0 x(t) + \sum_{n=1}^{N_C} \beta_n^{new} e^{i2\pi f_d(n)t} x\left(t - \tau_n\right) + \beta_{surv}^1 x\left(t - \tau_1^T\right) e^{i2\pi \nu_1^T t} + n_{surv}(t) \end{cases} \tag{2.23}$$

It is important to note that the first difference respect to the ideal case is the presence of the multipath component on the reference signal.

In order to simplify the analysis and determine the effects of multipath presence it's now assumed that the reference channel is free to multipath. and the surveillance channel is to direct signal.

Using equation (2.23) in equation (2.1) the output of the matched filter can be written as

$$M(\tau,\omega) \triangleq \sum_{m=1}^{N_T} \alpha_{ref} \beta_{surv}^m \chi\left(\tau - \tau_m^T, \omega - \nu_m^T\right) + \alpha_{ref} \beta_{surv}^1 \chi\left(\tau - \tau_1^T, \omega - \nu_1^T\right) + n_{out}(\tau,\omega) \tag{2.24}$$

The result is very similar to that obtained in a multi target scenario. The main difference is that the several contribution in the output signal are located at zero Doppler frequency.

2.4 PBR signal processing chain

In this section an advanced PBR signal processing architecture is presented in order to mitigate the main limitations of a simple matched filter architecture as underlined in the previous section. The scheme of a typically PBR signal processing chain is shown in Figure 2.5 [Cherniakov 2008].

A complete PR signal processing chain typically consists of the following steps:

- Data collection: reception of the direct signal from the transmitter and from the surveillance region on dedicated low-noise, linear, digital receivers.
- Reference signal conditioning
- Interference suppression
- Matched filter processing
- Target detection

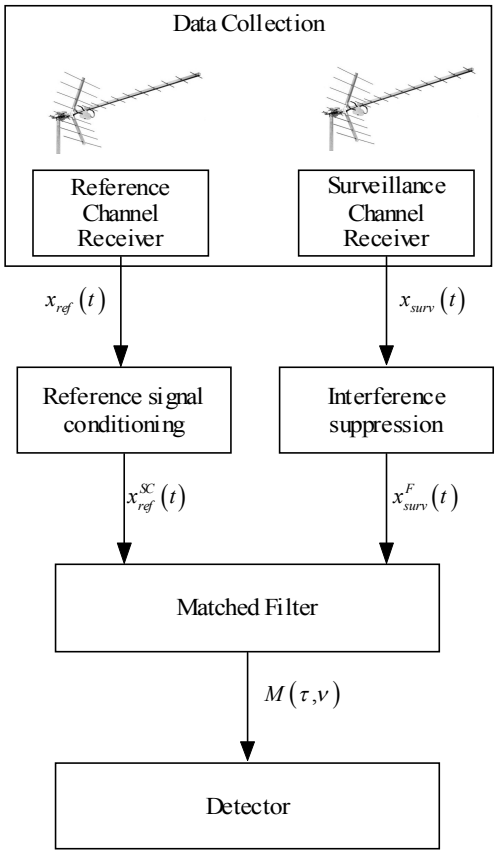

Figure 2.5 Typical PBR signal processing chain

2.4.1 Data collection considerations

The main requirements for the signal processing chain are:

- the availability of a reference signal, received directly from the transmitter
- the availability of the surveillance channel collected on the surveillance area.

In the simpler configuration analyzed in section 2.2 it is necessary to steer mechanically the two receiver antennas towards both the illuminators of opportunity and the surveillance area. The principal limitation of this configuration tends to be the problem of the reception of the transmitter signal in the echo channel that determines:

- the target signal is masked and it must be cancelled before matched filter
- requirement for high dynamic range

Therefore it is necessary to try to steer the echo channel antennas to minimize direct reception of the transmitter signal and reduce the direct signal before sampling. The simpler way is to site the receive antenna so that it is physically shielded from the direct path signal, using for example the terrain conformation or buildings. This technique can often provide adequate suppression but it can have several limits respect to the surveillance area. One other way to resolve this problem is that to use an antenna array and adopt analogue beamforming techniques in order to steer a deep null towards the transmitter before sampling [Kuschel 2008].
An antenna array configuration it is very interesting since we can apply digital beamforming techniques after sampling in order to implement an electronic scansion and the relative possibility to improve the interference cancellation.
In chapter 5 some digital beamforming techniques, used to collect the reference channel and the surveillance channel, will be presented.

2.4.2 Signal conditioning in the reference channel

In order to perform the matched filtering stage, it is necessary to cross-correlate the echo channel signals with the reference signal. In some circumstances, it may be necessary to perform some signal processing on the reference signal in order to:

- ✓improve its quality and the shape of the ambiguity function. For instance digital waveforms could contain some form of unwanted periodic structure which causes ambiguities in the ambiguity function.
- ✓remove unwanted multipath components within the reference signal. A good example of this is with digital audio-video broadcast (DAB, DVB-T) signals arising from a single frequency network (SFN). In this situation, the unprocessed reference signal would actually comprise the superposition of several identical, but time-shifted, copies of the reference signal from each transmitter within line-of-sight of the receiver. In this situation, it is necessary to reconstruct a pure reference signal. If this is not done, then even a single target would result in multiple detections.

2.4.3 Interference suppression in the surveillance channel

The scope of this block is that to mitigate and ideally to suppress below the noise floor the several interference components received on the surveillance channel. We want to recall the main target masking effects, as mentioned in the previous section:

- ➢Fraction of the direct signal received by the surveillance channel. This will be the dominant component and will occur at a particular incident angle.
- ➢Possible strong clutter/multipath echoes each characterized by a particular signal level and a particular incident angle, and possibly time varying and Doppler-shifted (ICM)
- ➢Possible strong interference received from other transmitters of opportunity specially in DVB-T or DAB single frequency network
- ➢Echoes from other strong targets

Different techniques have been proposed to resolve these problems and they can be summarized as:

- ✓Spatial cancellation
- ✓Spectral/temporal cancellation

The first option in reducing the interference received in the echo channels is to try spatially to filter out the signal through the receiver antenna pattern. The simpler and cheaper way is that to physically shield the surveillance antenna from the direct path as we have seen in the precedent sub-section. Another interesting way due to simplicity is that to physically steer a high directive antenna to ensure that the transmitter falls in a null or low sidelobe. This technique can be useful for direct path cancellation but it could have problems with respect to the cancellation of other contributions

If an antenna array rather than a single receiver antenna is used then the performance of sidelobe cancellation technique may be improved. An antenna array at the surveillance channel can improve the performances of the spatial cancellation. Beamforming techniques, applied to surveillance antenna array, can be configured in order to steer a null in the direction of the direct path signal. Both analogue and digital beamforming technique can be applied, particularly the first one could mitigate the problem of high dynamic range before sampling. In chapter 5 digital beamforming techniques will be analyzed and the signal processing chain will be opportunely modified.

Spectral-temporal cancellation of the interference is the second principal option. However, even after reducing the interference using the antenna pattern, it is necessary to filter the direct signal and clutter further by adaptive filtering in the time domain. The approach typically adopted is to use an adaptive noise canceller structure, in which the signal from the reference antenna is used to estimate the interference and then remove it from the echo channel. This approach relies on a reference channel containing no echo signals; otherwise they would also be removed. In chapter 4 temporal adaptive technique will be investigated and an alternative solution will be proposed.

2.4.4 Matched filter processing

After suppression of the DPI and clutter components the filtered surveillance channel signal $x_{surv}^{F}(t)$ is cross correlated with the modified reference signal $x_{ref}^{SC}(t)$ by the matched filter processor.

The output of the matched filter block, as seen in section 2.2, is obtained as

$$M(\tau,\nu)=\int_{0}^{T_{CUT}} x_{surv}^{F}(t)\,x_{ref}^{SC*}(t-\tau)\,e^{-j2\pi\nu t}\,dt \tag{2.25}$$

where $M(\tau,\nu)$ denotes the range–Doppler cross-correlation surface, $x_{surv}^{F}(t)$ is the filtered echo signal and $x_{ref}^{SC}(t)$ is the modified reference signal, delayed by an amount τ seconds and Doppler shifted by ν Hz

The cross correlation function is achieved by correlating the filtered surveillance signal $x_{surv}^{F}(t)$ with Doppler-shifted versions of the modified reference signal $x_{ref}^{SC}(t)$ to form a bank of filters matched to every possible Doppler frequency of interest. This calculation is one of the most computational expensive in a passive radar signal processing chain. In chapter 3 some algorithms used to calculate the cross correlation function will be presented.

2.4.5 Detector

Targets are detected on the cross-correlation surface by applying an adaptive threshold, and declaring all returns above this surface to be targets.

Having calculated the correlation surface, target detection is simply a matter of identifying which peaks cross a detection threshold. Providing the initial adaptive signal processing stage was effective and all significant reference signal leakages were removed, the target detection process is usually against a Gaussian noise floor. A simple constant false alarm rate (CFAR) algorithm could be therefore very effective.

2.5 Chapter summary

In this chapter the signal processing chain adopted in a typical passive radar scenario has been presented. The main obvious problem of non-cooperative passive radar is the necessity to estimate a copy of the transmitted signal. Therefore the simpler PBR radar system requires two antennas in order to collect the reference signal and the surveillance signal and to perform the matched filter receiver. The matched filter is the optimum receiver in presence of additive white noise and in a typical PBR scenario this simpler structure presents several drawbacks. The adopted model for both reference signal and received signal and a typical passive bistatic scenario have been described. The main block introduced in the signal processing chain is the interference suppression block before the matched filter. The scope of this block is that to mitigate and ideally to suppress below the noise floor the several interference components received on the surveillance channel. Both spatial and temporal cancellation techniques have been introduced and they will be respectively analyzed in chapter 4 and 5. It is worth noting that the main feature in a traditional PBR signal processing chain is the presence of the interference suppression block before the matched filter. In this thesis both spatial and temporal interference suppression techniques will be implemented after the matched filter block.

Chapter 3.

Matched filter processing

3.1 Introduction

The main block in a PBR signal processing chain is the matched filter as we have seen in the previous chapter. We want to recall that the output of the matched filter is the 2D cross correlation function and that this processing step serves two distinct purposes: provide the necessary signal processing gain to allow detection of the target echo; estimate the bistatic range and Doppler shift of the target. The evaluation of the 2D cross correlation function can be computationally expensive considering that large 2D range-Doppler maps might be required depending on the desired surveillance region and the resolution in both range and Doppler dimensions. This implies that, to evaluate the theoretical 2D cross correlation function, a large number of complex operations has to be performed which sets a strong limitation on real time processing [Howland 2005]. Sub optimum approaches can be exploited to reduce the computational cost if a small SNR degradation can be accepted. Different approaches have been proposed to this purpose based on different strategies [Howland 2005], [Cherniakov 2008]. In this chapter a comparative study between optimum and sub optimum methods is presented, both in terms of computational load and SNR loss. A new detailed formulation of the sub optimum batches algorithm is proposed. We demonstrate that the obtained algorithm is equivalent to the classical matched filter used in active pulse radar. This analysis constitutes the basis for the development of the adaptive signal processing techniques that will be presented in the further chapter. The exact matched filter formulation for OFDM waveforms is derived and we reveal that this approach is similar

to the batches algorithm. Specifically they are based on the same small Doppler approximation. Also in this case we underline the analogies with the classical stepped frequency approach used in active pulse radar.

The chapter is organized as follows. The optimum algorithms for "2D cross correlation evaluation are briefly described in section 3.2. Section 3.3 reports the description and the performance analysis of the batches algorithm. In section 3.4 the matched filter formulation for OFDM waveforms is reported.

3.2 Matched filter algorithms

The evaluation of the bistatic range-Doppler Cross-Correlation Function (2D-CCF) is the key step in the PBR processing chain as we have seen in chapter 2

$$M(\tau,\nu)=\int_{0}^{T_{int}} s_{surv}(t)s_{ref}{}^{*}(t-\tau)e^{-j2\pi\nu t}dt \quad 0\le\tau\le\tau_{\max} \quad -\nu_{\max}\le\nu\le\nu_{\max} \tag{3.1}$$

where

$M(\tau,\nu)$ represents the range-Doppler cross correlation function between the reference signal $s_{ref}(t)$ and the surveillance signal $s_{surv}(t)$, the variable τ denotes the time delay, corresponding to the bistatic time difference of arrival, $\tau_{\max}$ is the maximum delay of interest and it is related to the maximum non ambiguous bistatic range, ν denotes the frequency Doppler shift of interest, $\nu_{\max}$ is the maximum shift Doppler of interest and it is related to the maximum bistatic velocity of interest, T_{int} denotes the integration time or the so called Coherent Processing Interval (CPI). The integration time is typically chosen equal to $T_{obs}+\tau_{\max}$, where T_{obs} is the length of the reference signal, in order to have no integration losses.

It should be noted that if we refer to the chain processing of Figure 2.5 then we have to substitute $s_{ref}(t)$ and $s_{surv}(t)$ with $s_{ref}^{SC}(t)$ and $s_{surv}^{F}(t)$, being respectively the outputs of the signal conditioning block and the interference suppression block.

Assuming that the received signals are sampled at frequency f_s equation (3.1) can be expressed in the discrete domain as:

$$M[m,p]=\sum_{n=0}^{N-1} s_{surv}[n]\, s_{ref}^{*}[n-m]\, e^{-j2\pi\frac{p}{N}n} \quad 0\le m\le N_{delay}-1;\ 0\le p\le N_{doppler}-1 \qquad (3.2)$$

where

$s_{ref}[n]$ and $s_{surv}[n]$ are the surveillance and the reference signals sampled at time $t=nT_s=\dfrac{n}{f_s}$

N is the total number of samples corresponding to $\lfloor T_{\text{int}} f_s \rfloor$,

m represents the time delay bin ($\tau_m = m / f_s$),

p is the Doppler bin corresponding to $\nu_n = \dfrac{p}{N} f_s$

N_{delay} is the number of range bins corresponding to $\lfloor \tau_{\max} f_s \rfloor$,

$N_{Doppler}$ is the number of frequency Doppler bins corresponding to $\left\lfloor \dfrac{2\nu_{\max} N}{f_s} \right\rfloor$.

The cross-correlation function, defined in equation (3.1) or equivalently in its numerical form (3.2), can be efficiently calculated by means two different approaches [Cherniakov 2008], [Langelotti 2009]:

1. Frequency domain approach: the first way of looking at the definition is to view $M(\tau,\nu)$ as the Fourier transform, or the discrete Fourier Transform, of the signal $s_{surv}(t)s_{ref}{}^{*}(t-\tau)$.
2. Time domain approach: the second way of looking at the definition is to view $M(\tau,\nu)$ as the cross-correlation between $s_{surv}(t)$ and $s_{ref}(t)e^{j2\pi\nu t}$.

In the following sub-sections we consider both these approaches, time and frequency domain, and we define two alternative efficient implementations obtained exploiting the well known FFT algorithm to evaluate the Discrete Fourier Transform (DFT).

3.2.1 Direct Fourier transform

The most obvious way to implement the cross correlation processing would be to calculate the Fourier Transform, or the Discrete Fourier Transform, of the signal $s_{surv}(t)s_{ref}^{*}(t-\tau)$, known as mixing product and indicated here as $x_m(t,\tau)$.

The main steps of this approach, as schematically shown in Figure 3.1, can be summarized as:

- for each range bin calculate the signal $s_{ref}^{*}(t-\tau)$
- obtain the mixing product signal multiplying the signal $s_{ref}^{*}(t-\tau)$ and the signal $s_{surv}(t)$
- calculate the DFT of the mixing product for each range bin

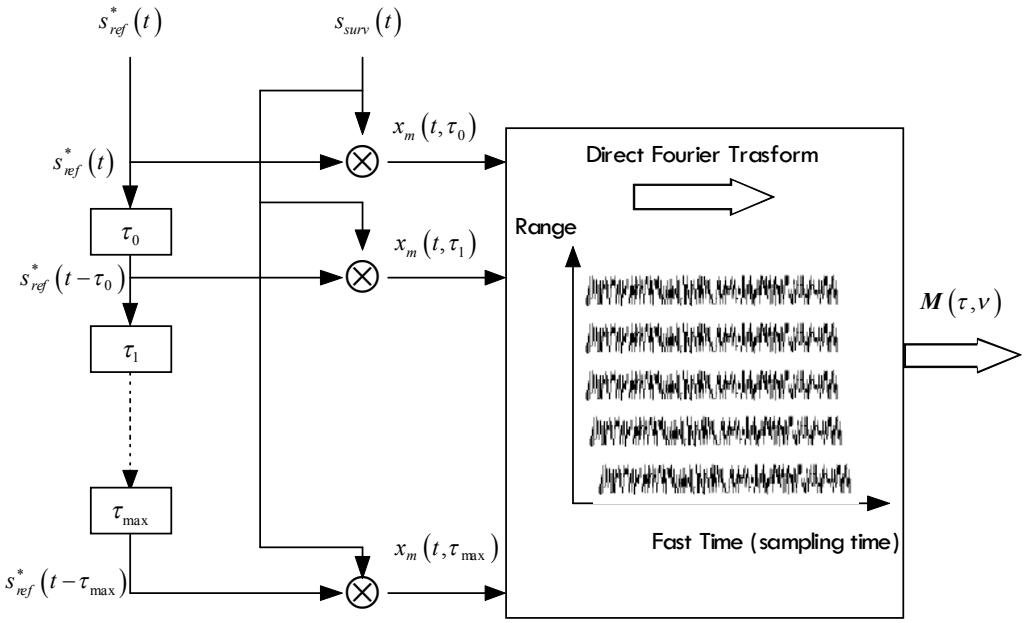

Figure 3.1 Cross correlation function in the frequency domain

It should be noted that this calculation must be done for each range of interest, therefore the iterations of this algorithm are limited to the maximum number of delays (N_{delay}) and this means that is possible to parallelize the algorithm over the range bins.

The computational load, defined as the number of complex multiplication, is

$$CL = \left[N\left(N_{Doppler} + 1\right)\right] N_{delay} \tag{3.3}$$

An alternative efficient implementation of this approach can be obtained exploiting the well known FFT algorithm. The main steps of the numerical algorithm are:

- for each time bin calculate the signal $s_{ref}{}^{*}(t-\tau)$
- obtain the mixing product signal multiplying the signal $s_{ref}{}^{*}(t-\tau)$ and the signal $s_{surv}(t)$
- calculate the FFT of the mixing product. The number of points in the FFT is N due to the length of the mixing product.
- discard $N - N_{Doppler}$ Doppler bins not of interest

Considering the reduced computational load of the FFT algorithm, the number of complex multiplication becomes

$$CL = \left[N + N\log_2\left(N\right)\right] N_{delay} = N\log_2\left(N\right) N_{delay} + NN_{delay} \tag{3.4}$$

Note that this algorithm allows the calculation of a limited number of delays N_{delay}, related to both maximum delay of interest and sampling frequency, but all possible Doppler shifts $N_{Doppler}$, limited only by the sampling frequency.

3.2.2 Cross correlation approach

The second way to implement the cross correlation processing would be to calculate the cross correlation between $s_{surv}(t)$ and $s_{ref}(t)e^{j2\pi\nu t}$. The main steps of this approach, schematically shown in Figure 3.2, can be summarized as:

- For each Doppler shift calculate a shifted copy of the reference signal $s_{ref}(t)e^{j2\pi\nu t}$
- Calculate the cross correlation between the surveillance channel $s_{surv}(t)$ and the signal obtained at the previous step

It should be noted that this calculation must be done for each Doppler of interest, therefore the iterations of this algorithm are limited to the maximum number of Doppler

shifts $N_{Doppler}$ and this means that is possible to parallelize the algorithm over the Doppler bins.

The computational load, defined as the number of complex multiplication, is

$$CL = \left[N\left(N_{delay}+1\right)\right] N_{Doppler} \tag{3.5}$$

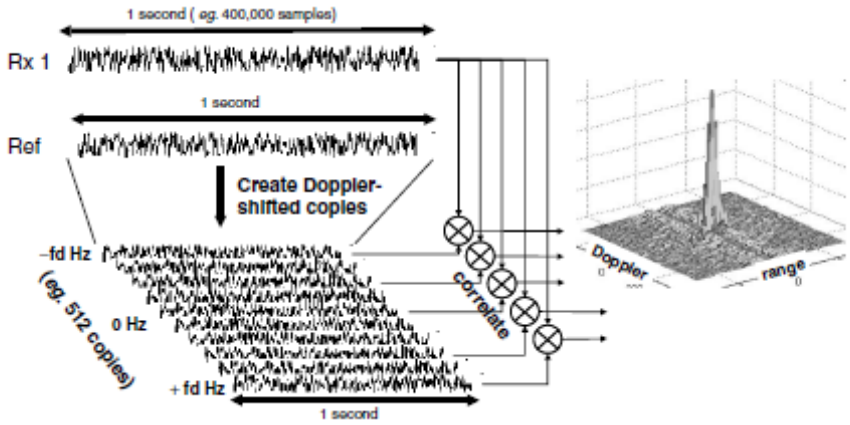

Figure 3.2 Cross correlation function in the time domain

A saving in computation is obtained by evaluating such cross-correlation in the frequency domain as:

- ➢Calculate the FFT of a shifted copy of the reference signal $s_{ref}(t)e^{j2\pi vt}$
- ➢Calculate the FFT of the surveillance signal $s_{surv}(t)$
- ➢Multiply the signals obtained at the previous two steps
- ➢Inverse the product signal in order to return in the range domain. The number of points in the IFFT is N.
- •Discard $N - N_{delay}$ range bins not of interest

The first step can be implemented more efficiently by simply calculating the FFT of $s_{ref}(t)$ and then rotating the elements of the transform with the appropriate number of places to impose the correct Doppler shift.

Considering the reduced computational load of the FFT algorithm, the number of complex multiplication becomes

$$CL = 2N\log_2(N) + \left[N + N\log_2(N)\right]N_{Doppler} = \\ = NN_{Doppler} + N\log_2(N)\left(N_{doppler} + 2\right) \tag{3.6}$$

As it is apparent from equations (3.6) and (3.4), the computational load for both algorithms increases with the number of integrated samples as Nlog2(N). However the final cost of the Correlation-FFT is essentially determined by the number $N_{Doppler}$ of considered Doppler bins, while the cost of the Direct-FFT is essentially determined by the number N_{delay} of range bins embedded in the 2D map. Thus the algorithm with the lowest number of operations depends on the extent of the 2D-CCF over the range and Doppler dimensions that is required for the specific application: if for example $N_{delay} > N_{Doppler}$ the Correlation-FFT algorithm requires less computation than the Direct- FFT.

3.3 Sub-optimum matched filter implementation

Further reduction of the computations required by the cross correlation function can be obtained by resorting to sub-optimum algorithms, if small degradations can be accepted in term of SNR. Notice that the required cost for both the time domain approach and the frequency domain approach optimum algorithms is strongly affected by the processing load required by the FFT of the long input sequences. Moreover, only a very small portion of the output FFTs (namely N_{delay} out of N, with $N_{delay} \ll N$, or $N_{Doppler}$ out of N, with $N_{Doppler} \ll N$) is required in the final 2D map while most of the obtained samples are discarded.

3.3.1 Batches algorithm

The processing developed in this section is analogous to the traditional radar processing method used for frequency modulated continuous wave (FMCW) signals, in which a number of snapshots of amplitude versus-range data are calculated, and then a Fourier

transform is used over each range bin to determine the Doppler shifts of targets at each range.

The reference signal $s_{ref}(t)$ can be divided into n_B batches of length T_B. The number of batches n_B is obtained as

$$\left\lfloor \frac{T_{obs}}{T_B} \right\rfloor \tag{3.7}$$

where T_{obs} is the length of the reference signal. With this assumption we can write the reference signal as

$$x_{ref}(t) = \sum_{i=0}^{n_B-1} x_i(t - iT_B) \tag{3.8}$$

The signal belonged to each block is defined as

$$x_i(t) = s_i(t)q(t) \tag{3.9}$$

where $s_i(t)$ is the transmitted signal, related to the waveforms of opportunity utilized, in the i-th block and $q(t)$ is defined as

$$q(t) = \begin{cases} 1 & t \in [0, T_B] \\ 0 & otherwise \end{cases} \tag{3.10}$$

Using equation (3.8) into equation (3.1), the output of the matched filter can be equivalently written as

$$M(\tau,\nu) = \sum_{i=0}^{n_B-1} \int_0^{T_{\text{int}}} x_{surv}(t) x_i^*(t - \tau - iT_B) e^{-j2\pi\nu t} dt \quad 0 \le \tau \le \tau_{\max} \quad -\nu_{\max} \le \nu \le \nu_{\max} \tag{3.11}$$

As $x_i^*(t - \tau - iT_B) \neq 0 \ \vee t \in [iT_B + \tau, iT_B + \tau + T_B]$ we can modify the integral as

$$M(\tau,\nu) = \sum_{i=0}^{n_B-1} \int_{iT_B+\tau}^{iT_B+\tau+T_B} x_{surv}(t) x_i^*(t - \tau - iT_B) e^{-j2\pi\nu t} dt \tag{3.12}$$

With a change of variable $\alpha = t - iT_B$, equation (3.12) becomes

$$M(\tau,\nu) = \sum_{i=0}^{n_B-1} e^{-j2\pi\nu iT_B} \int_{\tau}^{\tau+T_B} x_{surv}(\alpha + iT_B) x_i^*(\alpha - \tau) e^{-j2\pi\nu\alpha} d\alpha \tag{3.13}$$

As we have supposed $0 \le \tau \le \tau_{\max}$ and the surveillance channel a delayed replica of the reference signal $s_{ref}(t - \tau_T)$ with $0 \le \tau_T \le \tau_{\max}$, we can generally limit the integral,

equation (3.13), between $\left[0, T_B + \tau_{\max}\right]$. This fact should be more clear observing Figure 3.3.

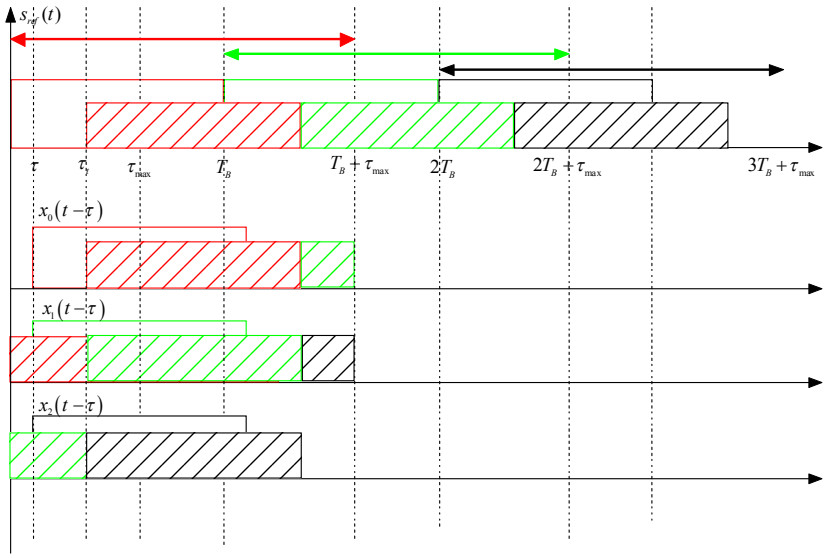

Figure 3.3 Batches algorithm description.

If we define the surveillance channel signal belonged to each block, as shown in Figure 3.4, as

$$x_{surv}^{i}(t) = x_{surv}(t) * rect\left(\frac{t - iT_b}{T_B + \tau_{\max}}\right) \tag{3.14}$$

the cross correlation function between the reference channel and the surveillance channel can be obtained as

$$M(\tau, \nu) = \sum_{i=0}^{n_B - 1} e^{-j2\pi\nu i T_B} \int_{0}^{T_B + \tau_{\max}} x_i^{surv}(\alpha) x_i^{*}(\alpha - \tau) e^{-j2\pi\nu\alpha} d\alpha \tag{3.15}$$

Using equation (1.10), equation (3.15) can be written as

$$M(\tau, \nu) = \sum_{i=0}^{n_B - 1} e^{-j2\pi\nu i T_B} \chi_i(\tau, \nu) \tag{3.16}$$

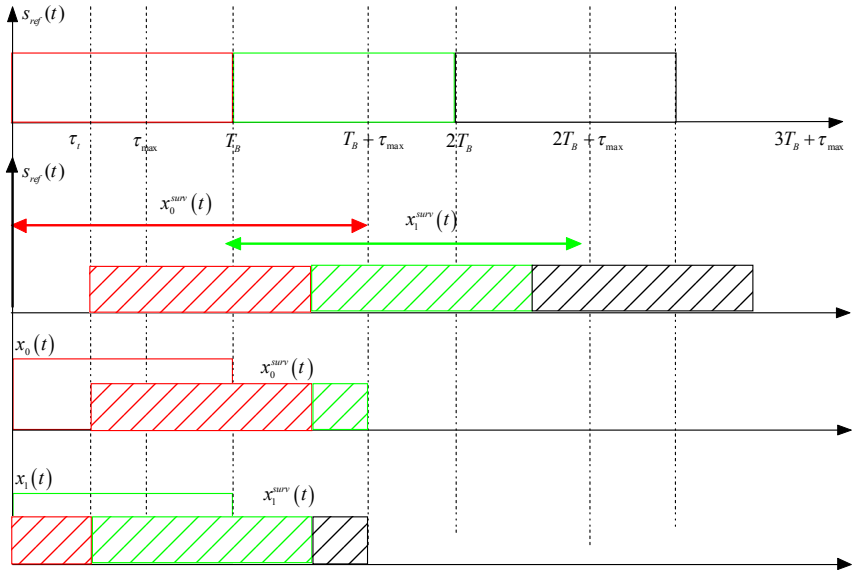

Figure 3.4 Batches algorithm: reference and surveillance signals segmentation

Observing equation (3.15) it is possible to conclude that the cross correlation function can be seen as the weighted sum of the cross correlation function between each block. It should be noted that in equation (3.15) the integral is really calculated between τ and $\tau + T_B$ as $x_i(t-\tau) \neq 0 \vee t \in [\tau, \tau + T_B]$.

We can write the numerical version of equation (3.15) as

$$M[m,p] = \sum_{i=0}^{n_B-1} e^{-j2\pi \frac{m}{n_B} i} \sum_{n=0}^{N_B'-1} x_i^{surv}[n] x_i^*[n-p] e^{-j2\pi \frac{m}{N} n} \qquad (3.17)$$

$$where \;\; 0 \leq p \leq N_{delay} - 1;\; 0 \leq m \leq N_{doppler} - 1$$

where

$x_i^{surv}[n]$ and $x_i[n]$ are the surveillance and the reference channel signals, relative to ith block, sampled at time $t = nT_s = \frac{n}{f_s}$

N_B' is the total number of samples corresponding to $\lfloor (T_B + \tau_{max}) f_s \rfloor$,

p represents the time delay bin ($\tau_p = p / f_s$),

m is the Doppler bin corresponding to $v_m = \frac{m}{N} f_s$

N_{delay} is the number of time bins corresponding to $\lfloor \tau_{max} f_s \rfloor$,

$N_{Doppler}$ is the number of frequency Doppler bins corresponding to $\left\lfloor \frac{2\nu_{\max} N}{f_s} \right\rfloor$.

Observing equation (3.15) when the product between T_B and the target Doppler shift is small compared to unity we can approximate the phase rotation within each block as constant

$$e^{-j2\pi\nu\alpha} \approx e^{-j2\pi\nu\frac{T_B}{2}} \quad \forall \nu \in [0, \nu_{\max}] \tag{3.18}$$

Then the Doppler shift has to be estimated based on the increasing accumulated phase shift between consecutive blocks and only a single correlator is needed. Equation (3.15) can be simplified to

$$M_b(\tau,\nu) = e^{-j\pi\nu T_B} \sum_{i=0}^{n_B-1} e^{-j2\pi\nu i T_B} \int_0^{T_B+\tau_{\max}} x_i^{surv}(t) x_i^*(\alpha-\tau) d\alpha \tag{3.19}$$

where the small Doppler approximation, defined in equation (3.18) has been supposed and the subscript b stands for "batches algorithm".

Defining the cross correlation between the i-th block as

$$x_{cc}^i(\tau) = \int_0^{T_B+\tau_{\max}} x_i^{surv}(t) x_i^*(\alpha-\tau) d\alpha \tag{3.20}$$

equation (3.19) can be written as

$$M_b(\tau,\nu) = e^{-j\pi\nu T_B} \sum_{i=0}^{n_B-1} e^{-j2\pi\nu i T_B} x_{cc}^i(\tau) \tag{3.21}$$

The numerical version of equation (3.19) can be written as

$$M_b(m,p) = \sum_{i=0}^{n_B-1} e^{-j2\pi\frac{mi}{n_B}} \sum_{n=0}^{N_B'-1} x_i^{surv}[n] x_i^*[n-m] \tag{3.22}$$

where we have supposed the small Doppler approximation

$$e^{-j2\pi\frac{p}{N}n} \approx 1 \tag{3.23}$$

The main steps of this approach, schematically shown in Figure 3.5, can be summarized as:

- Selection n_B consecutive batches of the reference channel $x_i(t)$ and surveillance channel $x_i^{surv}(t)$. The length of each block is $T_B + \tau_{\max}$ corresponding to $N_B^{'}$ samples
- Calculate the cross correlation, defined as $x_{cc}^i(\tau)$, n_B times between each batches $x_i(t)$ and $x_i^{surv}(t)$
- The Doppler dimension is then obtained by performing a FFT over the cross correlation values for each range bin

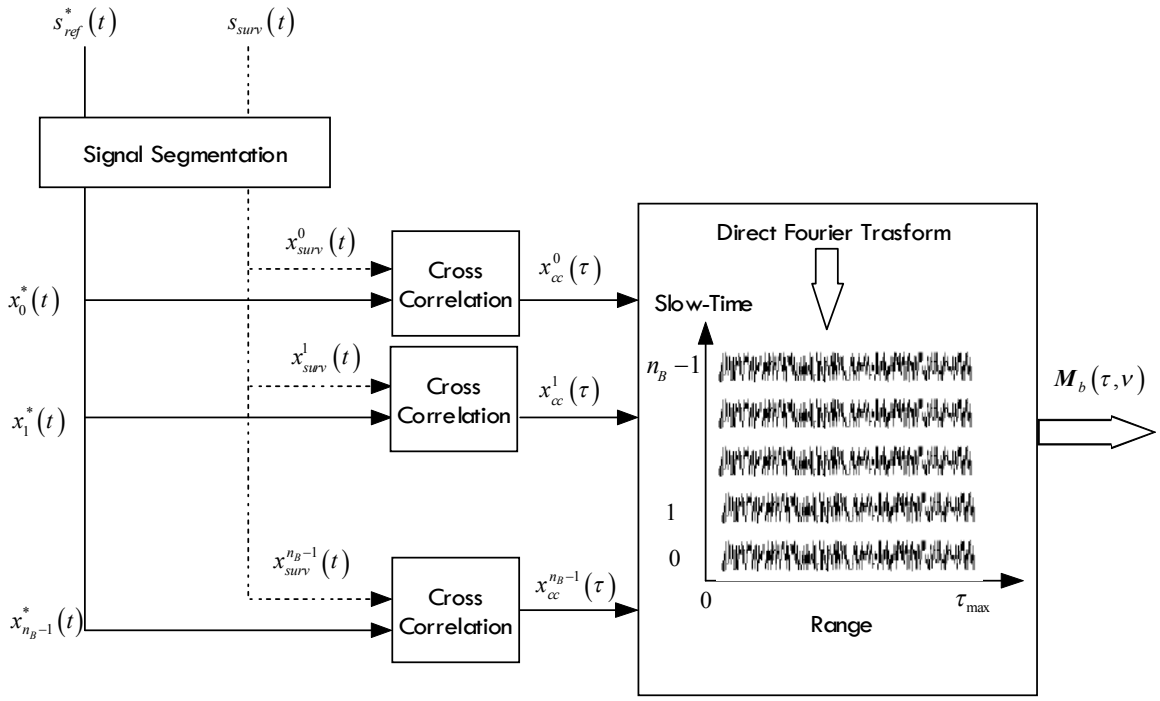

Figure 3.5 Batches algorithm scheme

Comparing Figure 3.5 with Figure 1.1 and equation (3.20) with equation (1.28) we can observe that the signal before the direct Fourier transform processing is equivalent to the classical range-slow time signal received by an active pulse radar

Modeling the received signal, as in chapter 1 the i-th matched filter output $x_{cc}^i(\tau)$ is given by

$$x_{cc}^i(\tau) = \int_0^{T_B+\tau_{\max}} \sqrt{E_t} b x_i^{surv}(t-\tau_a) e^{i\omega_{Da}t} x_i^*(\alpha-\tau) d\alpha \qquad (3.24)$$

Using equation(1.10), equation (3.24) can be modified as

$$x_{cc}^{i}(\tau) = \sqrt{E_t} b e^{i\omega_{Da} i T_B} \chi_i(\tau - \tau_a, -\omega_{Da}) \tag{3.25}$$

where $\chi_i(\tau,\omega)$ is the ambiguity function relative to the i-th batches.

The output of the matched filter receiver for the i-th batch is the ambiguity function of the transmitted batch scaled and shifted on the time delay corresponding to the location of the target and calculated at the target Doppler frequency.

Comparing equation (3.25) with equation (1.31) we can observe that we have similar losses related to the target Doppler shift as in the case of a pulse active radar.

To evaluate the losses of the batches algorithm respect to the optimum algorithm, shown in the previous section, we define the following parameter

$$Loss \triangleq \frac{M_b(\tau_T,\nu_T)}{M(\tau_T,\nu_T)} \tag{3.26}$$

where τ_T,ν_T are the time delay and Doppler shift of a single slowly fluctuating point target, $M(\tau_T,\nu_T)$ is the target peak calculated with optimum method and $M_b(\tau_T,\nu_T)$ is the target peak calculated with the batches algorithm sub-optimum method. We can calculate equation (3.26) by using equations (3.15) and (3.19)

$$Loss \triangleq \frac{\sum_{i=0}^{n_B-1}\int_0^{T_B+\tau_{\max}} \left|x_i(\alpha-\tau_T)\right|^2 e^{j2\pi\nu_T\alpha} d\alpha}{\sum_{i=0}^{n_B-1}\int_0^{T_B+\tau_{\max}} \left|x_i(\alpha-\tau_T)\right|^2 d\alpha} = \frac{\sum_{i=0}^{n_B-1}\chi_i(0,-\nu_T)}{\sum_{i=0}^{n_B-1}\chi_i(0,0)} \approx \frac{\overline{\chi}_i(0,-\nu_T)}{E_i} \tag{3.27}$$

We can observe that the losses depend on the target Doppler frequency and the shape of the ambiguity function. This fact can be explained considering that the losses are related only the small Doppler approximation

In Figure 3.6, considering a DVB-T transmitted waveform, the losses are evaluated respect to the variation of the batch length and the target Doppler frequency.

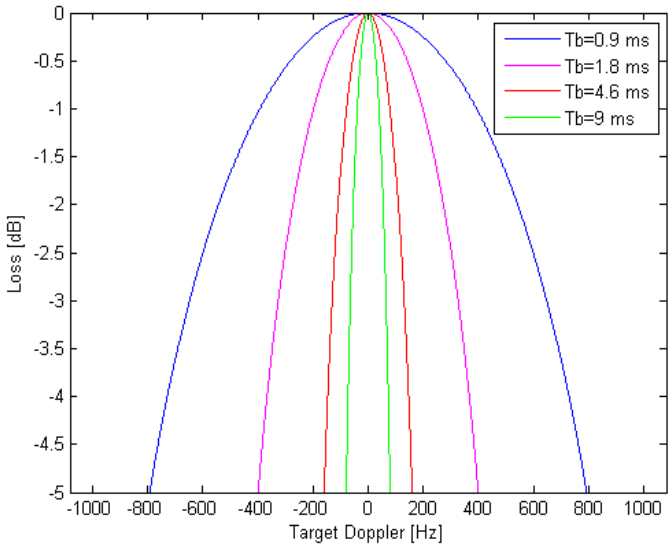

Figure 3.6 Batches algorithms losses

Greater the batches length and target Doppler, greater the losses of the batches algorithm. In order to reduce the losses due at eq.(3.22) we can impose

$$2\pi\nu_{\max}T_B \approx 0 \le \frac{\pi}{\gamma} \quad \text{then} \quad T_B < \frac{1}{2\nu_{\max}\gamma} \tag{3.28}$$

where γ is an integer greater than 10. Then equation .(3.28) guarantees that the exponential has a phase less than $\pi/10$.

The batch length T_B is also related to the maximum unambiguous Doppler frequency by the relation

$$T_B < \frac{1}{2\nu_{\max}} \tag{3.29}$$

Considering equations (3.28) and (3.29) we can impose the batch length as follows

$$T_B < \frac{1}{2\gamma\nu_{\max}} < \frac{1}{2\nu_{\max}} \tag{3.30}$$

An alternative implementation of the batches algorithm, proposed in [Langellotti 2009] and summarized in Figure 3.7, is based on the following steps:

- Multiply the reference signal $s_{ref}(t-\tau)$ and the surveillance signal $s_{surv}(t)$ obtaining the mixing product $x_m(t,\tau)$, as we have seen in the direct Fourier transform algorithm
- Selection n_B consecutive batches of the mixing product $x_m(t,\tau)$. The length of each block is T_B corresponding to N_B samples
- Sum the samples relative to each block in order to obtain n_B range profile.
- The Doppler dimension is then obtained by performing a FFT over the n_B range profiles.

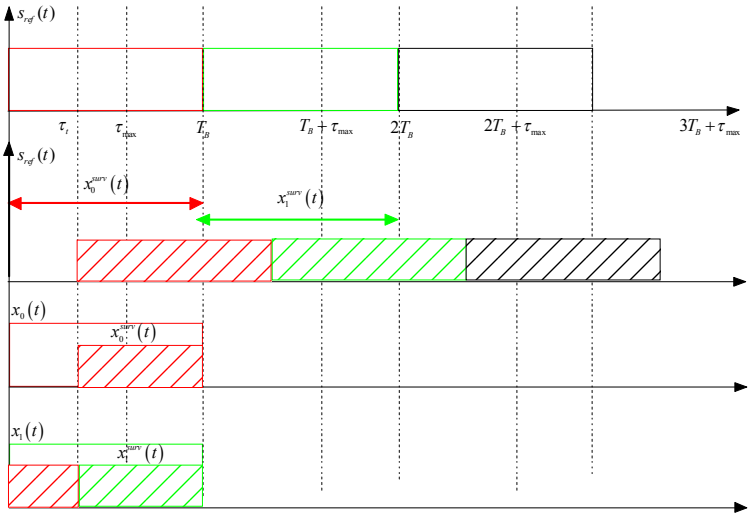

Figure 3.7 Traditional batches algorithm: reference and surveillance signal segmentation.

Comparing Figure 3.7 with Figure 3.4 we can conclude that the main difference of this traditional formulation is related to the segmentation of the surveillance signal. The losses related to this implementation depending both range and target Doppler. Considering only the range effect the SNR is reduced by a factor $\tau_{\max} / T_B$.

The computational loads of the two mentioned formulations are respectively

$$\begin{aligned} CL_1 &= N_B^{'} n_B N_{delay} + n_B \log_2(n_B) \\ CL_2 &= N N_{delay} + n_B \log_2(n_B) \end{aligned} \tag{3.31}$$

where the number of multiplications $n_B \log_2(n_B)$ is related to the last step for both algorithms. We can observe that the number of multiplications is greater, of about $CL1 - CL2 = \lfloor \tau_{\max} / f_s \rfloor N_{delay} n_B = N_{delay}^2 n_B$ multiplication, for the first algorithm.

The number of multiplications relative to the first algorithm can be reduced considering that the cross correlation can be implemented by using the FFT algorithm as follows

- Calculate the FFT of the reference signal block $x_i[n]$
- Calculate the FFT of the surveillance signal block $x_i^{surv}[n]$
- Multiply the signals obtained at the previous two steps
- Inverse the product signal in order to return in the time delay domain. The number of points in the IFFT is $N_B^{'}$

The computational load by using this implementation is given by

$$CL_1^{FFT} = \left[3N_B^{'} \log_2\left(N_B^{'}\right) + N_B^{'}\right] n_B + n_B \log_2(n_B) \tag{3.32}$$

In Figure 3.8 the computational load for the four defined algorithm has been shown respect to the number of range bin. We have supposed an integration time of 1 s, a maximum Doppler of 200 Hz and a sample frequency of 9 MHz. The batch length is calculated considering equation (3.28).

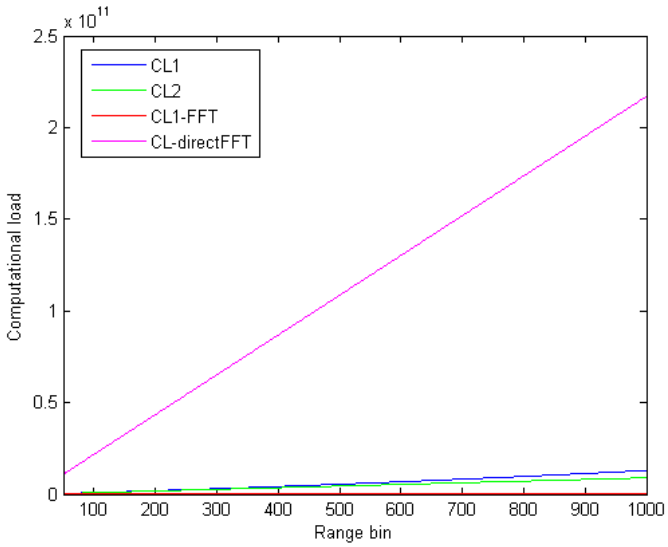

Figure 3.8 Batches algorithm: computational load

We can conclude that the proposed formulation of the batches algorithm is the best in term of computational load and SNR losses. In Figure 3.9 the time processing elapsed for batches algorithm and direct-FFT approach is shown.

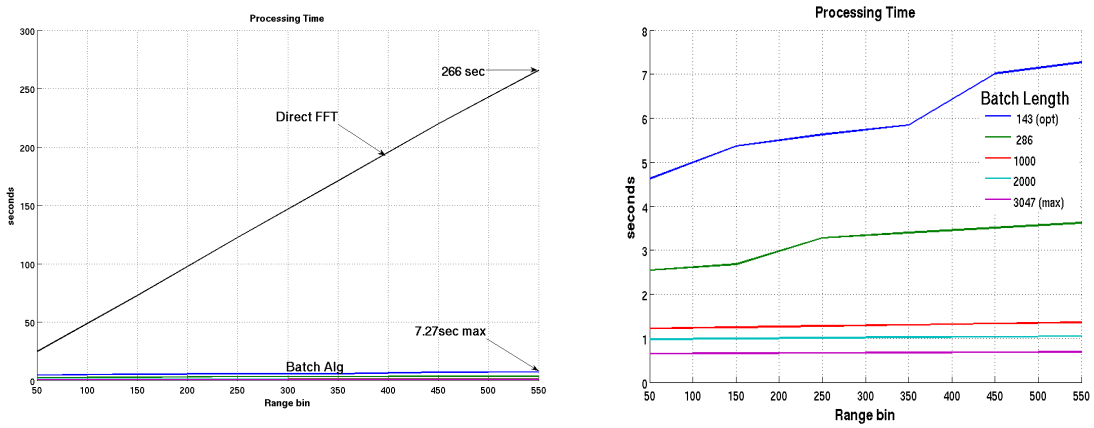

Figure 3.9 Time processing elapsed for batches algorithm and direct-FFT approach

We can conclude that the batch method is clearly faster than the direct-FFT method and the losses can be negligible with an opportune choice of the batch length.

3.4 Matched filter using OFDM waveforms

Earlier systems working with analog broadcast (TV/FM). With the advent of digital radio/television broadcasting (Digital Audio Broadcasting DAB, Digital Video Broadcasting DVB) a new generation of signal processing can be utilized to extract target information [Berger 2008-2010], [Bongioanni 2009], [Coleman 2008], [Gao 2006], [Glende 2007], [Kuschel 2008], [Langellotti 2010], [Poullin 2005-2010], [Saini 2005], [Tao 2010], [Yardley 2007]. We already mentioned the advantages of the digital signals in section 1.1. We are interested in investigating passive radar using orthogonal frequency division multiplexing (OFDM) modulated signals, as in the DAB or DVB-T scenario.

In [Berger 2008-2010] the exact matched filter formulation for OFDM waveforms has been derived. Thiswork is an extension of the signal processing, based on the application of FFT across block channel estimates, implemented in the CORA system.
In this section we introduce the matched filter formulation for OFDM waveforms and we reveal that this approach is equivalent to the batches algorithm based on the small Doppler approximation.

3.4.1 Principle of OFDM modulation

The purpose of this paragraph is just to briefly describe the principle of the OFDM modulation in order to derive the matched filter formulation using this type of modulation. For further details it is possible to analyze these], [Langellotti 2010], [Poullin 2005-2010], [ETSI 2009]. In a OFDM system of transmission the information is carried out by a large number of equally spaced carriers transmitted simultaneously.
By considering the complex elements $s_i[n]$ belonging to a finite alphabet and representing the transmitted digital data signal, the corresponding transmitted signal can be written

$$s(t) = \sum_{i=0}^{N_s-1} s_i(t - iT_U) \tag{3.33}$$

where $s_i(t)$ is the transmitted signal relative to the i-th symbol time defined as

$$s_{i,n}(t) = \sum_{n=-N/2}^{N/2-1} s_{i,n} e^{i2\pi \frac{n}{T_U} t} q(t) \tag{3.34}$$

and $q(t)$ is defined as

$$q(t) = \begin{cases} 1 & t \in [0, T_U] \\ 0 & otherwise \end{cases} \tag{3.35}$$

where T_U is the symbol duration.
It is easy to demonstrate that all these signals verify the orthogonality condition. The equidistant sub carriers, with a frequency step inversely proportional to the symbol duration T_U, constitute a “white” spectrum, as shown in Figure 3.10, obtained considering a OFDM DVB-T signal. In the case of DVB-T, there are two choices for

the number of carriers known as 2K-mode or 8K-mode. These are actually 1705 or 6817 carriers.

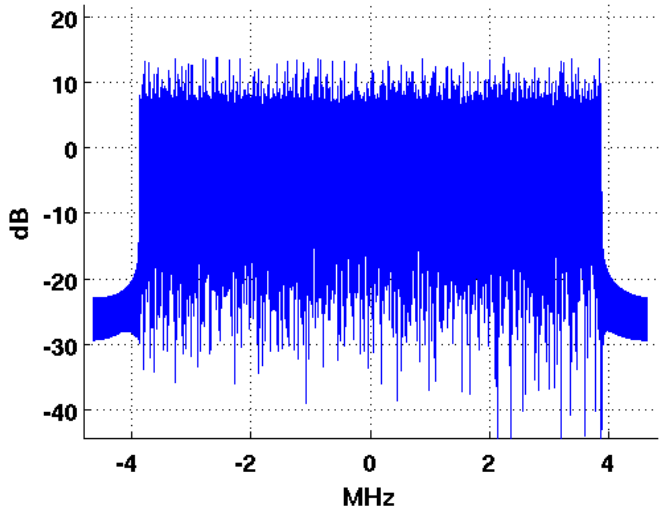

Figure 3.10 DVB-T spectrum

In an environment characterized by multipath, the orthogonality properties of the received signal are no satisfied. In order to avoid this limitation, a solution adopted, especially for DAB and DVB-T network, is that to transmit the elementary signal $s_{i,n}(t)$ over a duration T_S longer than T_U, as shown in Figure 3.11 The time difference $T_G = T_S - T_U$ between these durations is called guard interval. The guard interval length must to be longer than the propagation channel length in order to avoid signal analysis over transitory time duration and inter-symbolic interference. Under this assumption the transmitted signal could be written

$$s(t) = \sum_{i=0}^{N_s-1} \sum_{n=-N/2}^{N/2-1} s_{i,n} e^{i2\pi \frac{n}{T}(t-iT_S)} q'(t-iT_S) \tag{3.36}$$

where $q'(t)$ is defined as

$$q'(t) = \begin{cases} 1 & t \in [0, T_U + T_G] \\ 0 & otherwise \end{cases} \tag{3.37}$$

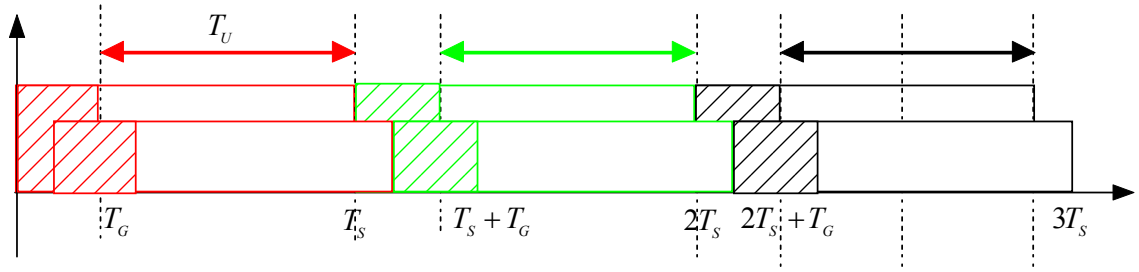

Figure 3.11 Guard interval concept

Using the orthogonality condition a simple decoding rule at the receiver is given by

$$\hat{s}_{i,n} = \int_{T_G}^{T_G+T_U} x(t+iT_s)e^{-j2\pi\frac{n}{T_U}t}\,dt \tag{3.38}$$

where $x(t)$ is the received signal in an multipath environment.

From a practical point of view this processing could be easily achieved using the FFT algorithm. Using a classical multipath radio channel model, as defined in section 2.3.3, the received signal can be written as

$$x(t)=\sum_{p=1}^{N_c} s\left(t-\tau_p\right) \tag{3.39}$$

and equation (3.38) becomes

$$\hat{s}_{i,n} = \int_{T_G}^{T_G+T_U}\left[\sum_{p=1}^{N_c}\sum_{n=-N/2}^{N/2-1} s_{i,n}e^{i2\pi\frac{n}{T_U}(t-\tau_p)}\right]e^{-j2\pi\frac{n}{T_U}t}\,dt \tag{3.40}$$

Considering the parts of signal used for decoding, the estimated symbols can be written as

$$\hat{s}_{i,n} = \sum_{p=1}^{N_c}\sum_{m=-N/2}^{N/2-1} s_{i,m}e^{i2\pi\frac{m}{T_U}\tau_p}\int_{T_G}^{T_G+T_U} e^{-j2\pi\frac{n-m}{T_U}t}\,dt = s_{i,n}\sum_{p=1}^{N_c} e^{i2\pi\frac{n}{T_U}\tau_p} = s_{i,n}H_{i,n} \tag{3.41}$$

where $H_{i,n}$ is the propagation channel response defined as

$$H_{i,n} \triangleq \sum_{p=1}^{N_c} e^{i2\pi\frac{n}{T_U}\tau_p} \tag{3.42}$$

Using the guard interval concept, the propagation channel response could be modeled with a complex coefficient for each transmitted frequency and symbol.

In order to estimate the transmitted symbols is necessary the estimation of the channel response.

3.4.2 Matched filter receiver

In this section we derive the matched filter formulation for OFDM waveforms.
Using equation (3.8), the output of the matched filter can be written as

$$M(\tau,\nu)=\int_0^{T_i} x_{surv}(t)x_{ref}^*(t-\tau)e^{-j2\pi\nu t}dt \quad 0\le\tau\le\tau_{\max} \quad -\nu_{\max}\le\nu\le\nu_{\max} \tag{3.43}$$

where $x_{ref}(t)=s(t)$ is the OFDM transmitted signal defined in equation (3.36), $x_{surv}(t)$ is the received signal, $T_i=N_ST_S+T_G$ is supposed a multiple of T_S.

As the reference signal $x_{ref}(t)$ is divided in block of length T_s, assuming that the largest possible delay $\tau_{\max}$ is smaller than the guard interval T_G, equation (3.43) can be rewritten as

$$M(\tau,\nu)=\sum_{i=0}^{N_S-1}\int_{iT_s}^{iT_s+T_G} x_{surv}(t)x_i^*(t-\tau-iT_S)e^{-j2\pi\nu t}dt \tag{3.44}$$

This formulation is equivalent to the batches algorithm processing described in the previous section, considering $T_B=T_S$ and $\tau_{\max}\le T_G$

At this point the properties of the OFDM modulation are taken into account, therefore the integration time in equation (3.44) is limited to T_U in relation to the decoding rule expressed in equation (3.38)

$$M(\tau,\nu)=\sum_{i=0}^{N_S-1}\int_{iT_s+T_G}^{iT_s+T_G+T_U} x_{surv}(t)x_i^*(t-\tau-iT_S)e^{-j2\pi\nu t}dt \tag{3.45}$$

With a variable change $\alpha=t-iT_S$, equation (3.45) becomes

$$M(\tau,\nu)=\sum_{i=0}^{N_S-1}e^{-j2\pi\nu iT_S}\int_{T_G}^{T_G+T_U} x_{surv}(\alpha+iT_S)x_i^*(\alpha-\tau)e^{-j2\pi\nu\alpha}d\alpha \tag{3.46}$$

We point out that by limiting the integration time in (3.44) to the interval $\left[iT_S + T_G, iT_S + T_G + T_U\right]$, as shown in Figure 3.12,the processing can be simplified but the SNR is reduced by a factor T_U / T_S. For instance considering a DVB-T signal with $T_G = T_U / 4$ we have about -2dB in SNR.

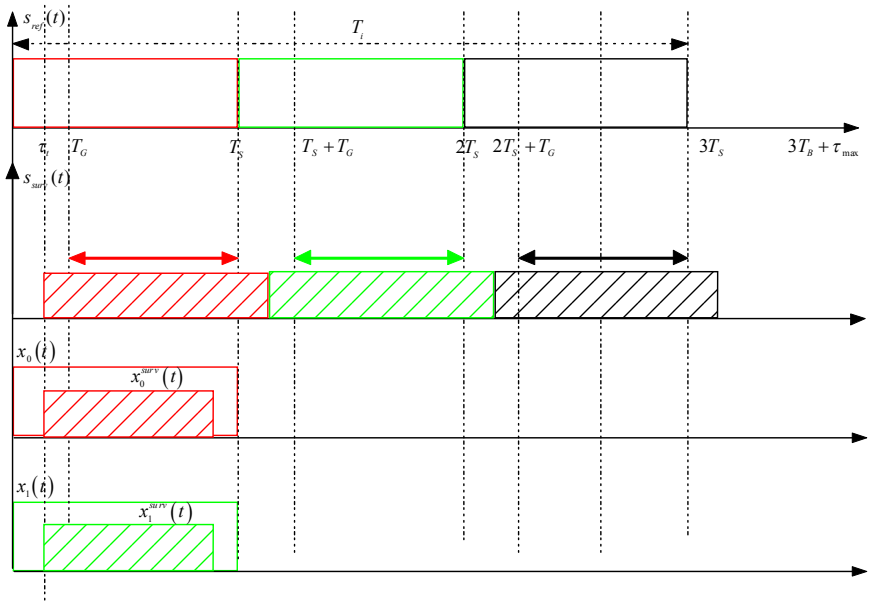

Figure 3.12 OFDM matched filter: reference and surveillance signals segmentation

Under the hypothesis of the small Doppler approximation, defined in equation (3.18), equation (3.46) can be simplified as

$$M(\tau,\nu) = \sum_{i=0}^{N_S-1} e^{-j2\pi\nu i T_S} \int_{T_G}^{T_G+T_U} x_{surv}(\alpha + iT_S) x_i^*(\alpha - \tau) d\alpha \qquad (3.47)$$

Far now we have the same expression of the batches algorithm considering different integration intervals. This formulation is very similar to the batches algorithm approach proposed in [Langellotti 2009] and described in the previous section.

Inserting the expression of the OFDM transmitted signal $x_{ref}(t) = s(t)$, defined in equation (3.36), into equation (3.47) we obtain

$$M(\tau,\nu) = \sum_{i=0}^{N_S-1} e^{-j2\pi\nu i T_S} \sum_{n=-N/2}^{N/2-1} e^{i2\pi\frac{n}{T_U}\tau} s_{i,n}^* \int_{T_G}^{T_G+T_U} x_{surv}(t + iT_S) e^{-i2\pi\frac{n}{T_U}t} dt \qquad (3.48)$$

Defining the channel estimate $\hat{H}_{i,n}$ relative to the n-th frequency in the i-th transmitted symbol as

$$\hat{H}_{i,n} \triangleq s_{i,n}^{*} \int_{T_G}^{T_G+T_U} x_{surv}(t+iT_S) e^{-i2\pi\frac{n}{T_U}t} \tag{3.49}$$

the processing can be seen as a 2-D discrete Fourier transform, that can be efficiently implemented as an 2D-FFT, of the OFDM channel estimates as follows

$$M(\tau,\nu) = \sum_{i=0}^{N_S-1} \sum_{n=-N/2}^{N/2-1} e^{i2\pi\frac{n}{T}\tau} e^{-j2\pi\nu iT_S} \hat{H}_{i,n} \tag{3.50}$$

We can write the numerical version of equation (3.50) as

$$M[m,p] = \sum_{i=0}^{N_S-1} \sum_{n=-N/2}^{N/2-1} e^{-j2\pi\frac{mi}{N_S}} e^{i2\pi\frac{np}{N}\tau} \hat{H}_{i,n} \quad 0 \le m \le N_{Doppler}-1;\ 0 \le p \le N_{Delay}-1 \tag{3.51}$$

where

N_S is the total number of symbols

N is the number of OFDM carriers

$\hat{H}_{i,n}$ is the channel estimate relative to the symbol ith and the carrier n-th

p represents the time delay bin ($\tau_p = p\frac{T_U}{N}$),

m is the Doppler bin corresponding to $\nu_m = m\frac{1}{N_S T_S}$

N_{delay} is the number of time bins corresponding to $\lfloor \tau_{\max} / \tau_p \rfloor$,

$N_{Doppler}$ is the number of frequency Doppler bins corresponding to $\lfloor 2\nu_{\max} N T_S \rfloor$.

The main steps of this algorithm, schematically shown in Figure 3.13 can be summarized as:

- the digital broadcast signal, received at the reference channel, is decoded and perfectly reconstructed. In other words the transmitted symbols are supposed known.
- the surveillance signal is divided into segments of length equal to useful time duration and the channel estimate $\hat{H}_{i,n}$ is obtained

- the inverse FFT across N carries is calculated and the range profiles are obtained
- the Doppler dimension is then obtained by performing N_S FFT over the range profiles.

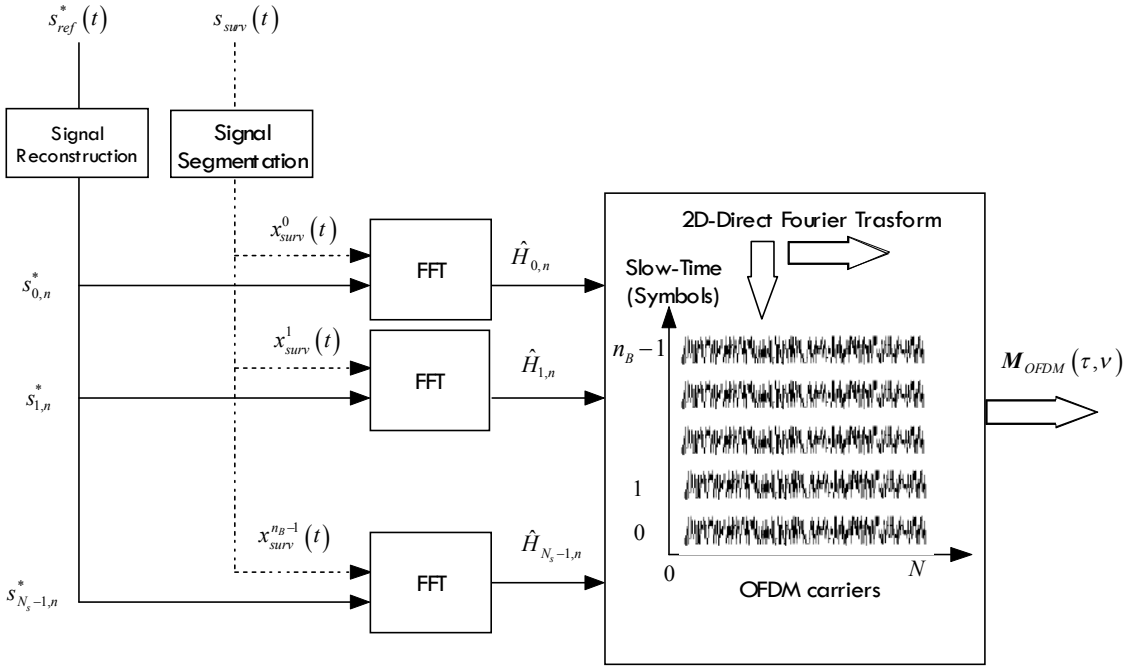

Figure 3.13 OFDM matched filter architecture

The main advantage, in term of computational load, of the OFDM matched filter is given by the possibility to calculate the output of the matched filter evaluating efficiently a 2D FFT.

The main drawbacks of this formulation can be summarized as:

1. necessity to estimate the transmitted symbols. This fact could not be a problem considering that a typical PBR signal processing chain requires the pre-processing block and the reconstruction of the transmitted signal as we have seen in chapter 2.
2. The maximum possible target delay has been assumed smaller than the guard interval. This assumption could represent a strong limit on the system performance.

3. The range bin of interest are strictly related to the FFT evaluated along the carrier frequency. For instance, only a very small portion of the output could be required in the final 2D map while most of the obtained samples are discarded.
4. The SNR losses depend on both range and Doppler considering that they are caused by both integration losses and small Doppler approximation.

At the end of this section we want to underline the analogies of the processing with the classical stepped frequency approach used in active radar system.

In active pulse radar system, for detecting targets in the strong background clutters, separation of the target requires high range and cross-range resolution in the system. Typically the high range resolution is obtained by utilizing shorter pulses and wideband-FM pulses, therefore, an expensive wideband receiver should be implemented. The alternative system to achieving high range resolution without using wideband receiver is the stepped frequency (SF) radar scheme performed synthetic range profile (SRP) processing. The principle of this radar is that the echoes of stepped frequency pulses are synthesized in the frequency domain to give the shorter pulses in the time domain thorough the IDFT. If we divide the 2D DFT processor, shown in Figure 3.13 and defined in equation (3.50), in two steps as schematically represented in Figure 3.14, the output of the matched filter is given by

$$M(\tau,\nu)=\sum_{i=0}^{N_S-1} e^{-j2\pi\nu iT_S} x_i(\tau) \tag{3.52}$$

where the range profiles for each transmitted symbol is obtained as

$$x_i(\tau)=\sum_{n=-N/2}^{N/2-1} e^{i2\pi\frac{n}{T}\tau}\hat{H}_{i,n} \tag{3.53}$$

We can observe that the output at the first DFT block, as shown in equation (3.53), is obtained in the same domain, slow time-range, of the stepped frequency approach.

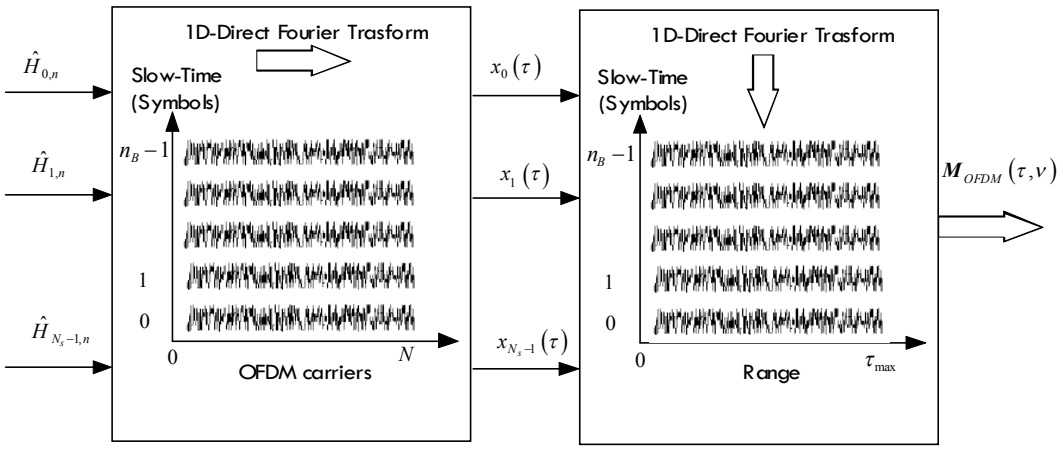

Figure 3.14 Modified OFDM matched filter architecture

3.5 Chapter summary

In this chapter a comparative study between optimum and sub optimum methods has been presented to evaluate the 2D-CCF for a passive bistatic radar. A new detailed formulation of the sub optimum batches algorithm has been proposed. The defined batches algorithm has been shown to yield comparable performance with respect to the optimum ones while strongly reducing the computational load. This solution can be regarded as an effective solution for real time PBR systems. We have demonstrated that the obtained algorithm allows us to process the received signal in a form similar to that of an active pulse radar. The exact matched filter formulation for OFDM waveforms has been derived. It has been shown that this approach is similar to the batches algorithm. Specifically they are based on the same small Doppler approximation but the OFDM formulation presents several drawbacks. Future studies will be done in order to resolve these problems and take advantages related to an implementation by using a 2D FFT. Also in this case we have underlined the analogies with the classical stepped frequency approach used in active pulse radar. This analysis constitutes the basis for the development and adaptation of the classical adaptive signal processing techniques, developed for active pulse radars, to a passive radar scenario.

Chapter 4.

Temporal adaptive processing

4.1 Introduction

The cancellation of the interference signal is a crucial issue for target detection in a passive bistatic scenario. Different techniques, both in spatial and temporal domain, have been proposed to resolve this problem. This section deals with the suppression of the direct signal and clutter echoes in a single receiver passive scenario, as described in section 2.3. Specifically in this chapter we investigate the spectral-temporal cancellation techniques. A variety of temporal adaptive processing have been developed for the removal of the interference component in the surveillance channel before the matched filter. Typically these techniques are based on the adaptive noise canceller structure. Another proposed technique, characterized by low popularity in the PBR radar community is the so called adaptive matched filter. This approach is derived as an extension of the direct FFT matched filter formulation analyzed in the previous chapter. The main advantage of the adaptive matched filter solution is the possibility to suppress strictly static clutter but affected by ICM. A new formulation of the adaptive matched filter is presented in this section. Specifically we define an adaptive matched filter based on the batches algorithm analyzed in the previous chapter.

The chapter is organized as follows. Section 4.2 introduces a literature review of the temporal adaptive techniques typically applied in a PBR scenario. Section 4.3 briefly introduces how the temporal adaptive algorithms can be embedded in a PBR signal processing chain. Specifically an advanced architecture based on the adaptive matched filter concept is defined. In section 4.4 we analyze the possibility to extend the classical temporal adaptive processing techniques, well known in literature and typically

developed in pulse-radar systems, to a passive radar scenario. In section 5.4 the results obtained with both simulated and real data are presented.

4.2 Temporal adaptive processing in a passive radar scenario

4.2.1 Motivations

Due to the characteristics of the transmitted waveform which is not under control of the radar designer, the ambiguity function could have a sidelobe level not much lower than its peak. It is therefore likely that potentially target echoes are masked essentially by the direct signal received by the sidelobe of the receiver antenna and by strong clutter echoes, as shown in section 2.3.. Thus the cancellation of the interference signal becomes a crucial issue for target detection. In section 2.4.3 we have already underlined the necessity to apply a interference suppression algorithm before the matched filter processor.

4.2.2 Literature review

A variety of temporal adaptive processing have been developed for the removal of DSI and multipath in the surveillance channel prior the matched filter. The main published works related to this argument can be substantially divided into two main categories:

1) Some classical well known adaptive algorithms used in different fields for many years have been applied to a PBR scenario. All these techniques are based on the adaptive noise canceller structure [Cherniakov 2008], [Howland 2005]. The goal of the noise canceller is that to estimate the unwanted interference signal from the reference channel and subtract it from the surveillance channel leaving only a true estimate of the desired signal. A careful review and comparison of the mentioned algorithms, specifically LMS, NLMS, RLS can be found in [Cardinali 2007], [Colone 2006], [Colone 2009], [Malanowski 2006]. In [Colone 2006], [Colone 2009] an effective cancellation filter for passive radar has been obtained by resorting to the Least Square (LS) approach. These mentioned filters act like a stop-band filter around zero Doppler assuming that the clutter echoes are potentially backscattered from the

first M range bins, where M is a filter parameter relate to the dimension of the filter and therefore to the computational load. In order to suppress strictly static clutter affected by ICM the LS algorithm has been extended to the so called Extensive Cancellation Algorithm (ECA) [Colone 2006], [Colone 2009]. However this approach is computationally intensive, since it corresponds to increasing the dimension of the weight vector whose evaluation requires the computation and the inversion an higher dimension matrix. Aiming at reducing the computational load of the ECA algorithm in [Colone 2009] a Sequential Cancellation Algorithm (SCA) has been proposed. In [Colone 2009] it has been demonstrated that the ECA and SCA techniques present better disturbance cancellation performance with respect to the transversal adaptive filter. Obviously the LS algorithm or ECA algorithm does not require a variable to control the rate of adaptation and this should help the algorithm to be more robust when used in different signal environments.

2) Another proposed technique, characterized by low popularity in the PBR radar community, is the adaptive matched filter [Kubica 2006]. Only few papers dealing with this alternative approach that are able to cope with clutter echoes with non zero-Doppler components. In [Kubica 2006]. an extension of the classical adaptive matched filter to noise-like signal has been proposed. The adapted matched filter can be used to suppress strictly static clutter but affected by ICM.

4.3 System architectures

This section briefly introduces how the mentioned adaptive algorithms can be embedded in a typical PBR signal processing architecture, shown in Figure 2.5 . Specifically section 4.3.1 deals with the classical PBR noise canceller structure, while section 4.3.2 introduces the adaptive matched filter architecture.

4.3.1 Traditional architecture

The traditional structure with an adaptive temporal filter, based on the noise canceller structure, for the removal of DSI and multipath in the surveillance channel prior the matched filter is shown in Figure 4.1. The adaptive algorithms based on the noise

canceller principle are well known and their exact description can be found in many papers and books, as seen in the previous section. In this section we presents the main aspects of this class of adaptive filters.

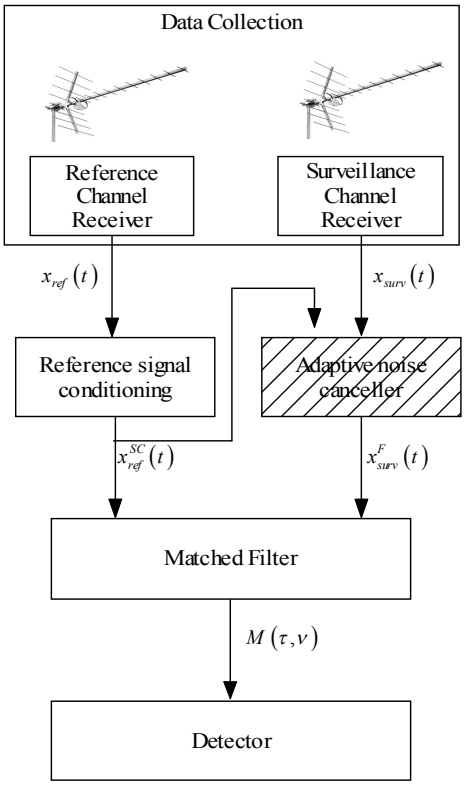

Figure 4.1 Temporal adaptive processing: traditional architecture

An adaptive noise canceller scheme is shown in Figure 4.2 [Cherniakov 2008], [Howland 2005]. The goal of the canceller is to detect the desired signal $d(n)$ received in the surveillance channel:

$$x(n) = d(n) + w_1(n) \tag{4.1}$$

where $w_1(n)$ is the unwanted interference. The signal from the reference antenna $w_2(n)$ is used to estimate the interference $w_1(n)$. The task of the adaptive filter is to estimate $\hat{w}_1(n)$ from $w_2(n)$. Then, this estimate is subtracted from the signal in the surveillance channel leaving only an estimate of the true echo signal:

$$e(n) = x(n) - \hat{w}_1(n) \tag{4.2}$$

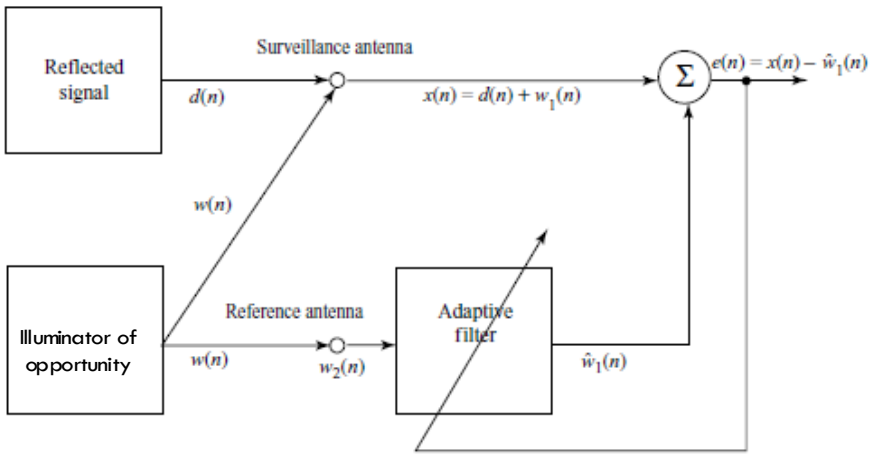

Figure 4.2 Adaptive noise canceller structure

The simplest of the adaptive filtering algorithms is the LMS algorithm which uses a transversal filter to produce the output of the filter and to update simultaneously the adaptive tap weights. The goal of the LMS algorithm is to minimize the least mean square of the output filter $e(n)$. The characteristic parameters of the algorithm are the step-size, which determines the rate of convergence, and the weight vector dimension M. This last parameter is selected by assuming that the clutter echoes are backscattered from the first M range bins.

It is characterized by simplicity and low computational complexity, but also by slow convergence. One of the typical modifications, in the normalization of the step size, of the LMS algorithm is the Normalized LMS. Another popular adaptive algorithm is the Recursive Least Square which is a recursive version of the Least Square algorithm. As for the LMS and NLMS algorithms, the length of the transversal filter is selected by assuming that the clutter echoes are backscattered from the first M range bins. The computational load of the RLS algorithm is higher than the LMS and NLMS algorithms but it has better convergence rate.

Another popular adaptive algorithm is Least Square Lattice (LSL). This filter is less popular and has many different variants [Cherniakov 2008], [Malanowski 2006].

We can conclude that the mentioned filters act like a stop-band filter around zero Doppler in the first M range bins.

An effective cancellation filter for passive radar can be achieved by resorting to the LS approach. The input data stream is arranged in block of equal length, and the filtering of input data proceeds on a block by block basis. The filter is adapted to non-stationary data by repeating the computation on a block by block basis, which makes it computationally demanding.

To derive the basic block LS algorithm, we consider the transversal filter structure. The goal of LS method is to find the tap weights vector in order to minimize the sum of error squares

$$\min_{\mathbf{w}} \mathrm{E}(\mathbf{w}) = \min_{\mathbf{w}} \sum_{i=0}^{N-1} \left| e(i) \right|^2 \tag{4.3}$$

where $\mathbf{w}$ is the tap weights vector and $e(i)$ is defined as follows

$$e(i) = x_{surv}(i) - \sum_{k=0}^{M-1} w_k^* x_{ref}(i-k) \tag{4.4}$$

The action of LS filter is like a notch filter in zero Doppler. We may want to delete also clutter components near the Zero-Doppler and it is possible to achieve by including Doppler shifted replicas of the reference signal. In this case the algorithm is named ECA (Extensive Cancellation Algorithm) [Colone 2006], [Colone 2009]. However this approach is computationally intensive, since it corresponds to increasing the dimension of the weight vector whose evaluation requires the computation and the inversion of the matrix with dimensions MxM which corresponds to $O[NM^2+M^2 \log M]$ complex products.

Obviously respect to the adaptive algorithm the LS algorithm or ECA algorithm does not require a variable to control the rate of adaptation. This should help the algorithm to be more robust when used in different signal environments.

4.3.2Adaptive matched filter architecture

The advanced architecture based on the adaptive matched filter is shown in Figure 4.3.

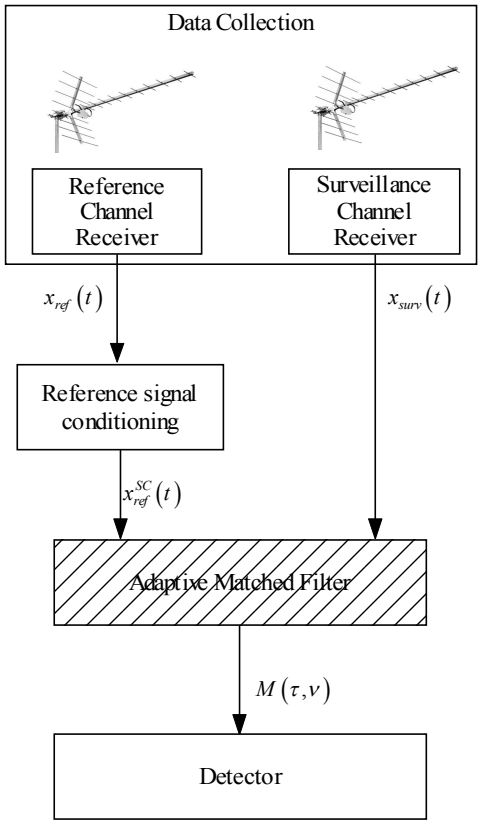

Figure 4.3 Temporal adaptive processing: adaptive matched filter

The adaptive matched filter block is an opportune modified version of the matched filter presented in the typical PBR signal processing architecture shown in Figure 2.5. The detailed description of this block will be presented in the next section. The main difference of this solution is the application of the interference suppression filter within the matched filter block and not before it.

It is important to note that the adaptive matched filter algorithm can be seen both as an alternative or as an extension of the adaptive noise canceller architecture, as shown in Figure 4.4. In this architecture the adaptive noise canceller could be uses to remove principally the direct signal and the adaptive matched filter could be used to improve the cancellation of the clutter affected by ICM.

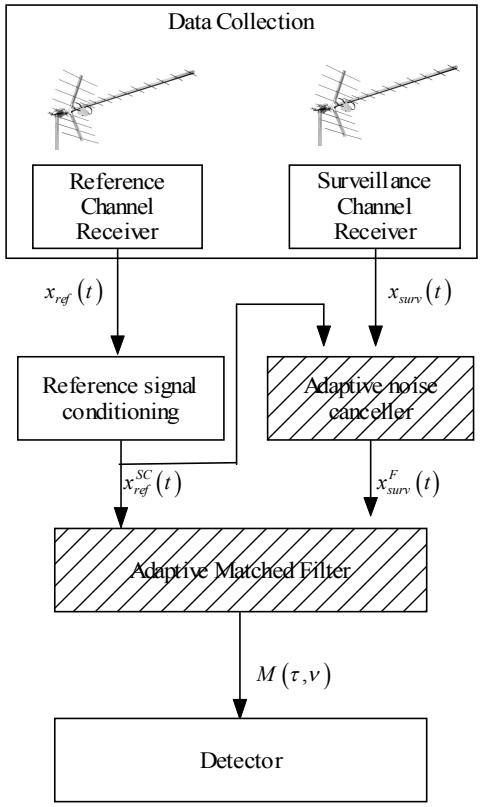

Figure 4.4 Temporal adaptive processing: adaptive matched filter plus adaptive noise canceller

4.4 Adaptive matched filter

In this section we define the adaptive matched filter architecture in a passive radar contest. In modern Doppler radar systems a key physical observable for separating moving targets from interference is the Doppler frequency. Doppler filtering techniques are well known in the field of active pulse radar as we have seen in section 1.2.3.

The classical processing consists in a uniform tapped delay-line liner combiner or FIR filter. For a pulse Doppler radar the delay is chosen to match the PRI. The goal of an adaptive Doppler filter is that to select the complex weighting factor in order to obtain an optimized Doppler filter response. The signal received from a passive radar is not in the slow time-range domain, therefore the classical temporal adaptive techniques, developed in the case of active radar, has to be extended to the passive radar scenario. Target detection, in a passive radar scenario, is typically performed by calculating the correlation between the reference signal and the received echo signal as shown in

chapter 3. Exploiting the main approaches to calculate the cross correlation function at the output of the matched filter we extend the defined matched filter processor to an adaptive matched filter architecture. We recall that the cross correlation algorithm can be implemented by using these main approaches:

- direct FFT: these algorithm evaluates the cross correlation by using the Fourier Transform of the so called mixing product, defined as the product between the received signal and a delayed version of the reference signal. The extension of the matched filter in this case has already analyzed in [Kubica 2006].
- batches algorithm: this algorithm calculates the Fourier Transform along each range bin snapshot obtained by calculating the cross correlation between reference signal and target signal batches. We have analyzed also the OFDM matched filter formulation in the case of OFDM modulations as in the case of DVB-T or DAB illuminators of opportunity.

In the next sub-sections temporal adaptive matched filter techniques will be defined in relation to each cross correlation algorithms.

4.4.1 Adaptive matched filter with direct FFT-approach

The direct FFF- approach has been described in section 3.2.1. In order to make the discussion more comprehensive we report below the expression of the direct FFT approach

$$M_{DFFT}(\tau,\nu) = DFT\left\{x_m(t,\tau)\right\} = \sum_{i=0}^{n_B-1} e^{-j2\pi\nu i T_C} x_m(iT_C,\tau) \tag{4.5}$$

where $x_m(t,\tau)$ is the mixing product defined as

$$x_m(t,\tau) = s_{surv}(t)s_{ref}{}^{*}(t-\tau) \tag{4.6}$$

and T_C is the sampling time.

The sampling time snapshot for the range cell τ can be written as

$$\boldsymbol{x}_m(\tau)=\begin{bmatrix} x_m(0,\tau) \\ \vdots \\ x_m\left((N-1)T_C,\tau\right) \end{bmatrix} \tag{4.7}$$

where N is the total number of samples.

Equation (4.5) can be written as

$$M_{DFFT}(\tau,\nu)=\boldsymbol{w}_{DFFT}^{H}(\nu)\,\boldsymbol{x}_m(\tau) \tag{4.8}$$

where the weighting filter $\boldsymbol{w}_{DFFT}$ is defined as

$$\boldsymbol{w}_{DFFT}(\nu)=\begin{bmatrix} 1 \\ \vdots \\ e^{j2\pi\nu(N-1)T_C} \end{bmatrix}=\boldsymbol{v}_{DFFT}(\nu) \tag{4.9}$$

where $\boldsymbol{v}_{DFFT}(\nu)$ is the temporal steering vector define in accordance with the sampling time T_C.. The filter defined in equation (4.9) is the temporal matched filter evaluated at the frequency of interest ν. The theory developed in chapter 1 can be applied in this case defining the vector $\boldsymbol{s}_0$, shown in equation (1.13), equal to the temporal steering vector $\boldsymbol{v}_{DFFT}(\nu)$. The natural extension of the matched filter formulation is the adaptive matched filter [Kubica 2006], as we have seen in chapter 1. Then the adaptive matched filter can be defined as

$$\boldsymbol{w}_{DFFT}(\nu)=\gamma\hat{\boldsymbol{R}}_i^{-1}\boldsymbol{v}_{DFFT}(\nu) \tag{4.10}$$

where $\hat{\boldsymbol{R}}_i \in \mathbb{C}^{NxN}$ is the estimated interference covariance matrix by using the SCM algorithm. The training data set $\Omega_{training}^{NxN_t}$ can be selected in the time delay domain before cross correlation, as shown in Figure 4.5.

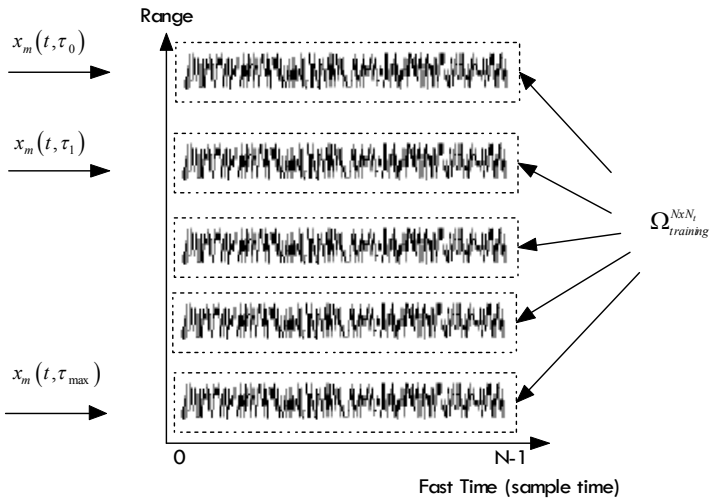

Figure 4.5 Training data set selection with direct FFT approach.

To obtain a useful estimate, the training data set has to be homogeneous over a number of training data relatively large compared to the value of N, following the well known Reed-Mallet-Brennan rule. Since the high dimension of the data sample N it is difficult to select a an homogeneous training data set. Another element that affects the interference correlation matrix estimation process is the presence of the useful signal all the time. In [Kubica 2006], the diagonal loading and the principal component methods are considered in order to attenuate these issues. The main problem related to this approach remains the high computational load as shown in section 3.2.1. The computation load is very high also in the case of the simple matched filter implementation, using an adaptive matched filter formulation the required computational load is increased in relation to the calculation and inversion of the covariance matrix. We want to underline that the dimension of the correlation matrix could be very large. For instance if we consider a typically integration time of 0.5 s and a sample frequency of 9 MHZ in a DVB-T passive radar scenario, the covariance matrix dimension could be 4 *10^6.

4.4.2 Adaptive matched filter with batches algorithm

The batches algorithm has been described in section 3.2.1. In order to make the discussion more comprehensive we report below the expression of the batches algorithm, defined in equations (3.19)

$$M_b(\tau,\nu) = \sum_{i=0}^{n_B-1} e^{-j2\pi\nu i T_B} x_{cc}^i(\tau) \tag{4.11}$$

Where

$$x_{cc}^i(\tau) = \int_0^{T_B+\tau_{\max}} x_i^{surv}(t) x_i^*(t-\tau)dt \tag{4.12}$$

We have demonstrated in chapter 3 that the signal $x_{cc}^i(\tau)$, before the Discrete Fourier transform, is equivalent to the classical range-slow time signal in an active pulse radar. The slow-time snapshot for the range cell τ can be written as

$$\boldsymbol{x}_{cc}(\tau) = \begin{bmatrix} x_{cc}^0(\tau) \\ \vdots \\ x_{cc}^{n_B-1}(\tau) \end{bmatrix} \tag{4.13}$$

and equation (4.11) can be written as

$$M_b(\tau,\nu) = \boldsymbol{w}_b^H(\nu)\boldsymbol{x}_{cc}(\tau) \qquad 0 \le \tau \le \tau_{\max} \tag{4.14}$$

where the weighting filter $\boldsymbol{v}_b^H(\nu)$ is defined as

$$\boldsymbol{w}_b^H(\nu) = \begin{bmatrix} 1 \\ \vdots \\ e^{j2\pi\nu(n_B-1)T_B} \end{bmatrix} = \boldsymbol{v}_b^H(\nu) \tag{4.15}$$

where $\boldsymbol{v}_b^H(\nu)$ is the temporal steering vector define in accordance with the batch duration T_B. The filter defined in equation (4.15) is the temporal matched filter evaluated at the frequency of interest ν. The theory developed in chapter 1 can be applied in this case defining the vector $\boldsymbol{s}_0$, shown in equation (1.13), equal to the temporal steering vector $\boldsymbol{v}_b(\nu)$. The natural extension of the matched filter is the adaptive matched filter, as we have seen in the previous section, which can be defined as

$$\boldsymbol{w}_b(\nu) = \gamma \hat{\boldsymbol{R}}_i^{-1} \boldsymbol{v}_b^H(\nu) \tag{4.16}$$

where $\hat{\boldsymbol{R}}_i \in \mathbb{C}^{n_B x n_B}$ is the estimated interference covariance matrix by using the SCM algorithm. . The training data set $\Omega_{training}^{n_B x N_t}$ can be selected in the range domain, as shown in Figure 4.6. A reasonable approach is to use surrounding range bins of the cell under test, that are likely to contain similar interference, without the cell under test and some guard cells to prevent so-called self nulling.

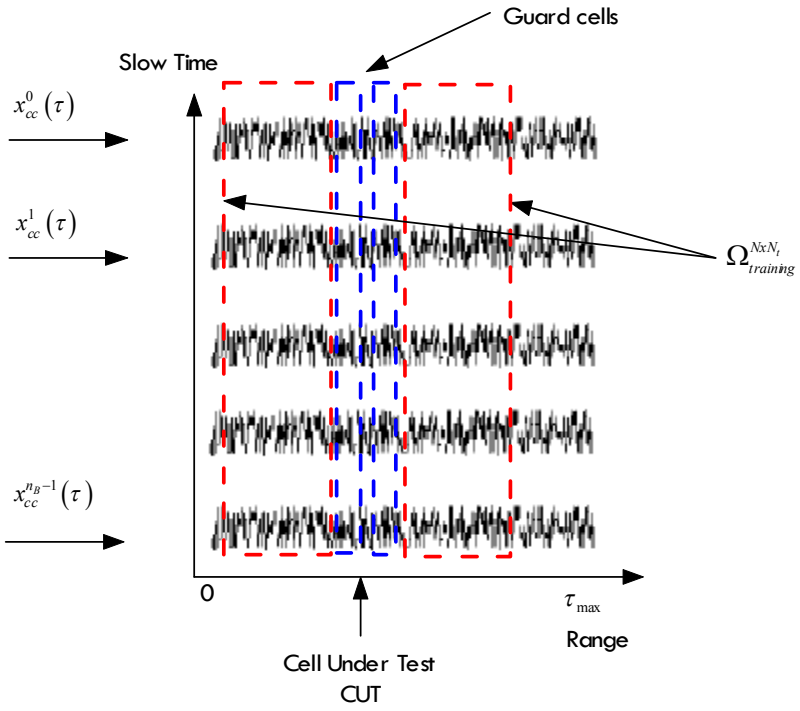

Figure 4.6 Training data set selection with batches algorithm approach.

We can observe that the training data selection is the same to the case of a pulse radar. The main advantages respect to the adaptive matched direct FFT filter are:

- the dimension of the slow-time snapshot for the range cell τ is n_B. This value is smaller than the number of samples N. Therefore the dimension of the correlation matrix is n_B and the associated computational load is reduced. In section 3.3.1 we have already shown the reduced computational load in the case of the matched filter implementation.

- to obtain a useful estimate, the training data set has to be homogeneous over a number of training data relatively large compared to the value of n_B. The ability of an adaptive filter to achieve a desired sidelobe level depends on the availability of sufficient sample support. For many practical applications, owing to either the non stationarity of the interference or operational considerations, a limited number of samples are available. A means of reducing the problems related to a limited sample support is to add a weighted identity matrix to the estimated correlation matrix. This technique is known as diagonal loading in literature. The minimum loading level should be at least equal to the noise power in order to achieve substantial improvements.
- after the range matched filter it is possible to separate the target component from interference component in order to avoid the presence of the useful signal in the training data set.

The mentioned advantages can be obtained considering that we have some losses related to the small Doppler approximation. These losses as we have demonstrated in section 3.3.1 can be reduced taking a smaller length batch. Smaller the dimension of the batch, greater the number of batches n_B and the dimension of the correlation matrix.

The final choice of the batch length will be a compromise between the losses and the opportune dimension of the correlation matrix in order to obtain good performances of the adaptive matched filter.

For instance if we consider a typically integration time of 0.5 s and a maximum Doppler frequency of 600 Hz, by using equation (3.28), the covariance matrix dimension could be 8*10^3.

4.4.3 Adaptive matched filter with OFDM waveforms

The matched filter with OFDM waveforms has been described in section 3.4. In order to make the discussion more comprehensive we report below the expression of the OFDM matched filter, defined in equations

$$M_{OFDM}(\tau,\nu)=\sum_{i=0}^{N_S-1}\sum_{n=-N/2}^{N/2-1}e^{i2\pi\frac{n}{T}\tau}e^{-j2\pi\nu iT_S}\hat{H}_{i,n} \tag{4.17}$$

where

$$\hat{H}_{i,n}\triangleq s_{i,n}^{*}\int_{T_G}^{T_G+T_U}x_{surv}(t+iT_S)e^{-i2\pi\frac{n}{T_U}t} \tag{4.18}$$

We have demonstrated in chapter 3 that the signal $x_i(\tau)$, after the first Discrete Fourier transform

$$x_i(\tau)=\sum_{n=-N/2}^{N/2-1}e^{i2\pi\frac{n}{T}\tau}\hat{H}_{i,n} \tag{4.19}$$

is equivalent to the classical range-slow time signal in an active pulse radar.

The slow-time snapshot for the range cell τ can be written as

$$\boldsymbol{x}(\tau)=\begin{bmatrix}x_0(\tau)\\ \vdots \\ x_{N_s-1}(\tau)\end{bmatrix} \tag{4.20}$$

and equation (4.17) becomes

$$M_{OFDM}(\tau,\nu)=\boldsymbol{w}_{OFDM}^{H}(\nu)\boldsymbol{x}(\tau)\qquad 0\le\tau\le\tau_{\max} \tag{4.21}$$

where the weighting filter $\boldsymbol{w}_{OFDM}^{H}(\nu)$ is defined as

$$\boldsymbol{w}_{OFDM}^{H}(\nu)=\begin{bmatrix}1\\ \vdots \\ e^{j2\pi\nu(N_s-1)T_S}\end{bmatrix}=\boldsymbol{v}_{OFDM}^{H}(\nu) \tag{4.22}$$

where $\boldsymbol{v}_b^{H}(\nu)$ is the temporal steering vector define in accordance with the symbol time T_S. The filter defined in equation (4.22) is the temporal matched filter evaluated at the frequency of interest ν. As we have seen for the batches algorithm we can extend the matched filter processor to the adaptive matched filter

$$\boldsymbol{w}_{OFDM}(\nu)=\gamma\hat{\boldsymbol{R}}_i^{-1}\boldsymbol{v}_{OFDM}^{H}(\nu) \tag{4.23}$$

where $\hat{\boldsymbol{R}}_i\in\mathbb{C}^{N_sxN_s}$ is the estimated interference covariance matrix by using the SCM algorithm. The training data set $\Omega_{training}^{N_sxN_t}$ can be selected in the range domain as we have seen in the case of batches algorithm (Figure 4.6).

The main advantages respect to the adaptive matched direct FFT filter are:

- the dimension of the slow-time snapshot for the range cell τ is N_s. This value is smaller than the number of samples N but it is comparable with n_B. Therefore the dimension of the correlation matrix is N_s and the associated computational load is similar to the batches algorithm.
- the losses related to the small Doppler approximation are similar to the batches algorithm losses. The OFDM algorithm has losses depending both range and target Doppler. Considering only the range effect the SNR is reduced by a factor $\tau_{\max} / T_U$.

4.5 Results

In this section the results relative to the proposed adaptive matched filter are shown. To evaluate the performance both simulated and real data are used.

4.5.1 Simulation results

To evaluate the performance of the temporal adaptive processing, we select a specific case. We consider a DVB-T signal received by each radiating element of the antenna array (Observation Time=0.3).
The simulated scenario is characterized by:

- direct signal with a Direct signal to Noise Ratio (DNR) of about 60dB
- two multipath echoes received at the range bins 10 and 20. The two multipath component have been simulated with a 6 Hz Doppler shift in order to consider the effect of ICM. In this way it is possible to compare the performance between Zero Doppler interference suppression and temporal adaptive processing
- a target located at range bin 100 with a 40 Hz Doppler shift.

To demonstrate the effect of the interference suppression we calculate the range-Doppler maps before and after the filtering. Specifically the range-Doppler map before

filtering is shown in Figure 4.7. The target is clearly masked by the direct and signal side lobes.

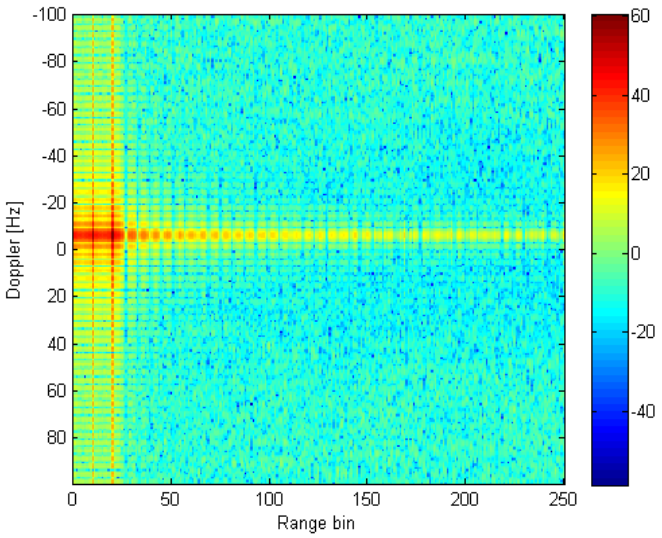

Figure 4.7 Range-Doppler map before filtering

In Figure 4.8 the range-Doppler map after the classical echo canceller filter is shown. Specifically we have used the ECA filter formulation. It is possible to note that the filter is not able to reduce the interference power located at non zero Doppler. In Figure 4.9 the range-Doppler map obtained by using an ideal temporal adaptive processing is shown. The term ideal refers to the case in which the training data set is composed by only the interference component received in the range cell under test. The interference correlation matrix is obtained by using diagonal loading.

In Figure 4.10 the range Doppler maps considering the presence of the target component in the training data set and by using the training data selection defined in the previous section is shown. The worse performance can be explained considering that the interference is non-homogeneous in the range domain as we can see observing Figure 4.7. This is a particular disadvantageous simulated case. The interference generally presents a more homogeneous characteristics as we will see in the next subsection considering real data.

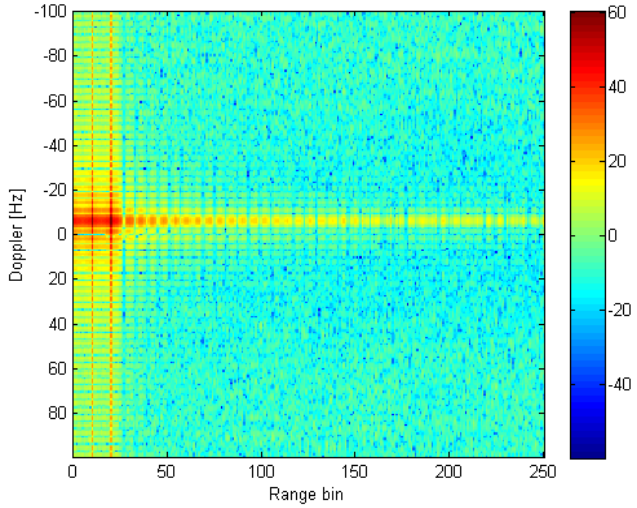

Figure 4.8 Range-Doppler map after ECA filter

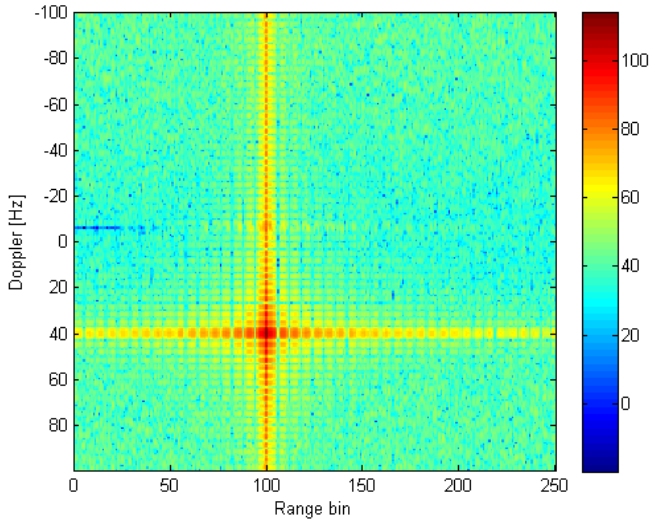

Figure 4.9 Range-Doppler map after optimum temporal adaptive processing

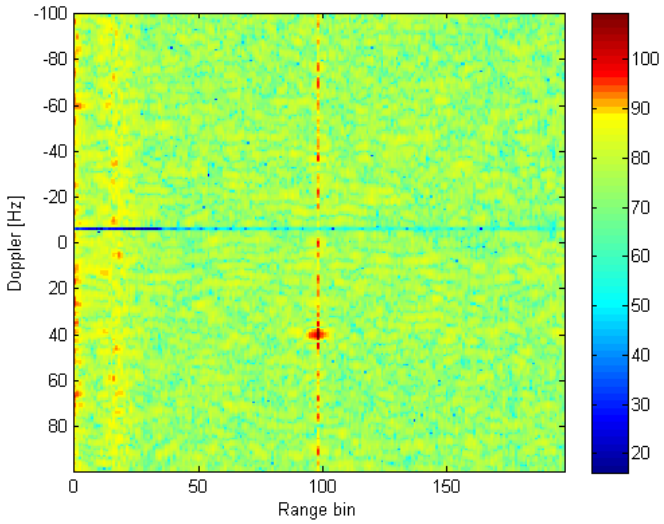

Figure 4.10 Range-Doppler map after temporal adaptive processing

4.5.2 Real-life measurements

The used real data has been acquired during a measurements campaign described in [Capria 2010], [Capria 2010_1]. In this work experimental results obtained with low-cost equipment have proven the feasibility of a DVB-T based passive radar system by using a software defined architecture. The experiment scenario geometry is shown in Figure 4.11.

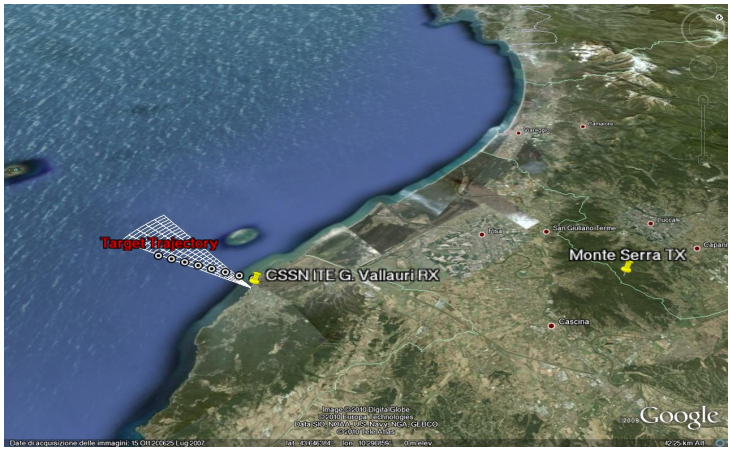

Figure 4.11 Experiment scenario geometry [Capria 2010].

Specifically the receiver was located at the “CSSN-ITE G. Vallauri” institute in Livorno, the used illuminator of opportunity was a DVB-T transmitter located on “Monte Serra” in Pisa (around 32 km far from the receiver) and the surveillance antenna was directed towards an area of sea in front of the receiver site. To demonstrate the effect of the interference suppression we calculate the range-Doppler maps before and after the filtering. Specifically the range-Doppler map before filtering is shown in Figure 4.12. The echo relative to the ship is clearly visible at a range bin 170 with a negative Doppler frequency equal to -15 Hz. In the range-Doppler map are clearly visible the direct signal component around zero Doppler and other interference components caused by both clutter and spurious introduced by the acquisition system. The range-Doppler map after filtering is shown in Figure 4.13.

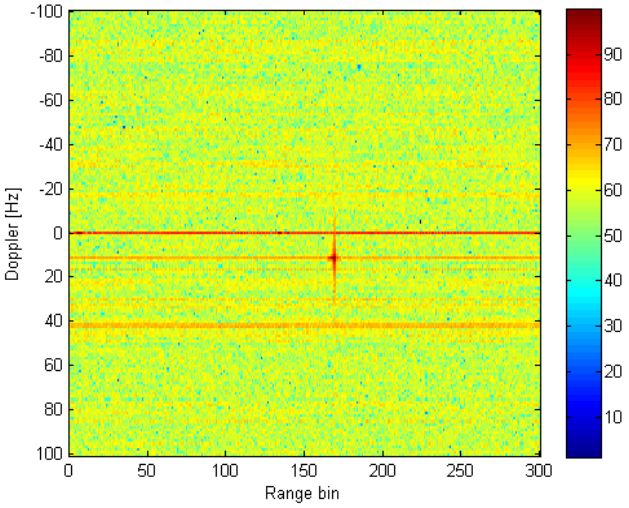

Figure 4.12 Range-Doppler map before filtering

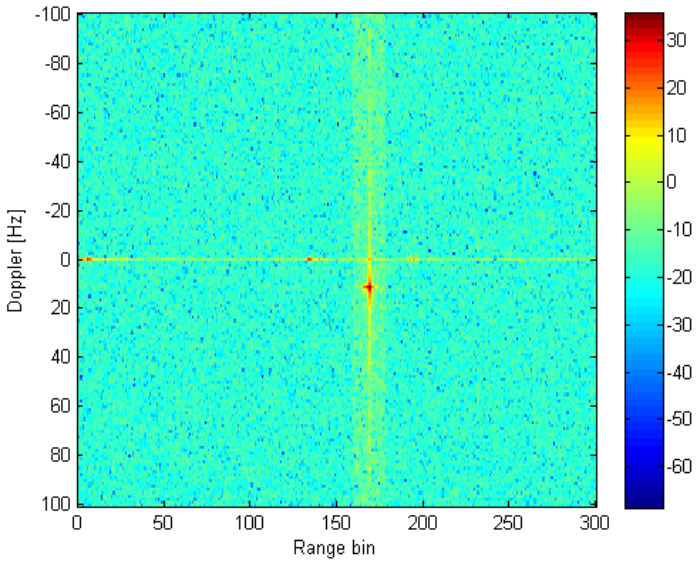

Figure 4.13 Range-Doppler map after filtering

4.6 Chapter summary

In this chapter we have investigated the use of spectral-temporal cancellation techniques in a single receiver passive radar. A variety of temporal adaptive processing have been developed for the removal of the interference component in the surveillance channel before the matched filter. Typically these techniques are based on the adaptive noise canceller structure. We have defined an adaptive matched filter solution based on the "batches" matched filter formulation. This solution is an alternative to the proposed adaptive matched filter technique base on the direct FFT approach.. The main advantages of this alternative solution are the possibility to suppress both static clutter and affected by ICM and the lower computational load.

The effectiveness of the proposed solution has been demonstrated considering both simulated and real data.

Chapter 5.

Spatial adaptive processing

5.1 Introduction

Simpler passive bistatic radar systems use only two antennas for the reception of both surveillance and reference signal. When the interference signal is especially strong the use of temporal adaptivity following the antenna side-lobes attenuation might still be unsatisfactory. Moreover the target DOA estimation is an essential step in the target localization and association problem. An alternative interesting approach might be based on the use of a phased array [Coleman 2008], [Fabrizio 2008-2009], [Howland 2005], [Kuschel 2008], [Malanoski 2008], [Villano 2009], [Zemmari 2009-2010.]In this way it is possible to electronically steer multiple beams in all directions in order to generate a set of directional beams on the surveillance area and in correspondence of the directions of the illuminators of opportunity. This chapter proposes the use of an antenna array and digital beamforming techniques in a PBR system. Typically digital beamforming techniques are applied directly on the received signal and before the matched filter. The main drawbacks of this solution are described and a new scheme, based on the application of digital adaptive beamforming after matched filter is proposed. The proposed technique improves the performances in terms of clutter cancellation on the surveillance channel.

The chapter is organized as follows. Section 5.2 introduces a literature review of the spatial adaptive techniques applied in a PBR scenario. In section 5.3 the theoretical background relative to the digital beamforming techniques is briefly describes and the single-sensor signal model, analysed in Chapter 2, has been extended to the case of an

array composed by K directive elements. Section 5.4 introduces the proposed adaptive digital beamforming technique. In section 5.5 the results of algorithm simulations are presented.

5.2 Digital beamforming in a passive radar scenario

5.2.1 Motivations

The main factors that motivate the use of digital beamforming techniques are:

1. improve the estimation of the target DOA (Direction of Arrival) and the possibility to attenuate the interference signal received on the surveillance channel. When the direct signal is especially strong, the use of the temporal adaptivity following the antenna sidelobe attenuation of the direct signal might still be unsatisfactory.
2. improve the estimation of a clean copy of the unknown source waveform in the reference channel.

As regard the first point we can observe that one of the main problem in a PCL radar is the localization of the target. Two main methods can be used in order to obtain the target coordinates:

- Single receiver configuration: estimate the angular direction of arrival (DOA) and calculate its intersection with the bistatic ellipse.
- Multistatic configuration: find the intersections points of bistatic ellipse originating from different illuminators of opportunity. Also in this case the DOA estimation is very important because it could limit the possible intersection points.

We can conclude that the measurement of target DOA are essential when estimating the location of a target using a simple bistatic configuration and are very helpful in resolving the target association problem with multiple transmitters.
The simplest way to estimate the target DOA is to sense the angle at which the returning target wavefront arrives at the radar. This is usually accomplished with a rotating

directive antenna, with a narrow radiation pattern. The direction in which the antenna points when the received signal is a maximum indicates the target DOA.
The angle of arrival can also be determined by measuring the phase difference between two separate receiving antennas as with an interferometer. This simplest and cheapest method have been implemented in one of the first passive radar system [45] by using only two receivers on the surveillance channel.
These two mentioned approaches have several problems in a actual passive radar scenario, as we have seen in chapter 2, because of the presence of several interferences in the surveillance channel. Therefore they could be implemented after a interference cancellation block by means high directive antennas and classical temporal filter exploited in Chapter 4.
These simple configurations presents several drawbacks:

- a single high directivity sensor cannot to look in several directions simultaneously and it can spatially discriminate separate targets by a mechanically rotation.
- the interference is reduced in the spatial domain by using only high directivity antennas. The single sensor spatial response or element pattern is strictly related to its physical and geometric properties, for this reason it cannot adapt its spatial response, which would require physically changing the aperture, in order to reject potentially strong sources that may interfere with the extraction of the signals of interest.

As regard the second point we can simply estimate the reference signal by using a single antenna pointed in the direction of the illuminator of opportunity, as we have seen in Chapter 2. It is possible to note that the use of a single reference antenna has several drawbacks:

- in a multistatic scenario in order to use multiple transmitters the beam of several antennas have to be pointed in different directions. Therefore it is necessary to use several antennas in order to capture the multiple reference signals.

• the element pattern of a single antenna could not sufficiently spatial attenuate the multipath signal received in the reference channel especially in the case of DVB-T or DAB SFN.

An alternative interesting approach might be based on the use of a planar phased array and digital beamforming technique. In this way it is possible to electronically steer multiple beams in all directions in order to generate a set of directional beams on the surveillance area and in correspondence of the directions of the illuminators of opportunity.

We can summarize the main goals of the digital beamforming stage as follows:

• form the direct signal beams on the direction of the transmitters of opportunity that we intend to use for implementing passive radar functionality. Ideally the reference beam attempts to minimize the corruption in the transmitted waveform estimate caused by the superposition of unwanted signal multipath components.

• form one or more surveillance beams in pre-determined directions selected for target search. Ideally the surveillance channel provides the maximum gain for target echoes while cancelling all interference components. A solution with multiple beams seems to be more practical since provides higher gain and potential capability of direction of arrival estimations.

5.2.2 Multi channel signal modelling

In this section the single-sensor signal model, analysed in Chapter 2, has been extended to the case of an array composed by K directive elements as shown in Figure 5.1.

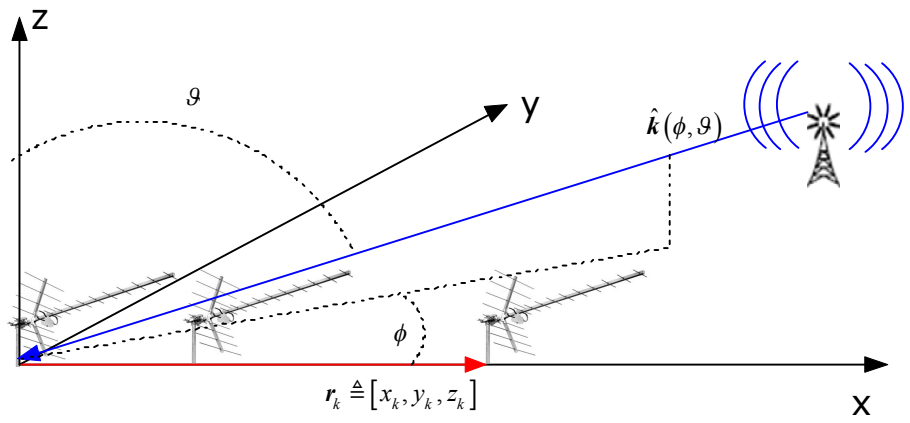

Figure 5.1 Multi channel signal modelling

After defining the antenna structure, in particular the position of the array elements $\boldsymbol{r}_k$, the different components of the received signal are defined by their spatial steering vector as

$$\mathbf{v}(\phi,\vartheta) = \begin{bmatrix} G_0(\phi,\vartheta)1 \\ G_1(\phi,\vartheta)e^{i2\pi f_0\tau_1} \\ \vdots \\ G_{K-1}(\phi,\vartheta)e^{i2\pi f_0\tau_{K-1}} \end{bmatrix} \tag{5.1}$$

where τ_k represents the intra element delay due to their different spatial position and $G_k(\phi,\vartheta)$ is the k-th element pattern calculated at the angular direction (ϕ,ϑ). The delay τ_k is determined as a function of the direction of arrival and of the array element positions as:

$$\tau_k = \frac{\hat{\boldsymbol{k}}(\phi,\vartheta)\boldsymbol{r}_k}{c} = \frac{\cos(\phi)\sin(\vartheta)x_k + \sin(\phi)\sin(\vartheta)y_k + \cos(\vartheta)z_k}{c} \tag{5.2}$$

where $\hat{\boldsymbol{k}}(\phi,\vartheta)$ is an unit vector pointing in the (ϕ,ϑ) angular direction, $\boldsymbol{r}_k$ is the k-th array element vector position. It is assumed that the transmitted waveform is narrowband.

The array received signal coming from a generic source located at (ϕ,ϑ) can be modelled as:

$$\mathbf{x}(t) = x(t)\,\mathbf{v}(\phi,\vartheta) \tag{5.3}$$

where $x(t)$ is the transmitted signal.

Considering the single channel model, defined in chapter 2, the multichannel signal model can be defined as follows

$$\begin{aligned}\boldsymbol{x}(t) &= \beta_0 x(t)\boldsymbol{v}(\phi_D,\vartheta_D) + \sum_{n=1}^{N_C} x(t-\tau_n)\sum_{k=1}^{N_n}\boldsymbol{v}(\phi_{n,k},\vartheta_{n,k})\alpha_{n,k}e^{i\theta_{n,k}} + \\ &+\beta_{surv}^{1}\, x(t-\tau_1^T)e^{i2\pi v_1^T t}\boldsymbol{v}(\phi_1^T,\vartheta_1^T) + \boldsymbol{n}(t)\end{aligned} \tag{5.4}$$

where (ϕ_D,ϑ_D) is the transmitter angular location, $(\phi_{n,k},\vartheta_{n,k})$ is the single multipath path angular position and (ϕ_1^T,ϑ_1^T) is the target angular location. The statistical characterization of the model has already been presented in chapter 2.

5.3 Digital beamforming overview

5.3.1 Basic terminology and concepts

In its most general form, a beamformer processor produces its output by forming a weighted combination of signals from the K elements of the sensor array, that is,

$$y(t) = \sum_{k=0}^{K-1} w_k x_k(t) = \boldsymbol{w}^H \boldsymbol{x}(t) \tag{5.5}$$

where $\boldsymbol{w}$ is the column vector of beamforming weights and $\boldsymbol{x}(t)$ is the array received signal [Van Trees 2002], [Manolakis 2005]. We assume throughout that the data and weights are complex since a quadrature receiver is used at each sensor to generate in phase and quadrature (I and Q) data. Each sensors is supposed to have any necessary receiver electronics and an A/D converter if beamforming is performed digitally.

Both surveillance and reference channel can be obtained by filtering the received array signal by means opportune weight vectors as shown in Figure 5.2

$$\begin{cases} x_{ref}(t) = \boldsymbol{w}_{ref}^H \boldsymbol{x}(t) \\ x_{surv}(t) = \boldsymbol{w}_{surv}^H \boldsymbol{x}(t) \end{cases} \tag{5.6}$$

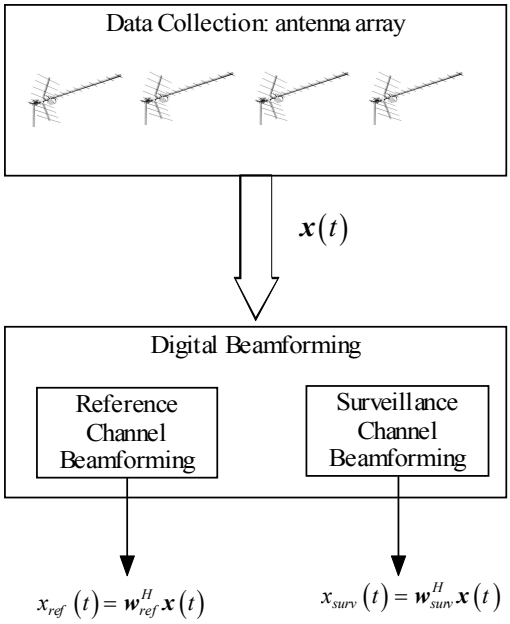

Figure 5.2 Digital beamforming in PBR systems

Beamforming algorithms can be classified as either data independent or data dependent (adaptive), depending on how the weights are chosen. The weights in a data independent beamformer do not depend on the array data and are chosen to present a specified response for all signal-interference scenarios. The weights in an adaptive beamformer are chosen based on the statistics of the array data to "optimize" the array response. In general, the statistically adaptive beamformer places nulls in the directions of interfering sources in an attempt to maximize the signal to noise ratio at the beamformer output.

5.3.2 Data independent beamforming

The simpler data independent beamforming is the so called conventional beamforming. The weights of the conventional beamformer are chosen as

$$\boldsymbol{w} = \boldsymbol{v}(\phi, \vartheta) \tag{5.7}$$

where $\boldsymbol{v}(\phi,\vartheta)$ is the spatial steering vector, defined in equation (5.1) and evaluated at the angular direction (ϕ,ϑ) .of interest. Both the surveillance and reference channel can be obtained as

$$\begin{cases} \boldsymbol{w}_{ref} = \boldsymbol{v}(\phi_D,\vartheta_D) \\ \boldsymbol{w}_{surv} = \boldsymbol{v}(\phi_T,\vartheta_T) \end{cases} \tag{5.8}$$

where (ϕ_D,ϑ_D) is the angular location relative to the illuminator of opportunity and (ϕ_T,ϑ_T) is the target angular location. More generally (ϕ_T,ϑ_T) represents the surveillance beams in pre-determined directions selected for target search.

The conventional beamformer is optimum in terms of output SNR when the noise field is spatially white. In many practical applications, including passive radar, the noise field is generally not spatially white. The sub optimality of the conventional beamforming is most noticeable when powerful interference leaks through the sidelobes and potentially mask a weak signal incident from the steer direction.

The use of window functions to taper or shade the sensor outputs prior to conventional beamforming lowers the sidelobes of the beampatterns at the expense of increasing the main lobe width and reducing the main lobe maxima. A wide selection of window function may be used and the specific choice depends on the tradeoff between sidelobe level and main lobe width. The tapered beamforming is generally preferred over the untapered version because it is more immune to interference in the side lobe region and the wider main lobe is more robust to slight errors between the steer direction and the DOA of the desired signal. The price often paid for computational advantages of conventional beamforming is the sub optimality in output SINR.

The methods, defined as general data independent response design, apply to design of beamformers that approximate an arbitrary desired response. This is of interest in several different applications. For instance, we may wish to receive any signal arriving from a range of directions, in which case the desired response is unity over the entire range. As another example, we may know that there is a strong source of interference arriving from a certain range of directions, in which case the desired response is zero in this range. These two examples are analogous to bandpass and bandstop FIR filtering.

In the majority of cases, the problem can be stated as a model matching minimization scheme. In the model matching scheme, the concept is to define a model which resembles the ideal output response of the beamformer, and try and match this response. The optimization problem to be solved can be formulated as follows

$$\min_{\mathbf{w}} \left| \mathbf{A}^H \mathbf{w} - \mathbf{r}_d \right|^2 \tag{5.9}$$

where $\mathbf{A}$ is the steering matrix with the steering vectors associated to the directions where the desired output is provided and $\mathbf{r}_d$ is the ideal output response. The solution is given by [Van Veen 1998]

$$\mathbf{w} = \left(\mathbf{A}^H \mathbf{A} \right)^{-1} \mathbf{A}^H \mathbf{r}_d^T \tag{5.10}$$

If the ideal response is set to one in the angular direction of interest and zero in the interference angular direction we obtain the so called null steering technique.

5.3.3 Data dependent beamforming

In data dependent beamforming the weights are chosen based on the statistics of the data received at the array. In particular the data dependent optimum weight vector is synthesized by using the information contained in the received signal spatial covariance matrix. As we have seen in section 1.2.2 the optimum solution of an adaptive filter is related to the interference correlation matrix. In the case of spatial adaptive techniques the interference correlation matrix is defined in the spatial domain as

$$\boldsymbol{R}_i(t) \triangleq E\left\{ \boldsymbol{x}_i(t) \boldsymbol{x}_i^H(t) \right\} \tag{5.11}$$

where we have indicated with $\boldsymbol{x}_i(t)$ the interference component belonged to the received signal $\boldsymbol{x}(t)$.

It is important to note that the interference is given by

- the direct signal and relative multipath in the surveillance channel
- the target signal, the multipath signal and the signal transmitted by other illuminators of opportunity in a SFN in the reference channel

As we have mentioned in section 1.2.2 this is a typically case in which we cannot estimate signal free correlation matrix. The SCM correlation matrix estimation is given by

$$\hat{\boldsymbol{R}}_i = \frac{1}{N_t}\sum_{m=1}^{N_t} \boldsymbol{x}\left(mT_C\right)\boldsymbol{x}^H\left(mT_C\right) \tag{5.12}$$

where T_C is the sampling time and the training data set is chosen in sampling time domain as shown in Figure 5.3

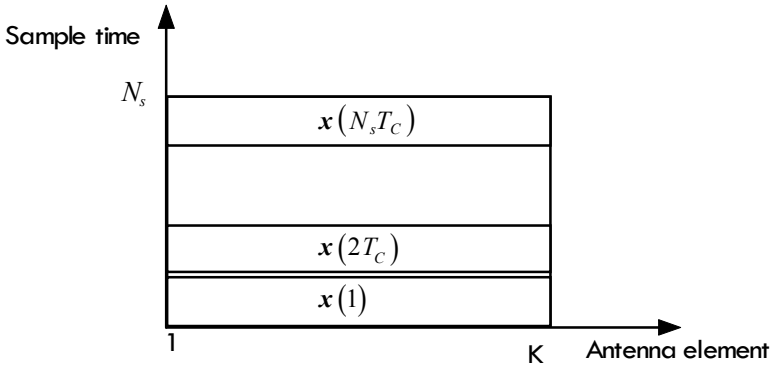

Figure 5.3 Data training selection

5.4 System architectures

In this section we define two possible PBR signal processing architectures based on the application of digital beamforming techniques. The first one is based on the elaboration of the array received signal, as we have seen in the previous paragraphs. The second one is based on the application of digital beamforming techniques after the matched filter.

5.4.1 Traditional architecture

A standard PBR beamforming approach, that may be used to generate the reference and surveillance channel, applies directly the beamforming weighting vector to the array snapshot $\boldsymbol{x}\left(t\right)$ received in the CPI as shown in Figure 5.4. Both data dependent and data independent beamforming techniques, mentioned in the previous paragraph, can be developed in the reference channel and in the surveillance channel.

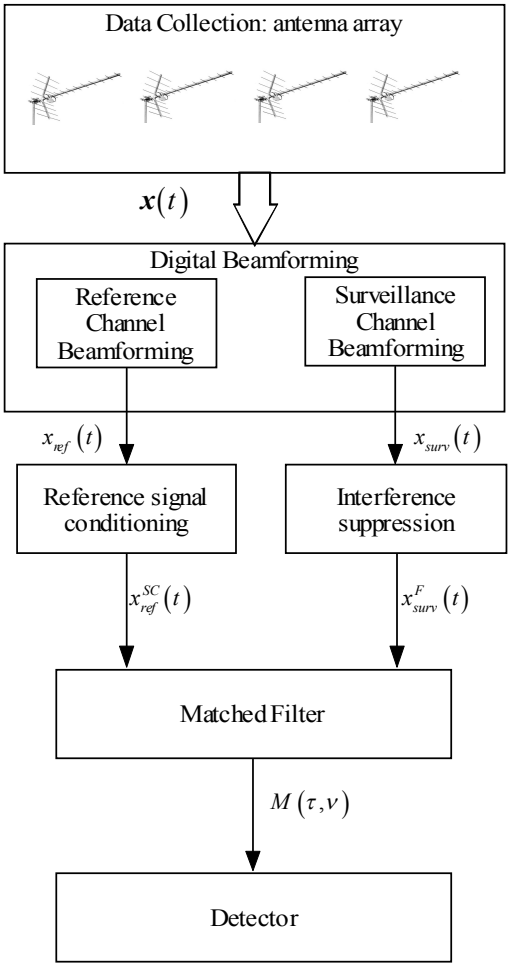

Figure 5.4 Traditional architecture

Reference channel beamforming

In a multistatic scenario, for the reference channel the desired signal is the direct path signal from a certain transmitter, whereas the direct paths of other transmitters and multipath are regarded as the interference. The presence of this components on the reference signal will lead to ambiguities that will obscure the target, as we have seen in chapter 2. Since typically the receiver and the transmitter are both stationary we can suppose transmitter DOAs known. Alternatively we can adopt a method to perform an automatic estimation of the direction of the illuminators of opportunity. For the DOA estimation a number of traditional algorithms can be considered including Capon, Bartlett, MUSIC.

Typically the reference beamformer is based on data independent techniques as shown in section 5.3.2 [Fabrizio 2009]. In a multistatic scenario null steering techniques could be an optimum solution. The resulted deterministic filter generates a main beam in the direction of the desired opportunity emitter and notches in the directions of the others, possibly with a high directivity and low SLL to reduce the other interference contributions. In a practical application it is necessary to form nulls of a certain width in order to: avoid the mistakes relative to the estimation of the interference DOA and to attenuate the multipath generated by the distributed clutter.
In [Zemmari 2009-2010], either the conventional beamformer or the data dependenr beamformer, based on the concepts developed in section 5.3.3, have been proposed.
The application of traditional data dependent techniques presents the problem relative to the cancellation of the desired signal. The reason is as follows: it is impossible to estimate the interference covariance matrix without the presence of the desired signal. In [Tao 2010] a technique based on the general side lobe canceller (GSC) structure has been proposed to remove the effect of desired signal in the covariance matrix estimation.

Surveillance channel beamforming

A shortcoming of conventionally formed surveillance beams is that the powerful DSI from the transmitter may not be sufficiently attenuated by the resulting antenna pattern sidelobes. For this reason the surveillance channel beamformer is typically implemented by using data dependent techniques, as shown in section 5.3.3. This architecture is widely used in most of the passive radar system but has two potential disadvantages:

1. Adaptive techniques applied to this domain attempt to cancel the global disturbance interference energy, most of which does not actually masked the potential target since it is concentrated around zero Doppler frequency.
2. As we have already mentioned the target signal is included in the training data set and it could be self cancelled.

Some techniques have been proposed to avoid these problems. In [Fabrizio 2009]. the loaded sample matrix inverse (LSMI) has been analyzed while in [Zemmari 2009-2010] the eigenvector Projection (EVP) method a eigen-decomposition method is investigated.

In [Tao 2010] it is shown that the noise-subspace can be estimated from the power of the covariance matrix avoiding the direct eigen-decomposition.

5.4.2 Proposed architecture

Alternatively to the previous architecture the array data can be transformed to the range-Doppler domain prior to the surveillance channel adaptive beamforming. In this architecture the adaptive beamforming is performed in the range-Doppler domain instead of the sampling time domain This new architecture is shown in Figure 5.5. The reference signal can be extracted as we have seen in the previous section. More specifically, each receiver output is filtered using the conventional estimate of the reference waveform to produce K range-Doppler maps denoted by $M_k(\tau,\nu)$ for $k = 0,1,...,K$. The range-Doppler maps can be obtained either with the matched filter algorithms developed in chapter 3 or with the adaptive matched filter developed in chapter 4. At each range-Doppler bin the complex multi-channel outputs may be assembled into the spatial snapshot vector $\boldsymbol{M}(\tau,\nu) \in \mathbb{C}^{Kx1}$.

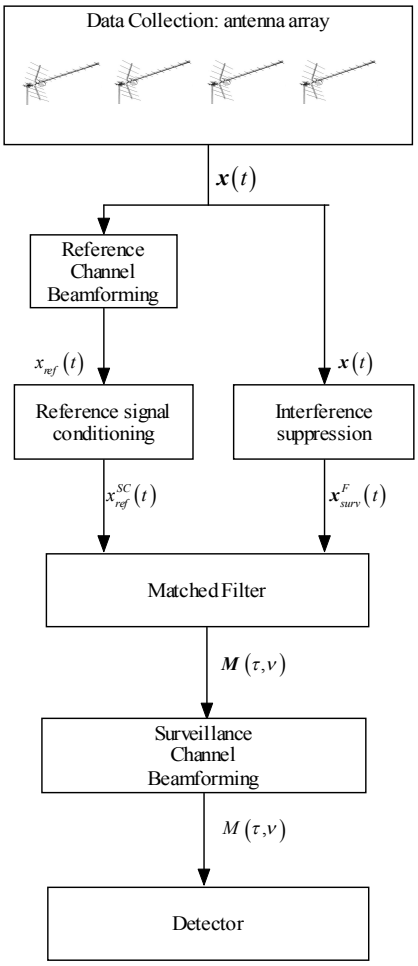

Figure 5.5 Advanced architecture

The spatial snapshot for the range cell τ and frequency Doppler ν can be written as

$$\boldsymbol{M}(\tau,\nu)=\begin{bmatrix} M_0(\tau,\nu) \\ \vdots \\ M_{K-1}(\tau,\nu) \end{bmatrix} \approx M_0(\tau,\nu)\boldsymbol{v}_s(\phi,\vartheta) \tag{5.13}$$

The spatial matched filter evaluated at the angular direction of interest can be written as

$$\boldsymbol{w}_{conv}(\phi,\vartheta)=\boldsymbol{v}_s(\phi,\vartheta) \tag{5.14}$$

The theory developed in chapter 1 can be applied in this case defining the vector $\boldsymbol{s}_0$, shown in equation (1.13), equal to the spatial steering vector $\boldsymbol{v}_s(\phi,\vartheta)$ The natural extension of the matched filter is the adaptive matched filter which can be defined as

$$\boldsymbol{w}(\phi,\vartheta)=\gamma\hat{\boldsymbol{R}}_i^{-1}\boldsymbol{v}_s^H(\phi,\vartheta) \tag{5.15}$$

where $\hat{\boldsymbol{R}}_i \in \mathbb{C}^{KxK}$ is the estimated spatial interference covariance matrix by using the SCM algorithm. The training data set $\Omega_{training}^{KxN_t}$ can be selected in the range-Doppler domain, as shown in Figure 5.6. A reasonable approach is to use surrounding range-Doppler bins of the cell under test, that are likely to contain similar interference, without the cell under test and some guard cells to prevent so-called self nulling.

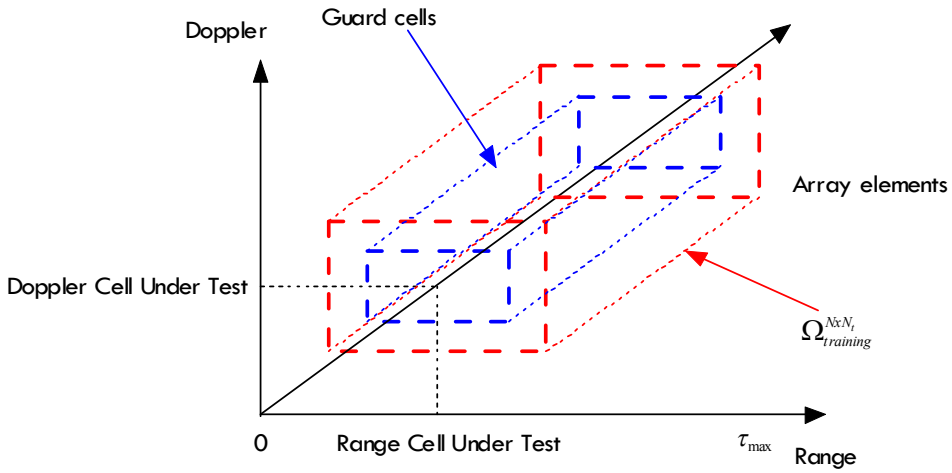

Figure 5.6 Training data set selection

Once obtained the signal in the range-Doppler domain we can applied all the classical adaptive beamforming techniques. The implemented techniques are chosen to have an adaptive algorithm is not complex from both implementation and computational load to facilitate a real time application. We discussed the optimum beamformer that maximizes the signal-to-interference-plus-noise ratio. This optimum beamformer can be obtained also as the solution of a constrained minimization problem, namely

$$\min_{\boldsymbol{w}} \left\{ \boldsymbol{w}^H \boldsymbol{R}_i \boldsymbol{w} \right\} \quad subject\ to \quad \boldsymbol{w}^H \mathbf{v}(\phi, \vartheta) = 1 \tag{5.16}$$

where $\boldsymbol{w}^H \boldsymbol{R}_i \boldsymbol{w}$ is the interference output power. It is possible to demonstrate that the solution is given by

$$\mathbf{w}(\phi,\vartheta)=\frac{\boldsymbol{R}_i^{-1}\mathbf{v}(\phi,\vartheta)}{\mathbf{v}^H(\phi,\vartheta)\boldsymbol{R}_i^{-1}\mathbf{v}(\phi,\vartheta)} \tag{5.17}$$

This result is the same of the equation (5.15) with the proportionality constant γ equal to $\gamma=1/\left(\mathbf{v}^H(\phi,\vartheta)\boldsymbol{R}_i^{-1}\mathbf{v}(\phi,\vartheta)\right)$.

Due to this alternative formulation the optimum beamformer is commonly referred to as the Minimum Variance Distorsionless Response (MVDR) beamformer. However, some applications may require additional constrain on the beamformer output. One common use of additional constrains is for the case when the interference DOA (ϕ_i,ϑ_i) is known a priori. In this case we want to reject the echo received from this angle and we can impose also the null constrain, that is

$$\min_{\boldsymbol{w}}\left\{\boldsymbol{w}^H\boldsymbol{R}_i\boldsymbol{w}\right\} \quad subject\,to \quad \boldsymbol{w}^H\mathbf{v}(\phi,\vartheta)=1 \;\; and \;\; \boldsymbol{w}^H\mathbf{v}(\phi_i,\vartheta_i)=0 \tag{5.18}$$

Once we have determined a set of constrains in order to obtain a desired response at a set of angles we can have a constrained optimization problem

$$\min_{\boldsymbol{w}}\left\{\boldsymbol{w}^H\boldsymbol{R}_i\boldsymbol{w}\right\} \quad subject\,to \quad \boldsymbol{C}^H\mathbf{v}(\phi,\vartheta)=\boldsymbol{r}_d \tag{5.19}$$

where **C** is the constraint matrix and is $\boldsymbol{r}_d$ the desired beamformer response. The result is known as the Linearly Constrained Minimum Variance (LCMV) beamformer and the solution is given by

$$\boldsymbol{w}_{LCMV}=\hat{\boldsymbol{R}}_i^{-1}\boldsymbol{C}\left(\boldsymbol{C}^H\hat{\boldsymbol{R}}_i^{-1}\boldsymbol{C}\right)^{-1}\boldsymbol{r}_d \tag{5.20}$$

As we have seen in chapter 2, the received signal has a dynamic range of easily 80-90 dB between the direct signal and target signal which cannot be handled by analog-to-digital converters. This makes additional analog attenuation of the direct signal in the form of null steering or directional antennas before the sampling. For instance in [Berger 2010] an analog null steering attenuates the direct signal to a level of clutter reducing the required dynamic range. The received signal after analog beamformer, denoted as $\boldsymbol{x}_{AB}(t)$, is shown in Figure 5.7. This signal is obtained in the angular

domain and not in the array element domain. In this case we can apply sub-optimum techniques known as beamspace partially adaptive techniques.

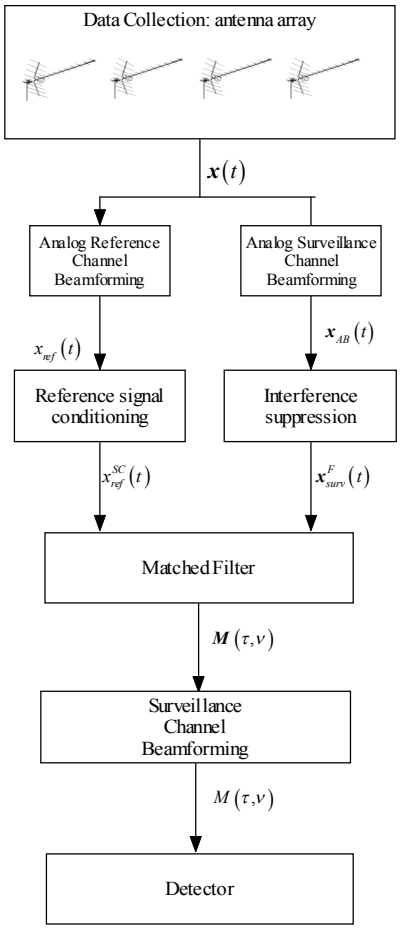

Figure 5.7 Analog beamforming architecture

5.5 Simulation results

To evaluate the performances of the proposed adaptive beamforming techniques a DVB-T-based multichannel passive radar has been simulated. The antenna array is a uniform linear array consists of eight elements. The simulated scenario is characterized by:

- A transmitting station located at $(0°, 90°)$

- Two multipath echoes received from the angular direction $(10°,90°)$ and $(15°,90°)$. In addition, the signal from the path I is simulated at the range bin 13, whereas the signal from the path II is simulated at range bin $7\,7T_C$ and it has a 3 Hz Doppler shift in order to simulate ICM.
- a target located at $(60°,90°)$ and at range bin 20 has a 40 Hz Doppler frequency shift.
- a target located at $(80°,90°)$ and at a range bin 13 has a -20 Hz Doppler frequency shift

The powers of the two target echoes are 20 dB lower than the noise power whereas the power of the two multipath echoes is 60 dB greater than the target power. The power of the direct path is 80 dB greater than target power.

To demonstrate the effect of the interference suppression by spatial filtering we calculate the range-Doppler maps before and after the defined spatial adaptive signal processing. Specifically in Figure 5.8 the range-Doppler map $M_0(\tau,\nu)$ considering the first array element is shown, whereas in Figure 5.9 the range-Doppler map $M_0(\tau,\nu)$ considering only the target components is shown.

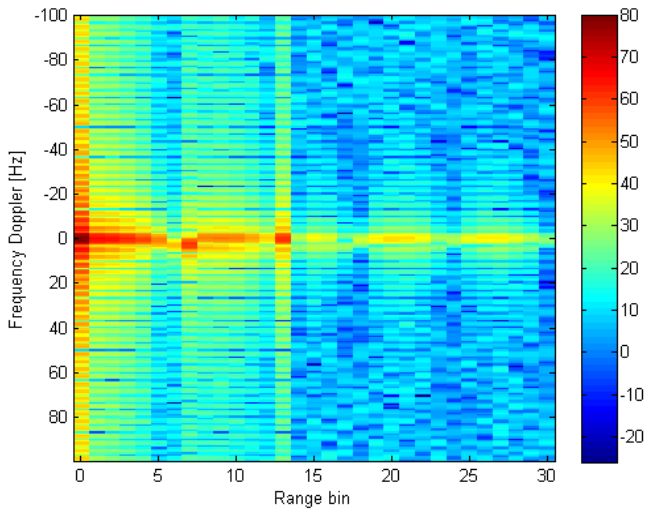

Figure 5.8 Range-Doppler map before spatial adaptive processing

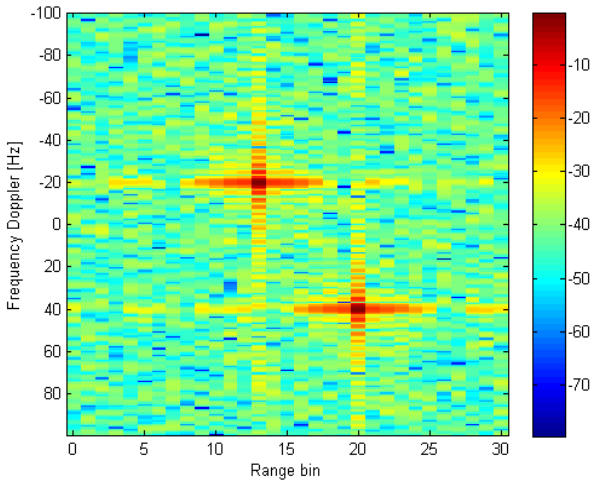

Figure 5.9 Range-Doppler map considering only target components

In Figure 5.10 the range-Doppler map, evaluated at the first target angular location is shown.

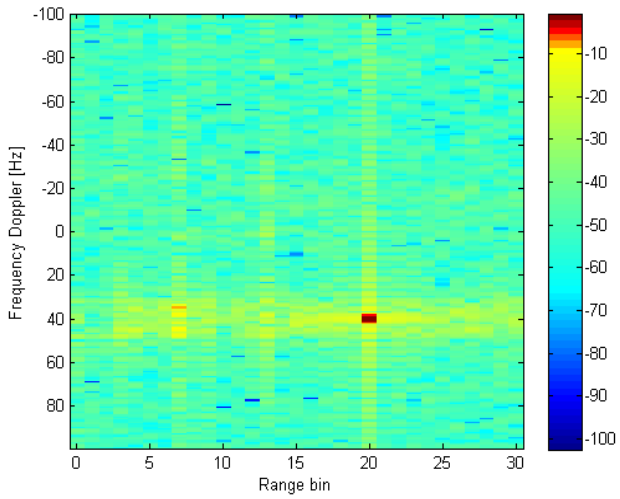

Figure 5.10 Range-Doppler map after spatial adaptive processing relative to the first target

In Figure 5.11 the range-Doppler map, evaluated at the second target angular location is shown.

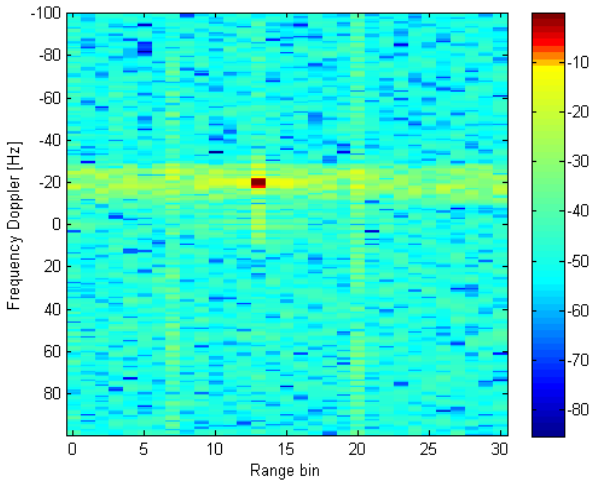

Figure 5.11 Range-Doppler map after spatial adaptive processing relative to the second target

It is evident from Figure 5.10 and Figure 5.11 that the use of the proposed spatial adaptive technique improves the target detection.

We have considered a more complicated DVB-T passive radar scenario. Specifically the simulated scenario is shown in Figure 5.12. Five targets moving on five different trajectories and two transmitter of opportunity have been considered. In Table 1 the main parameters of the IOs and the receiver are reported.

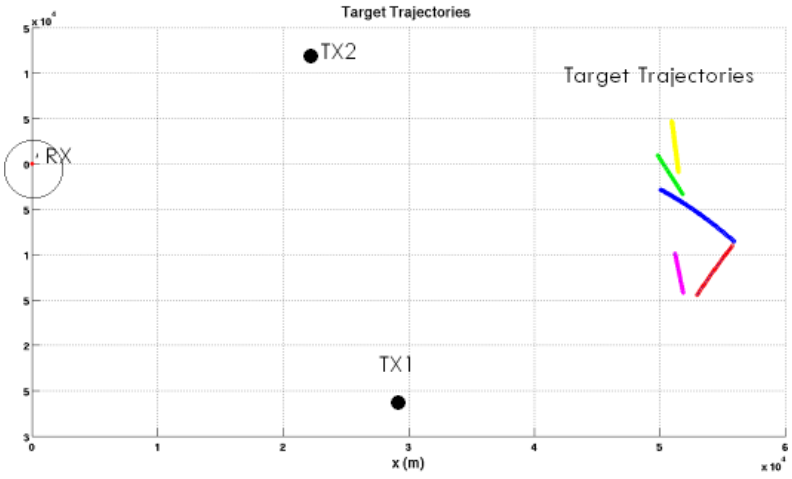

Figure 5.12 Simulated scenario

	Latitude	Longitude	ERP (W)	Baseline Length (km)	Azimuth (w.r.t. receiver‟s position)	DPI (dBm)
TX1 (Reference)	40º 27‟ 8.47‟‟‟ N	3º 50‟ 52.24‟‟‟ W	20000	39.46	131.85º	-41.52
TX2	40º 47‟ 57‟‟‟ N	3º 55‟ 58.7‟‟‟ W	24.6	25.19	61.12º	-66.72

	Latitude	Longitude	Altitude	Surveillance azimuth sector	*Azimuth width*	Bistatic angles
Receiver	40º 41‟ 23.8” N	3º 50‟ 52.24‟‟‟ W	1868 m	69.76º - 110.14º	40.38º	35° - 60°

Central. freq.	**Integration time**	**Radiating element**	**Array Config.**
850 MHz	0.2 sec	Cardiod pattern HPBW=120° G=8dB	UCA 8 elements

Table 1: System parameters

The simulated antenna is a Uniform Circular Array with 8 cardioid elements as shown in Figure 5.13

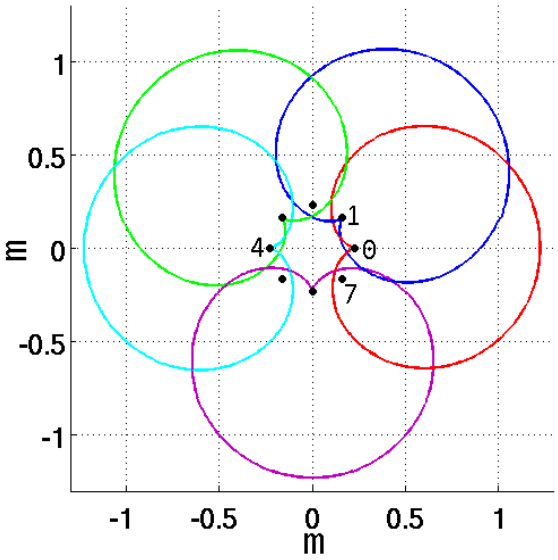

Figure 5.13 Uniform Circular Array with pattern cardiod elements

Table 2 shows the angular sectors where the multipath has been generated considering the signal model defined in section 5.2.2. Specifically the multipath around TX1 and TX" and the multipath around the target positions (Ground Clutter) have been simulated.

	Sectors of the multipath (deg)
Multipath around PIO4	-52°, - 32°
Multipath around PIO5	18°, 38°
Ground clutter	-25°,38°

Table 2: Simulated multipath angular sectors

Figure 5.14 shows the element radiation patterns and highlights the angular sectors corresponding to multipath and ground clutter. The black dot lines highlight the multipath angular regions around the IOs, whereas the orange dot lines are related to the ground clutter.

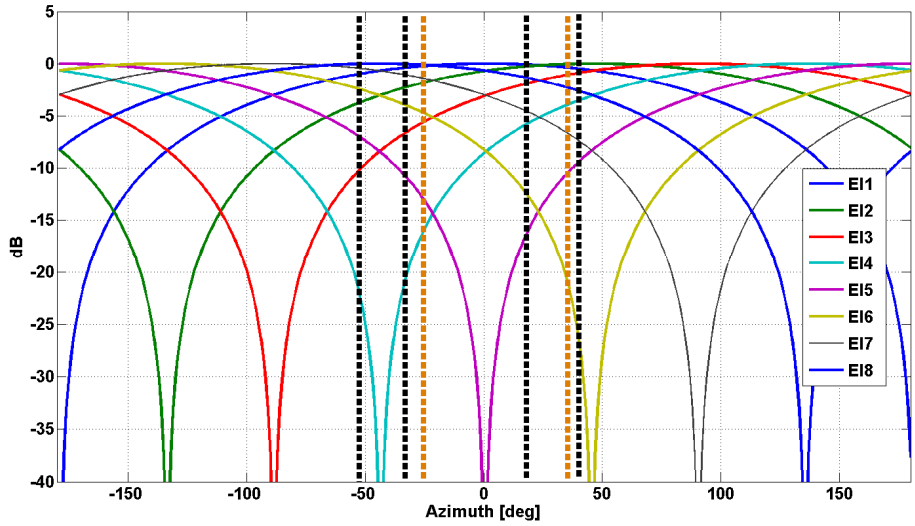

Figure 5.14 Simulated ground clutter and multipath directions

To demonstrate the effect of the interference suppression by spatial filtering we calculate the range-Doppler maps before and after the defined spatial adaptive signal processing. Specifically in Figure 5.16 the range-Doppler map $M_0(\tau,\nu)$ considering the first array element is shown. We can observe from Figure 5.16 that the five targets are completely masked by the interference.

To evaluate the disturbance cancellation capability of adaptive algorithms, the Signal Interference Noise Ratio SINR can be defined as follows

$$SINR_{dB} = 10\log_{10}\left(\frac{P_{\text{Target}}}{P_{\text{Clutter}}}\right) \tag{5.21}$$

where P_{Clutter} is the power of returns of clutter and P_{Target} is the power of the target where the target is located within the range-doppler map. The SINR, defined in equation (5.21) and evaluated considering both the received signal and the signal after ECA filtering is shown in Figure 5.15.

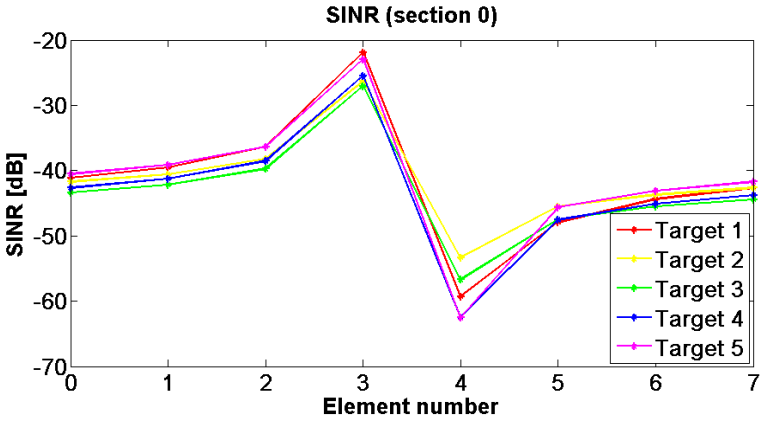

a) Received signal

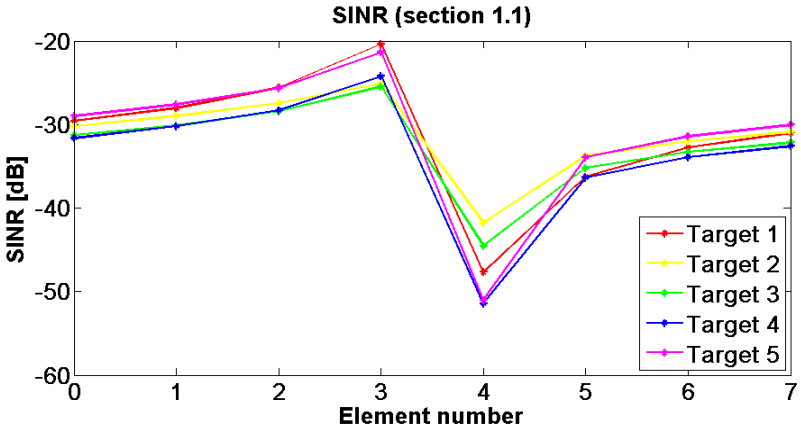

b) After ECA filter

Figure 5.15 SINR before spatial adaptive processing

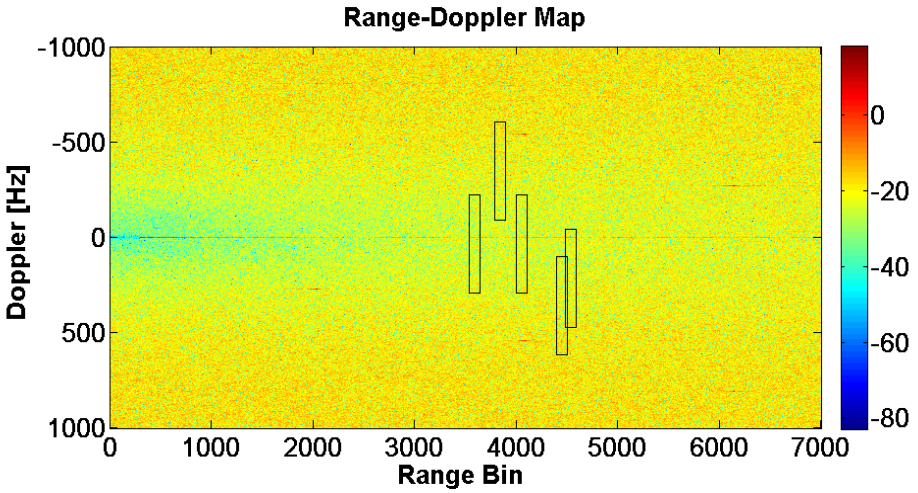

Figure 5.16 Range Doppler map relative to array element 1.

The zoomed views of the range-Doppler region after spatial filtering occupied by targets and underlined in Figure 5.16 are shown in Figure 5.17. It should be noted that all targets are clearly visible after filtering.

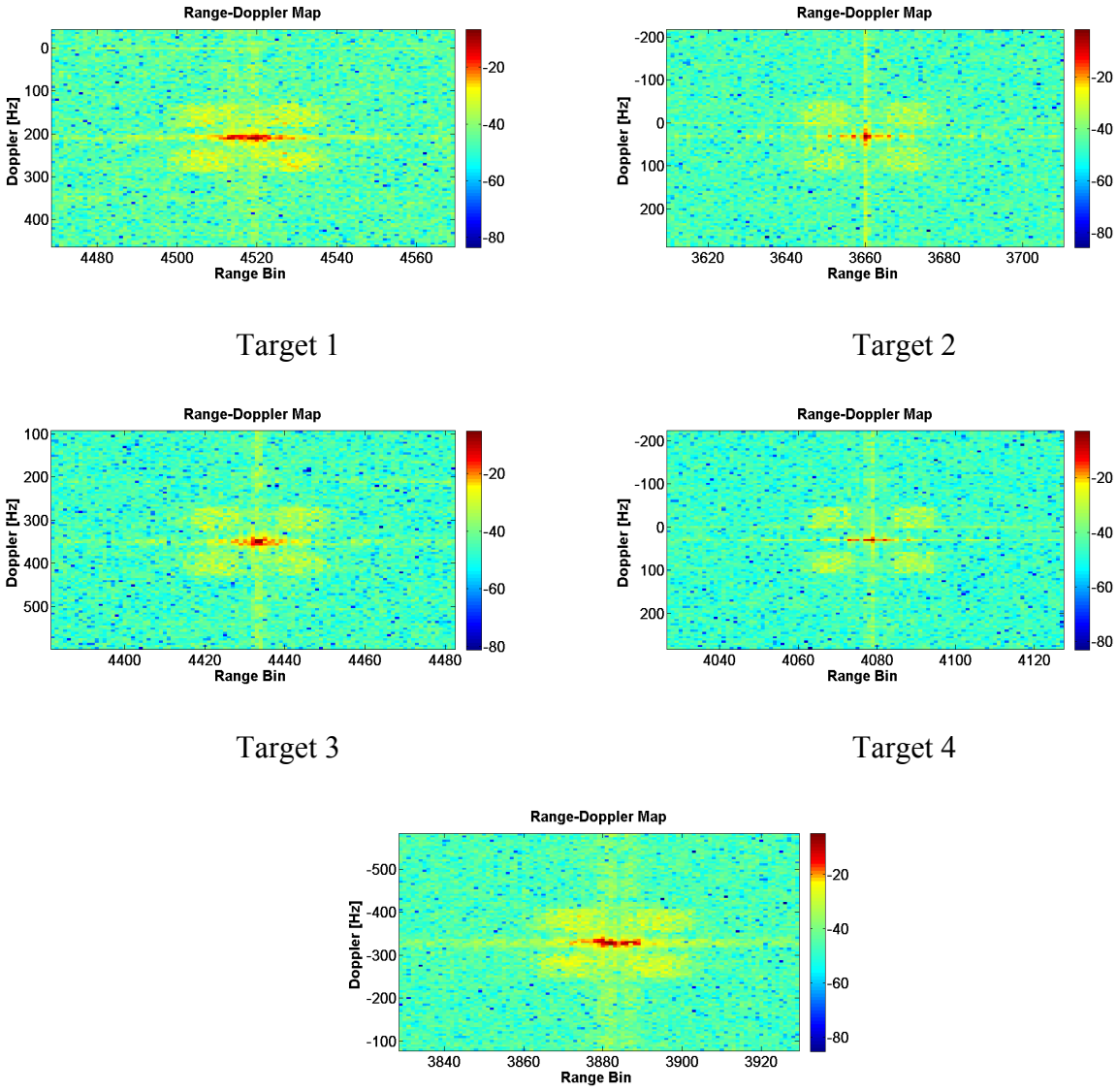

Figure 5.17 Range Doppler map after filtering

It is straightforward to observe the ability of the SAP approach to suppress the interferences and to achieve a good SINR as shown in Figure 5.18..

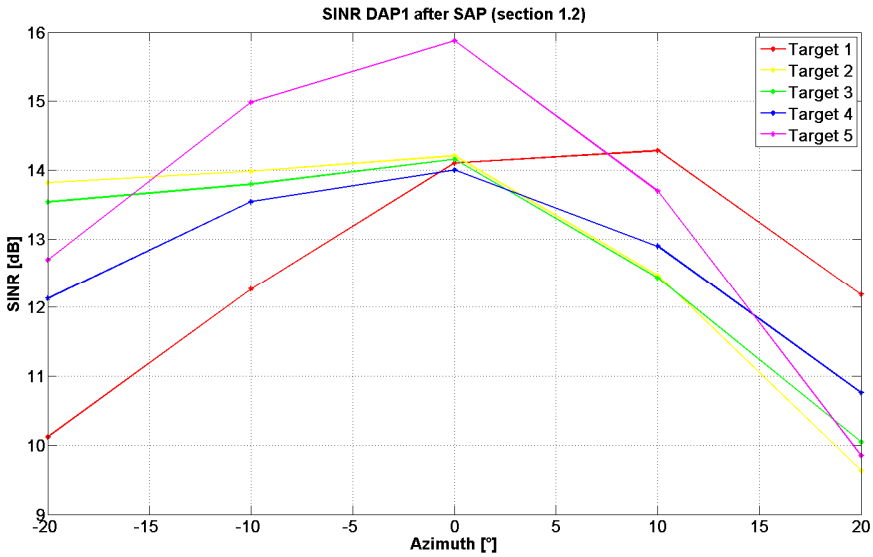

Figure 5.18 SINR after spatial adaptive processing

5.6 Chapter summary

In this chapter the main advantages of a multichannel passive radar system using digital beamforming techniques have been detailed. The main advantages are: form at the same time multiple beams to collect reference and surveillance channel, improve the target localization process and the interference suppression. The main drawbacks of a traditional solution based on the application of digital beamforming techniques before the matched filter have been underlined. A new scheme, based on the application of digital adaptive beamforming after matched filter has been proposed. The proposed technique improves the performances in terms of clutter cancellation on the surveillance channel. Once defined a multichannel signal model the effectiveness of the proposed solution has been demonstrated on the simulated data.

Chapter 6.

Space-time adaptive processing

6.1 Introduction

The traditional temporal adaptive processing techniques, based on the noise-canceller structure, cannot be efficient in presence of Internal Clutter Motion (for instance in the presence of sea clutter) since it is not able to reduce non-zero Doppler interference. In order to avoid this problem temporal adaptive techniques, developed for active pulse radar, have been extended to a passive radar scenario. This analysis has been carried out in chapter 4. In chapter 5 we extended the study to a multichannel passive radar and spatial adaptive processing has been analyzed to improve the interference cancellation. In presence of a moving PBR, as in a moving platform active radar, the clutter spectrum exhibits an angular direction–dependent mean frequency. The classical algorithms, used in a moving active radar and known as Ground Moving Target Indication techniques, are based on Space Time Adaptive Processing (STAP) techniques. In the STAP literature, it is assumed that the available signal is composed by the echoes from a pulse-Doppler radar, as we have mentioned in chapter 1. Their employment in a PBR scenario requires some adaptations. Using the theory developed in the previous chapters, we examine the feasibility of applying STAP processing to bistatic passive radars and we show how the classical STAP techniques can be applied to a PBR system that operates in a continuous mode.

The chapter is organized as follows. The main works proposed in literature dealing with moving passive radar are listed in Section 6.1. Section 6.2 introduces how the 1D temporal and spatial adaptive techniques, presented in the previous chapters, can be

extended to STAP techniques. Therefore the applicability of STAP techniques in a passive radar scenario is demonstrated. In Section 6.4 the classical STAP algorithms are reformulated in the contest of the passive radar receiver. In section 6.5 the results of the proposed algorithm simulations are presented.

6.2 Literature review

Most of the published works dealing with passive radar considerer stationary ground based systems. A feasibility study on applying passive radar technology to a moving receiver platform has been started in [Dawidowicz 2008], [Dawidowicz 2009], [Kulpa 2011], [Kulpa 2011_1], [Raout 2006-2010], with some experiments carried out using a ground vehicle and airborne platform. The first results obtained and the advantages of a passive radar system show its high potential for future research development. With a moving PBR, as in a moving active radar, the main issue is the suppression of clutter. In a mobile system, the Doppler shift relative to a stationary ground object echoes is non-zero and it is strictly related to its angular location. Bistatic geometry is in general more complex than monostatic geometry. The potential of STAP for bistatic radar has been discussed in detail in [Klemm 2000]. The clutter Doppler spectrum, especially by using a wide antenna field of view, may be wide enough to mask targets of interest present at the same range cell. The target detection by filtering the clutter in frequency Doppler domain is difficult with a single antenna. An improvement in clutter suppression can be achieved by using an antenna array and two-dimensional signal processing. Space-Time adaptive processing is typically used to filter out interferences in GMTI radars in order to detect slow moving target. STAP offers a benefit over a separate spatial and temporal processing when there is a correlation between the clutter signal direction of arrival and its Doppler frequency. The basics of STAP are well understood. For an introduction the paper by Brennan, et al. [Brennan 1973], the report by Ward [Ward 1994] and the textbooks by Klemm [Klemm 2002] and Guerci [Guerci 2003] are recommended.

6.3 Applicability of STAP to passive bistatic radars

Space-Time processing is a technique widely used in active radar installed on mobile platforms. A block diagram of a STAP-based receiver applied to an active pulse radar is depicted in Figure 6.1. Matched filter is done separately on the returns from each pulse after which the signals are sampled and sent to the STAP digital processor.

The k-th matched filter output $s_{cc}^{m}(\tau, \boldsymbol{r}_k)$ can be seen as the cross correlation between the transmitted pulse $u_p(t)$ and the received signal collected into the m-th PRI $s_R^m(t, \boldsymbol{r}_k)$

$$s_{cc}^{m}(\tau, \boldsymbol{r}_k) = \int_0^{PRI} s_R^m(t, \boldsymbol{r}_k) u_p^*(\alpha - \tau) d\alpha \tag{6.1}$$

For each PRI, L time (range) samples are collected to cover the desired range interval. The data available to the STAP signal processor consists of M pulses on each of K elements for each range bin. This multidimensional data set is often visualized as the space-time-range cube of complex samples as shown in Figure 6.1. The space dimension corresponds to consecutive elements of the antenna array and the time dimension, also called "slow time", corresponds to the echoes received from consecutive transmitted pulses.

Considering a fixed range gate which is to be tested for target presence, the two-dimensional STAP processor can be defined as a linear filter that combines the collected spatial and temporal samples $s_{cc}^{m}(\tau, \boldsymbol{r}_k)$ to produce a scalar output. The spatial and temporal samples $s_{cc}^{m}(\tau, \boldsymbol{r}_k)$ can be arranged into a matrix $\boldsymbol{S}_{cc}(\tau) \in \mathbb{C}^{KxM}$. We want to recall that the beamforming is an operation that combines the columns of $\boldsymbol{S}_{cc}(\tau) \in \mathbb{C}^{KxM}$, while the temporal or Doppler filtering operation combines the rows of $\boldsymbol{S}_{cc}(\tau) \in \mathbb{C}^{KxM}$. The STAP processor can be represented by an KM-dimensional weight vector and its output can be defined as the inner product of the weight vector $\boldsymbol{w} \in \mathbb{C}^{KMx1}$ and the space-time snapshot of interest $\boldsymbol{s}_{cc}(\tau)$ obtained by stacking the columns of $\boldsymbol{S}_{cc}(\tau) \in \mathbb{C}^{KxM}$. Since the target DOA and velocity are unknown a priori, a STAP processor typically computes multiple weight vectors that form a filter bank to cover all potential target DOA and Doppler frequencies. Ideally the STAP processor

provides coherent gain on target while forming angle and Doppler response nulls to suppress clutter and jamming.

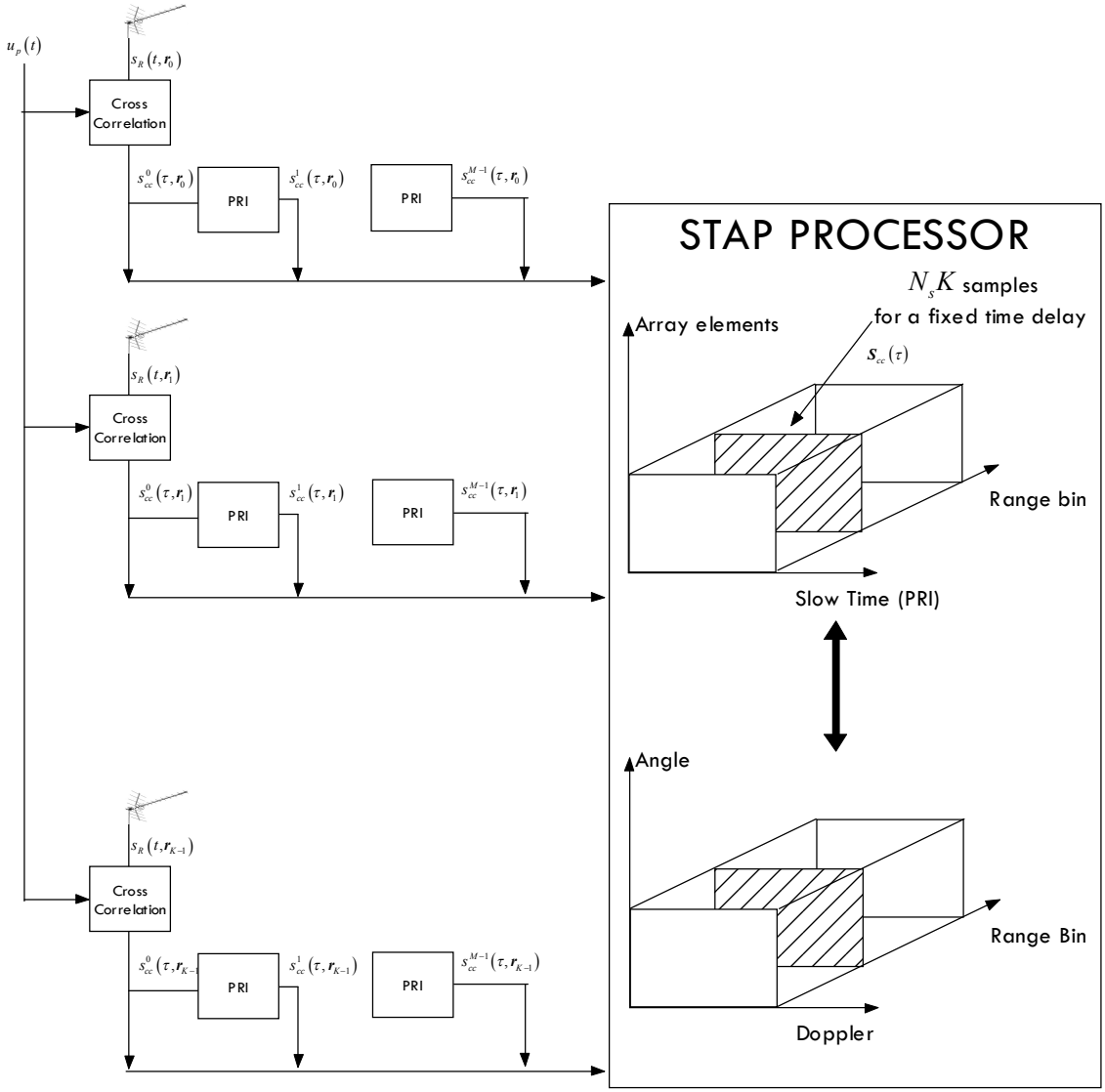

Figure 6.1 STAP processing in active pulse radars.

A PBR system operates in a continuous mode and the received signal is not available in the classical array elements-slow time-range domain. In a PBR system the detection is performed by using the matched filter processing as we have seen in chapter 3. Each receiver output $x(t,\boldsymbol{r}_k)$ can be cross correlated with the estimate of the reference signal to produce K range-Doppler maps denoted by $M_k(\tau,\nu)$ and defined as

$$M_k(\tau,\nu)=\int_0^{T_{\text{int}}} x(t,\boldsymbol{r}_k)x_{ref}^*(t-\tau)e^{-i2\pi\nu t}dt \tag{6.2}$$

where $x_{ref}(t)$ can be obtained at the output of the reference channel beamforming, as shown in chapter 5. A typical block diagram of an array passive radar system is depicted in Figure 6.2. As the target is illuminated continuously, Doppler modulation of the received signal is taken into account during the integration time and not only in the slow time as we have seen in the case of an active pulse radar. The output of each matched filter is directly obtained in the range-Doppler domain. Therefore the standard STAP techniques cannot be applied directly to this signal. The K range-Doppler maps $M_k(\tau,\nu)$ can be combined by using a spatial matched filter or an adaptive spatial processing as we have described in chapter 5. Exploiting the cross correlation algorithms, defined in chapter 3, and the extended temporal adaptive matched filter, analyzed in chapter 4, we can obtain an useful signal to STAP processor. Specifically in the next subsections we define two possible signals, obtained at the output of the array passive radar receiver, that can be used by a standard STAP processor. The first one is based on the direct FFT matched filter approach and it has been proposed in literature [Kulpa 2011], [Raout 2006-2010]. The second one is based on both batches and OFDM matched filter architecture.

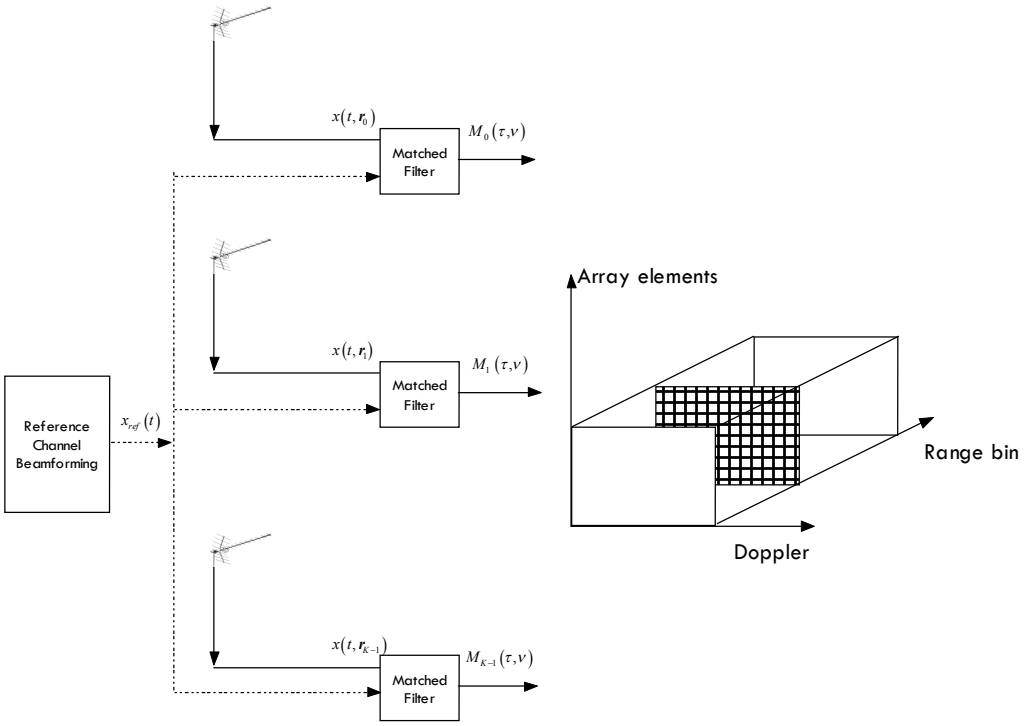

Figure 6.2 Array passive radar system.

6.3.1 STAP with direct FFT approach

In [Raout 2006-2010] it has been demonstrated that by computing the appropriate mixing product, the signal is converted into a pulse-Doppler like signal, hence making the application of STAP to arbitrary signals straightforward. As noted in section 3.2.1 the output of each matched filter, defined in equation (6.2) can be seen as the Fourier transform of the mixing product $x_m(t,\tau,\mathbf{r}_k)$

$$M_k(\tau,\nu)=\int_0^{T_{\text{int}}} x(t,\mathbf{r}_k)x_{ref}^*(t-\tau)e^{-i2\pi\nu t}dt=\int_0^{T_{\text{int}}} x_m(t,\tau,\mathbf{r}_k)e^{-i2\pi\nu t}dt \tag{6.3}$$

The signal $x_m(t,\tau,\mathbf{r}_k)$ is the mixing product, defined in section 3.2.1, between the reference signal and the received signal at the k-th element. The block diagram of an array passive radar system, shown in Figure 6.2, can be modified as shown in Figure 6.3.

The signal obtained at the output of the temporal matched filter in the section 1 is exactly the same obtained in Figure 6.2. This fact can be explained considering that the direct FFT algorithm is an optimum approach as we have demonstrated in section 3.2.1. Using a temporal adaptive processing instead of a temporal matched filter, as defined in chapter 4, we can obtain a signal processing architecture based on the application of sequential 1D temporal and spatial processing. Then we may process the data obtained in section 0 (see Figure 6.3) from one range bin in the two-dimensional domain having sampling time t as one dimension and space or array elements as second dimension. The block diagram of the direct FFT-STAP processing is shown in Figure 6.4. The inputs to the STAP processor are the mixing products from each receiver antenna array calculated for a specific range bin. This signal is not exactly equivalent to the received signal by a active pulse radar because the mixing product is obtained before the cross correlation block.

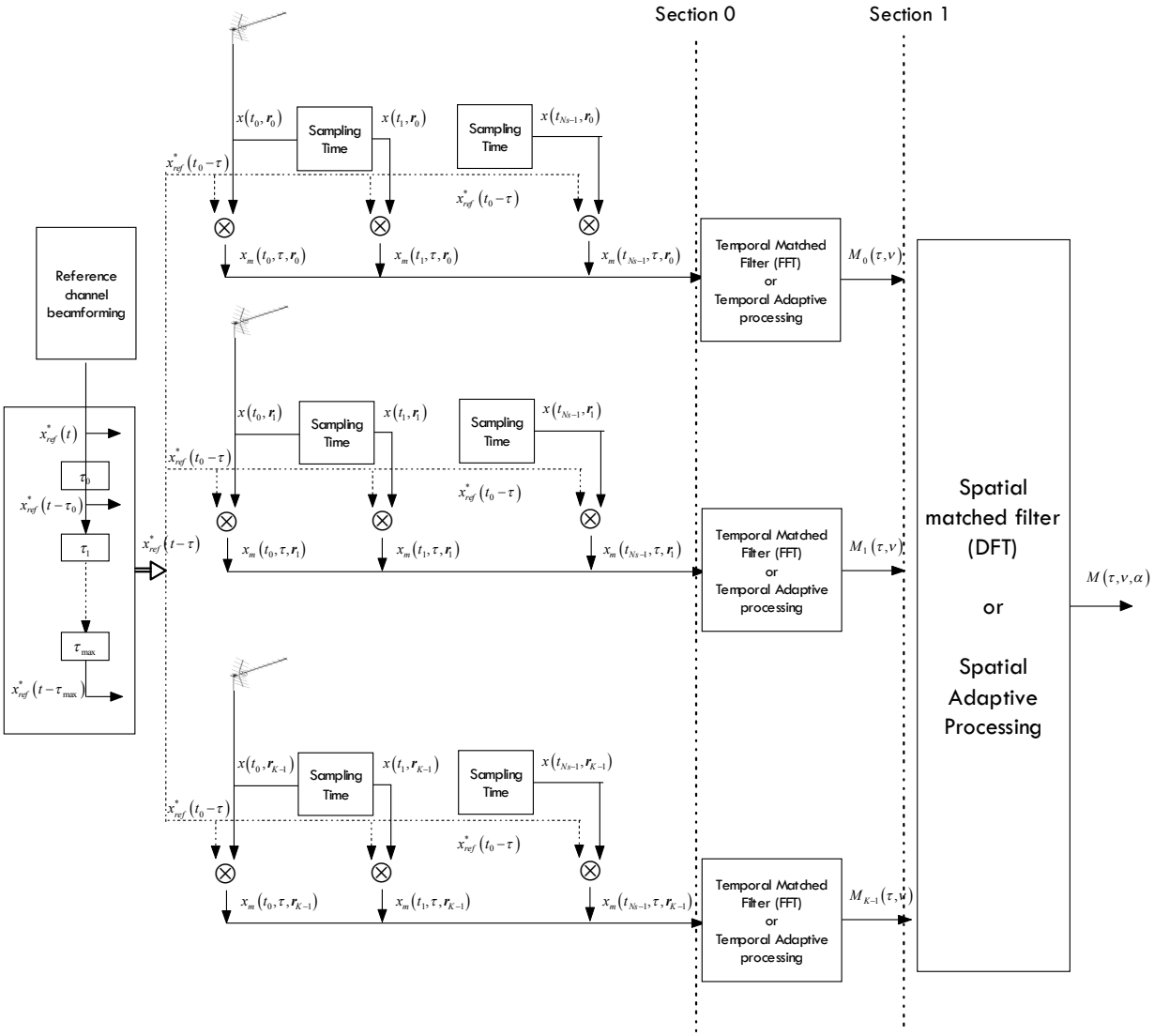

Figure 6.3 Array passive radar system with direct FFT approach

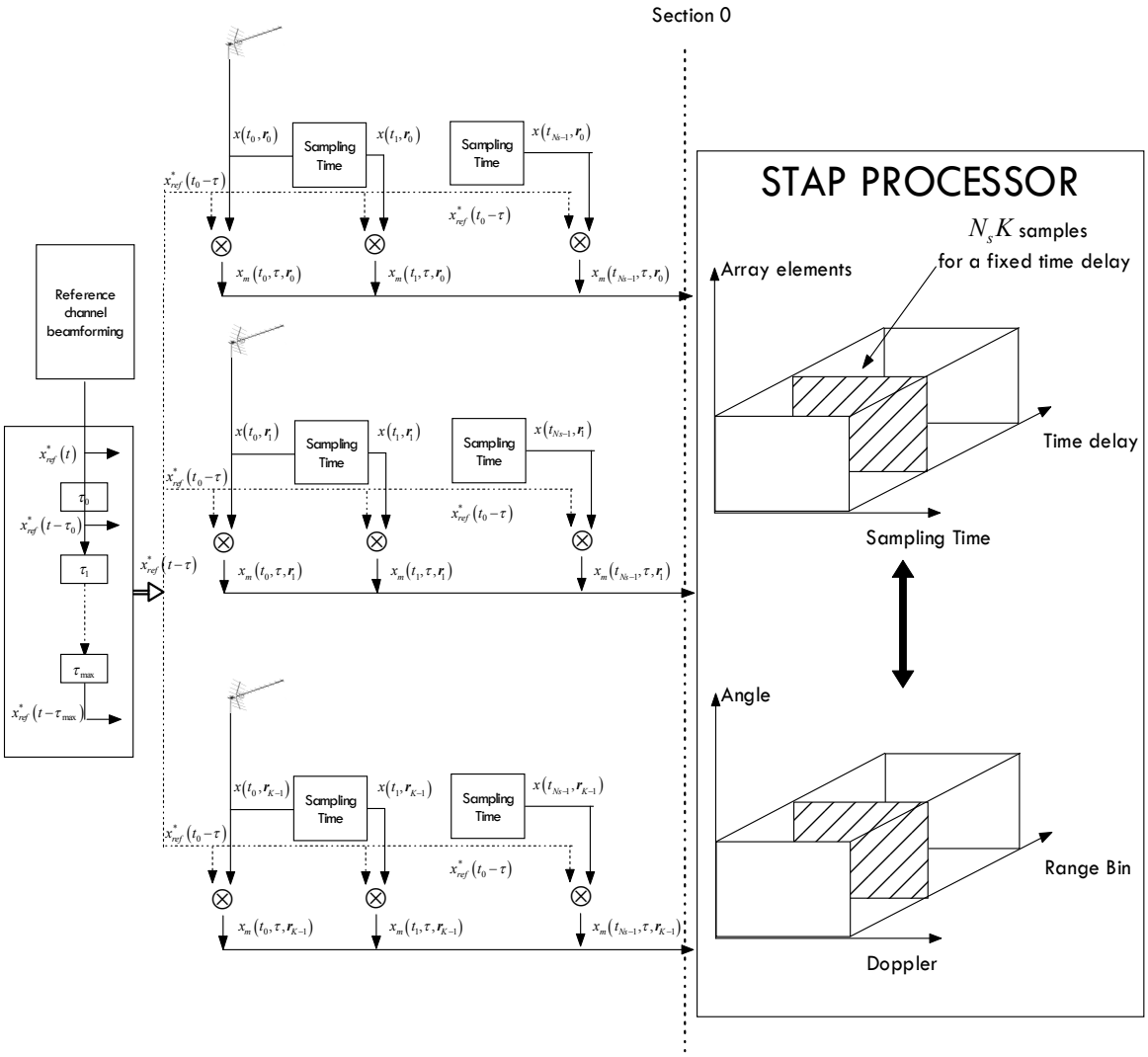

Figure 6.4 PBR-direct-FFT-STAP architecture

6.3.2 STAP with the batches algorithm

Alternatively to the previous architecture the input signal to the STAP processor can be calculated considering respectively the batches algorithm and the OFDM matched filter defined in Chapter 3. As noted in section 3.3.1 the output of each matched filter, defined in equation (6.2) can be seen as

$$M_k(\tau,\nu) = \sum_{i=0}^{n_B-1} e^{-j2\pi\nu i T_B} \int_0^{T_B+\tau_{\max}} x^i(t,\boldsymbol{r}_k) x_i^*(t-\tau) e^{-j2\pi\nu t} dt = \\ = \sum_{i=0}^{n_B-1} e^{-j2\pi\nu i T_B} x_{cc}^i(\tau,\boldsymbol{r}_k) \tag{6.4}$$

This signal $x_{cc}^i(\tau,\boldsymbol{r}_k)$ is the cross correlation, defined in section 3.3.1, between the i-th reference signal batch and the i-th received signal batch at the k-th array element.

The block diagram of an array passive radar system, shown in Figure 6.2, can be modified as shown in Figure 6.5. The signal obtained at the output of the temporal matched filter in the section 1 is not exactly the same obtained in Figure 6.2. This fact can be explained considering that the batches algorithm is a sub-optimum approach as we have widely demonstrated in section 3.3.1. Using a temporal adaptive processing instead of the temporal matched filter, as defined in chapter 4, we can obtain a signal processing architecture based on the application of sequential 1D temporal and spatial processing. Then we may process the data obtained in section 0 from one range bin in the two-dimensional domain having “slow time” or batch time as one dimension and space as second dimension. We can observe that the signal obtained in section 0 is equivalent to the classical range-slow time signal received by an active pulse radar. All STAP techniques defined for active pulse radar can be applied to this signal. The block diagram of the batches-STAP processing is shown in Figure 6.6.

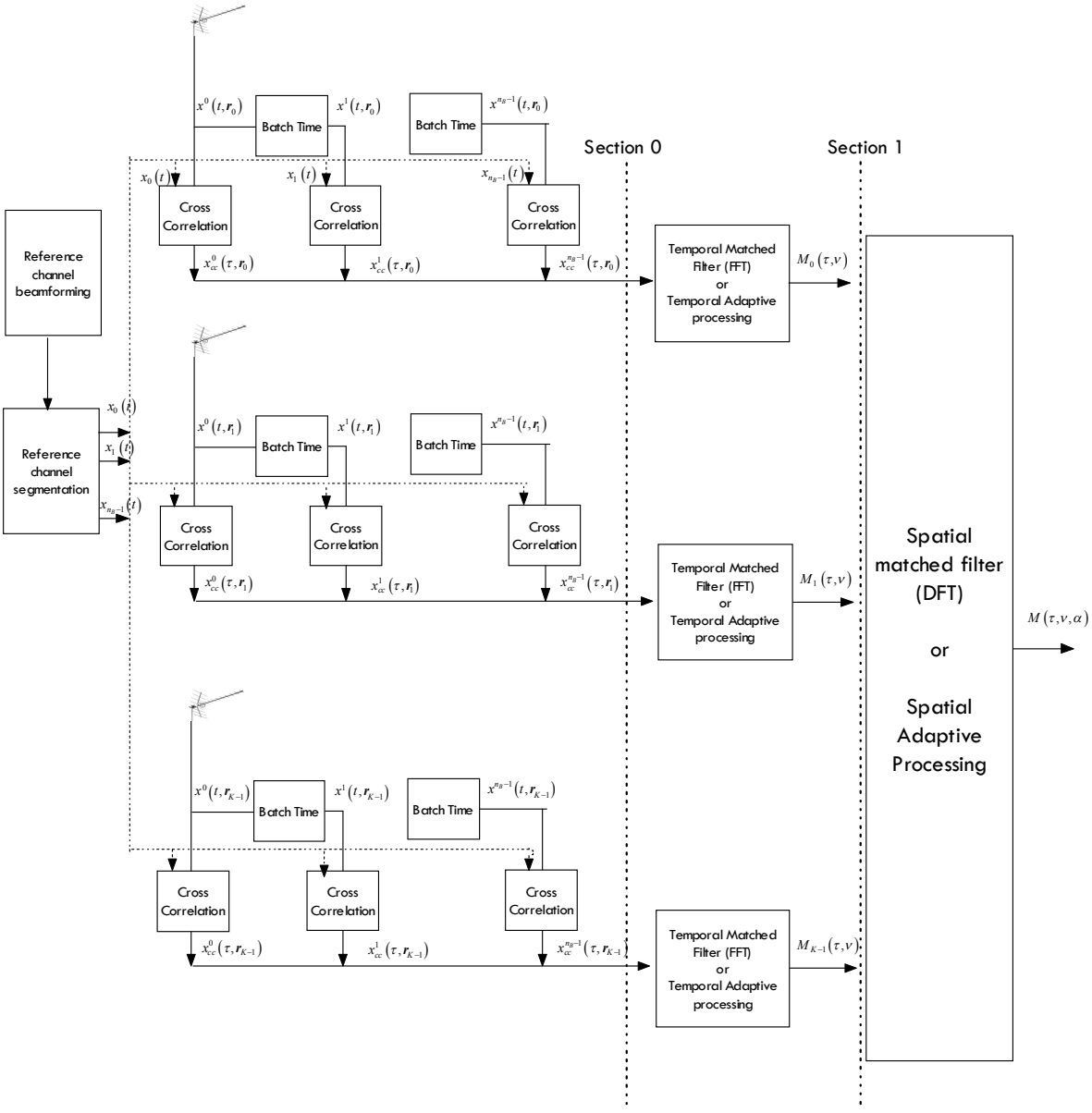

Figure 6.5 Array passive radar system with batches approach

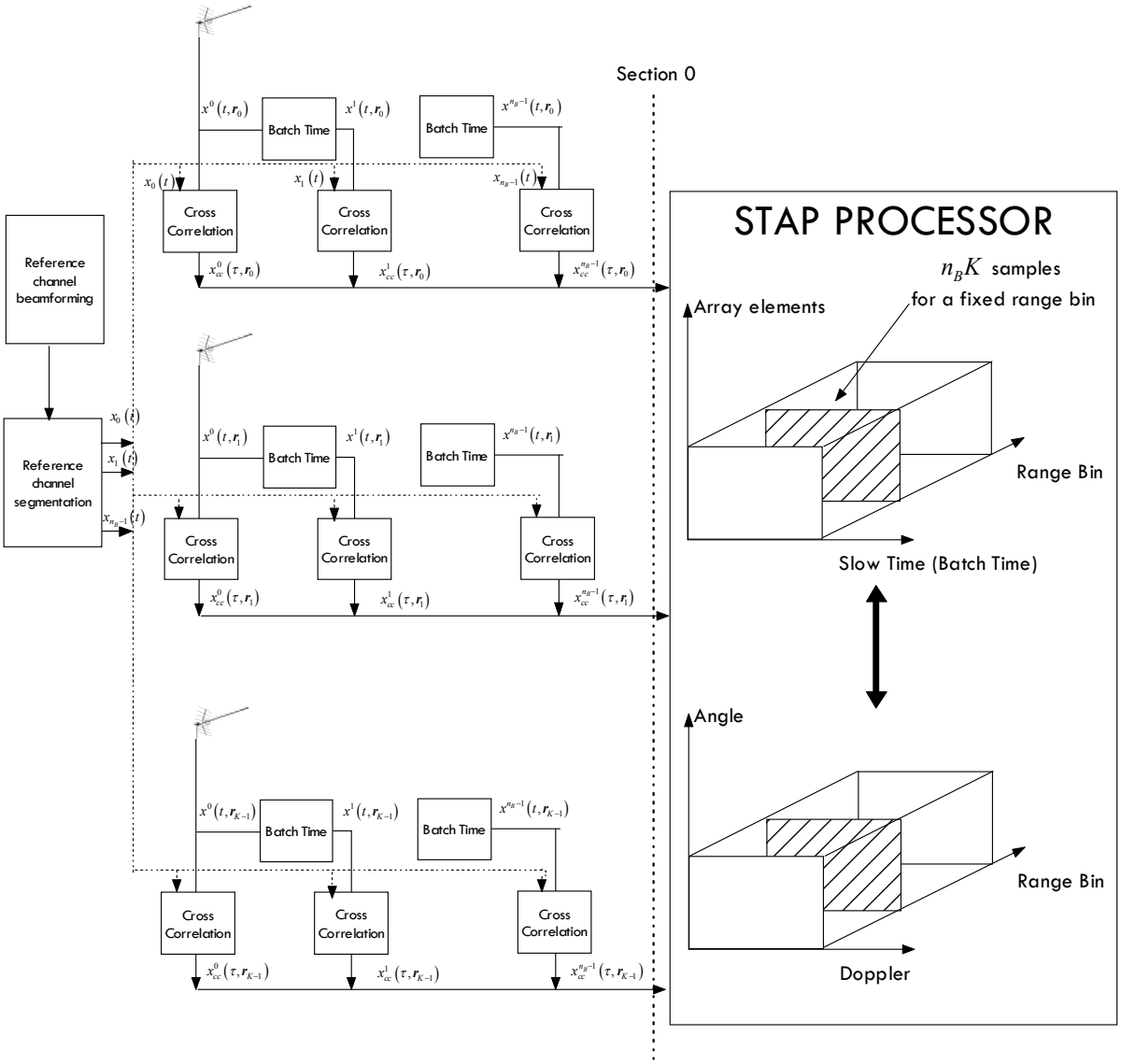

Figure 6.6 PBR-batches-STAP architecture

Considering the theoretical development of the previous chapters the batch-STAP architecture can be easily defined for the OFDM modulation as shown in Figure 6.7.

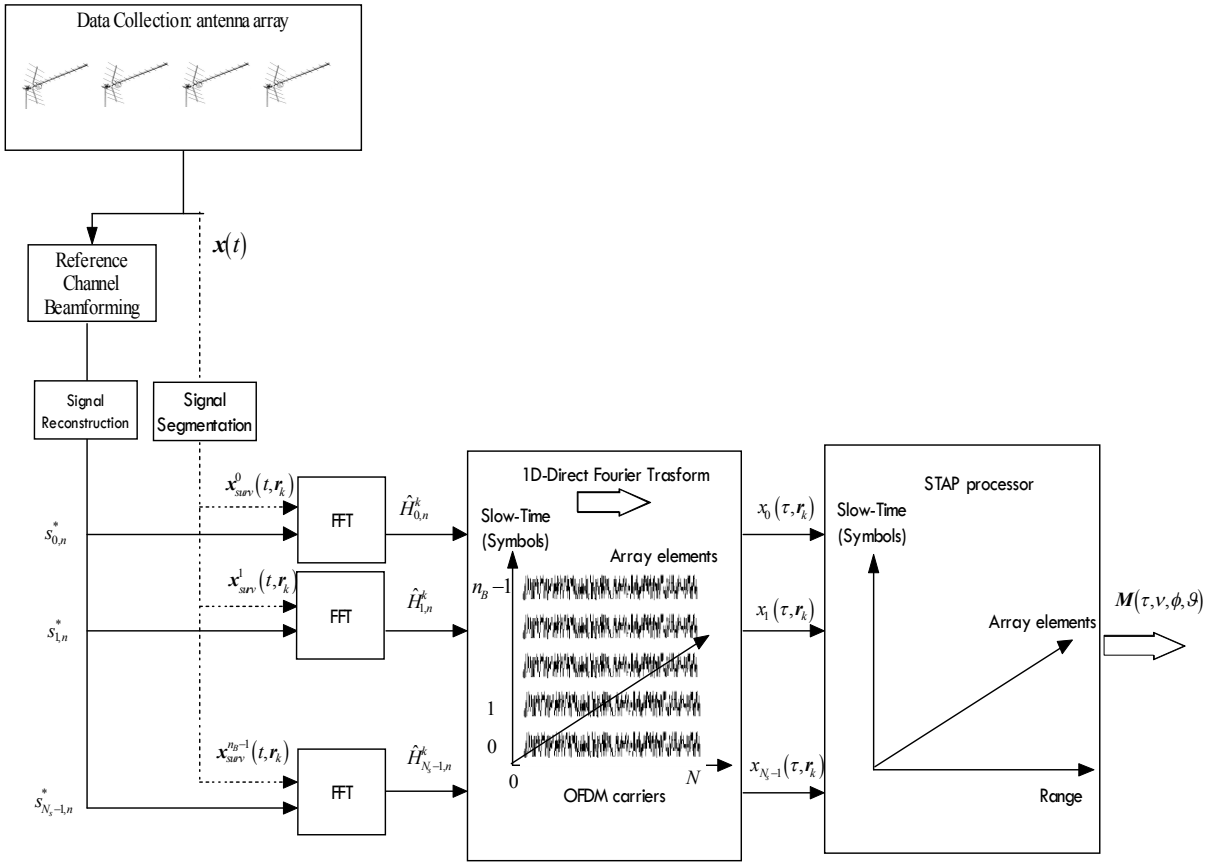

Figure 6.7 PBR -OFDM-STAP architecture

Each receiver output is matched filter using the conventional estimate of the reference waveform to produce $x_i(\tau, \boldsymbol{r}_k)$ as we have seen in Chapter 3. We can observe that the signal $x_i(\tau, \boldsymbol{r}_k)$ is in the domain of the classical STAP data cube.

6.4 STAP algorithms

Defining the spatial steering vector $\boldsymbol{v}_s(\phi, \vartheta)$ as in equation (5.1) and the temporal steering vector $\boldsymbol{v}_{DFFT}(\nu)$ as in equation (4.9) we can obtain the space-time steering vector as

$$\boldsymbol{v}_{ST}(\nu,\phi,\vartheta)=\boldsymbol{v}_{DFFT}(\nu)\otimes\boldsymbol{v}_{s}(\phi,\vartheta) \tag{6.5}$$

where $\otimes$ is the Kronecker product.

For each τ the complex multi-channel outputs may be assembled into the space-time snapshot vector $\boldsymbol{x}(\tau)\in\mathbb{C}^{NKx1}$ as

$$\boldsymbol{x}(\tau)=\left[\boldsymbol{x}(t,\tau,\boldsymbol{r}_0)\quad ...\quad \boldsymbol{x}(t,\tau,\boldsymbol{r}_{K-1})\right] \tag{6.6}$$

The space-time matched filter evaluated at both the angular direction and frequency Doppler of interest can be written as

$$\boldsymbol{w}_{conv}(\nu,\phi,\vartheta)=\boldsymbol{v}_{ST}(\nu,\phi,\vartheta) \tag{6.7}$$

The theory developed in chapter 1 can be applied in this case defining the vector $\boldsymbol{s}_0$, shown in equation (1.13), equal to the space-time steering vector. $\boldsymbol{v}_{ST}(\nu,\phi,\vartheta)$. Also in this case the natural extension of the matched filter is the adaptive matched filter which can be defined as

$$\boldsymbol{w}(\nu,\phi,\vartheta)=\gamma\hat{\boldsymbol{R}}_i^{-1}\boldsymbol{v}_{ST}^{H}(\nu,\phi,\vartheta) \tag{6.8}$$

where $\hat{\boldsymbol{R}}_i\in\mathbb{C}^{NKxNK}$ is the estimated interference covariance matrix by using the SCM algorithm.

The space-time snapshot considering the direct-FFT and the batches approaches can be respectively defined as

$$\begin{aligned}\boldsymbol{x}_{DFFT}(\tau)&=\left[\boldsymbol{x}_m(\tau,\boldsymbol{r}_0)\quad ...\quad \boldsymbol{x}_m(\tau,\boldsymbol{r}_{K-1})\right]\in\mathbb{C}^{N_sKx1}\\ \boldsymbol{x}_B(\tau)&=\left[\boldsymbol{x}_{cc}(\tau,\boldsymbol{r}_0)\quad ...\quad \boldsymbol{x}_{cc}(t,\tau,\boldsymbol{r}_{K-1})\right]\in\mathbb{C}^{n_BKx1}\end{aligned} \tag{6.9}$$

The dimension of the interference correlation matrix $\hat{\boldsymbol{R}}_i\in\mathbb{C}^{NKxNK}$ is related to

- the number of the sensors array K and the number of samples N_s for the direct FFT approach
- the number of the sensors array K and the number of batches n_B for the batches approach

The training data set $\Omega_{training}^{NxN_t}$ can be selected in the range domain τ for both approaches. It is important to recall that in the case of the direct-FFT approach, the input signal to the STAP processor is not exactly equivalent to the received signal by a

active pulse radar because the mixing product is obtained before the cross correlation block.

The main advantages of the proposed architecture, based on the batches algorithm, can be summarized as:

- the dimension of the space-time snapshot for the range cell τ is $n_B K$. This value is smaller than $N_s K$. Therefore the dimension of the correlation matrix is $n_B K$ and the associated computational load is reduced.
- to obtain a useful estimate, the training data set has to be homogeneous over a number of training data relatively large compared to the value of $n_B K$. Several techniques have been developed to resolve this issue.
- after the range matched filter it is possible to separate the target component from interference component in order to avoid the presence of the useful signal in the training data set.

From equation (6.8) we can see that the STAP filter can be obtained in a similar way to both adaptive beamforming and temporal processing as we have shown in the previous chapters. In the STAP processing the dimension of the interference correlation matrix $\hat{\boldsymbol{R}}_i \in \mathbb{C}^{NKxNK}$ is related to the number of sensors array K and the number of samples N. Therefore the dimension of the space-time interference-plus-noise correlation matrix is greater for STAP than for the separate 1-D temporal and spatial adaptive processing. Therefore the problems related to the estimation and the inversion of the interference correlation matrix are amplified. Several techniques, well known in the GMTI-STAP literature, have been developed to reduce the number of samples required to perform a useful estimation [Ward 1994], [Klemm 2002], [Guerci 2003]. In this first studies we used a method based on the diagonal loading algorithm to demonstrate the applicability of STAP techniques to a passive radar scenario. Other interesting types of algorithms, like the Joint Domain Localized (JDL) method or the Principal Component method, have been proposed considering the traditional architecture [Raout 2006-2010] Further studies about the applications of these other classical techniques on the proposed architecture will be done.

6.5 Simulation results

The considered PBR scenario assumes that a moving receiver platform is equipped with a side-looking ULA composed by eight elements. The radar receiver moves along axes x with a constant velocity $V_p\hat{\boldsymbol{x}}$.

The simulations are performed utilizing DVB-T signals of a carrier frequency equal to 800 MHz and a bandwidth of 8 MHz. The sampling frequency of the system is equal to 9 MHZ and the integration time is equal to 600 ms. The detailed geometry of the radar scene is presented in Figure 6.8.

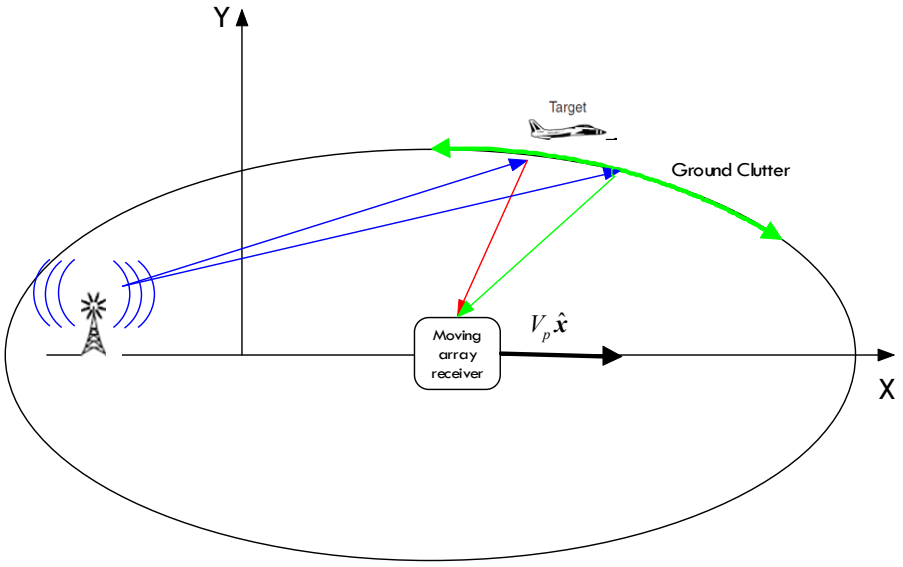

Figure 6.8 PBR simulation geometry

The range-Doppler map evaluated before applying the STAP processor is shown in Figure 6.9. The target is clearly masked by the interference echoes. The range-Doppler map after the application of the STAP filter is shown in Figure 6.10.

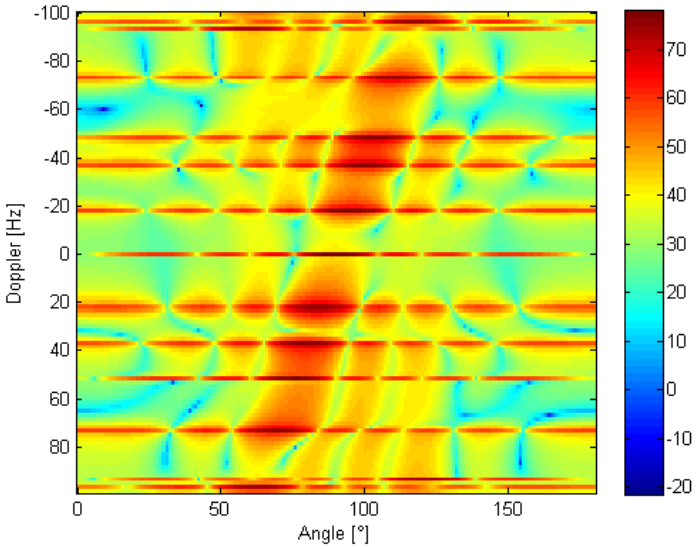

Figure 6.9 Range-Doppler map before STAP

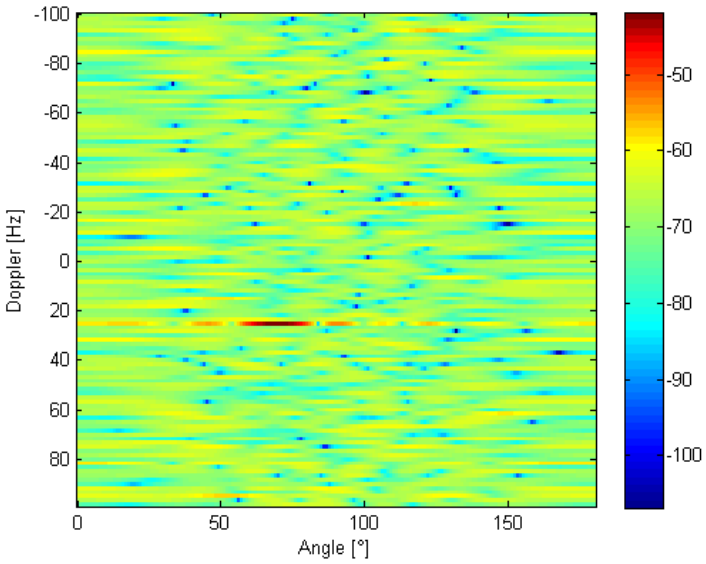

Figure 6.10 Range-Doppler map after STAP

6.6 Chapter summary

In this chapter we have demonstrated how the 1D temporal and spatial adaptive techniques can be extended to STAP techniques. In presence of a moving platform active radar an improvement in clutter suppression can be achieved by using an antenna

array and two-dimensional STAP signal processing. In the STAP literature, it is assumed that the available signal is formed by the echoes from a pulse-Doppler radar. We have shown how the classical STAP techniques can be applied to a PBR system that operates in a continuous mode. An alternative solution to work on the mixing product has been proposed and its advantages have been described. In this first studies we have used a simple technique to demonstrate the applicability of the STAP techniques to a passive radar scenario. The effectiveness of the proposed solution has been demonstrated on the simulated data. Further studies about the applications of other classical techniques on the proposed architecture will be done.

Chapter 7.

Conclusions

In this thesis the applicability of adaptive signal processing techniques in a multichannel passive bistatic radar has been investigated. The main features of the signal processing chain adopted in a typical passive radar scenario has been presented and a comparative study between optimum and sub optimum methods has been presented to evaluate the "2D cross correlation function" for a passive bistatic radar. A new detailed formulation of the sub optimum "batches algorithm" has been proposed. The defined batches algorithm has been shown to yield comparable performance with respect to the optimus ones while strongly reducing the computational load. The exact matched filter formulation for OFDM waveforms has been derived and it has been shown that this approach is similar to the batches algorithm considering the same small Doppler approximation. The analogies of this approach with the classical techniques used in active pulse radars have been underlined.

A variety of temporal adaptive signal processing techniques have been developed for the removal of the interference component in the surveillance channel before the matched filter. Typically these techniques are based on the adaptive noise canceller structure. We have defined an adaptive matched filter solution as an extension of the batches matched filter formulation. The main advantages of this alternative solution are the possibility to suppress both static clutter and affected by ICM together with a lower computational load.

The main advantages of a multichannel passive radar system making use of digital beamforming and the main drawbacks of a traditional solution based on the application of digital beamforming techniques before the matched filter have been underlined. A new scheme, based on the application of digital adaptive beamforming after matched filter has been proposed.

In presence of a moving platform active radar an improvement in clutter suppression can be achieved by using an antenna array and two-dimensional STAP signal processing. In the STAP literature, it is assumed that the available signal is formed by the echoes from a pulse-Doppler radar. We have shown how the classical STAP techniques can be applied to a PBR system that operates in a continuous mode. We demonstrated how the proposed 1D temporal and spatial adaptive techniques can be extended to STAP techniques.

A PBR system operates in a continuous mode, therefore the received signal is not available in the classical array elements- slow time- range domain such as in an active pulse radar. The results presented in this thesis show how the adaptive processing techniques, well known in active pulse radars, can be successfully applied in a passive radars scenario. Using a suitable signal processing architecture we have defined an equivalent signal to that of an active pulse radar and we have demonstrated the applicability of standard signal processing techniques to this type of signals.

References

[Backer 2005] C.J Baker, H D Griffiths and I. Papoutsis 'Passive coherent location radar systems: Part 2: Waveform properties' IEE Proceedings Radar Sonar and Navigation. Special issue: Passive Radar system Volume 152 Number 3 june 2005 pages 160-169.

[Berger 2008] C. R. Berger, S. Zhou, and P. Willett, "Signal extraction using compressed sensing for passive radar with OFDM signals," in Proc. Int. Conf. Inf. Fusion, Cologne, Germany, Jun. 2008.

[Berger 2010] C. R. Berger, B. Demissie, J. Heckenbach, P. Willett, S. Zhou, " Signal Processing for Passive Radar Using OFDM Waveforms", IEEE Journal of Selected Topics in Signal Processing, Vol. 4, no. 1, February 2010.

[Bongioanni 2009] C. Bongioanni, F. Colone, D. Langellotti, P. Lombardo, T. Bucciarelli, "A New Approach for DVB-T Cross-Ambiguity Function Evaluation", EURAD 2009, Rome, Italy, 30 September-2 October 2009.

[Brennan 1973] L.E. Brennan, I.S. Reed, "Theory of adaptive radar", March 1973, IEEE transaction on aerospace and electronic systems, Vol. 9, No 2.

[Capria 2010] A. Capria, M. Conti, D. Petri, M. Martorella, F. Berizzi, E. Dalle Mese,R. Soleti, V. Carulli, "Ship Detection with DVB-T Software Defined Passive Radar", Proceedings of 2010 IEEE GOLD Remote Sensing Conference, April 29-30, 2010, Italian Naval Academy, Livorno, Italy.

[Capria 2010_1] A. Capria, M. Conti, D. Petri, M. Martorella, F. Berizzi, E. Dalle Mese,R. Soleti, V. Carulli, "Costal Ship Detection by DVB-T Software Defined Passive Radar: Experimental Results", Proceedings of GTTI 2010, June 21-23, 2010,

Brescia, Italy.

[Cardinali 2007] R. Cardinali, F. Colone, P. Lombardo, O. Crognale, A. Cosmi, A. Lauri, “Multipath cancellation on reference antenna for passive radar which exploits FM transmissions”, The IET International Radar Conference (Radar07), 15-18 October 2007, Edinburgh (UK).

[Cherniakov 2008] M. Cherniakov “Bistatic Radar: Emerging Technology”, 2008 John Wiley & Sons, P. E. Howland, H. D. Griffiths and C. J. Baker, Chapter 7 “Passive Bistatic Radar Systems”.

[Coleman 2008] C. Coleman, H. Yardley, and R. Watson, “A practical bistatic passive radar system for use with DAB and DRM illuminators,” in Proc. IEEE Radar Conf., May 2008, pp. 1514–1519.

[Coleman 2008_1] C Coleman, H Yardley “Passive bistatic radar based on target illuminations by digital audio broadcasting”, IET Radar Sonar and Navigation, Volume 2, Issue 5, October 2008, pp. 366-375.

[Colone 2006] F. Colone, R. Cardinali, P. Lombardo, “Cancellation of clutter and multipath in passive radar using a sequential approach”, IEEE 2006 Radar Conference, Verona, April 24-27, 2006.

[Colone 2009] F. Colone, D. W. O'Hagan, P. Lombardo, C. J. Baker "A multistage processing algorithm for disturbance removal and target detection in Passive Bistatic Radar", IEEE Trans. On Aerospace and Electronic Systems, Volume 45, Issue 2, April 2009, pp. 698-721.

[Dawidowicz 2008] B. Dawidowicz; K. S. Kulpa, "Experimental results from PCL radar on moving platform," Radar Symposium, 2008 International, pp.1-4, 21-23 May 2008.

[Dawidowicz 2009] B. Dawidowicz, K. S. Kulpa, M. Malanowski, "Suppression of the ground clutter in airborne PCL radar using DPCA technique," Radar Conference, 2009. EuRAD 2009. European, pp.306-309, Sept. 30 2009-Oct. 2 2009.

[ETSI 2009] Digital Video Broadcasting (DVB); DVB Digital Video

Broadcasting (DVB); Framing structure, channel coding and modulation for digital terrestrial television, ETSI EN 300 744 V1.6.1 (2009-01).

[Fabrizio 2008] G. Fabrizio, F. Colone, P. Lombardo, A. Farina, "Passive Radar in the High Frequency Band", 2008 IEEE Radar Conference, Rome, Italy, May 26-30, 2008.

[Fabrizio 2009] G. Fabrizio, F. Colone, P. Lombardo, A. Farina, "Adaptive beamforming for high-frequency over-the-horizon passive radar", IET Radar Sonar and Navigation, August 2009, Volume 3, Issue 4, pp. 384 – 405.

[Gao 2006] Z. Gao, R. Tao, Y. Ma, and T. Shao, "DVB-T Signal Cross-Ambiguity Functions Improvement for Passive Radar", Radar, 2006. CIE '06. International Conference on, pp.1-4, 16-19 Oct. 2006.

[Glende 2007] M. Glende, J. Heckenbach, H. Kuschel, S. Mueller, J. Schell, and C. Shumacher, "Experimental passive radar systems using digital illuminators (DAB/DVB-T)", in Proc. Int. Radar Symp., Cologne, Germany, Sep. 2007, pp. 1443-1448.

[Griffiths 1986] H.D. Griffiths, N.R.W. Long, "Television based bistatic radar". IEE Proceedings, Pt. F (Communication Radar Signal Processing), 133, 7 (1986), 649—657.

[Griffiths 2003] H.D. Griffiths, C.J. Baker, H. Ghaleb, R. Ramakrishnan and E. Willlman, "Measurement and analysis of ambiguity functions of off-air signals for passive coherent location", Electron. Lett., June 2003, 39, (13), pp. 1005-1007.

[Griffiths 2003_1] H.D. Griffiths, 'From a different perspective: principles, practice and potential of bistatic radar', Proc. International Conference RADAR 2003, Adelaide, Australia, pp1–7, 3–5 September 2003.

[Griffiths 2005] H.D. Griffiths, C.J. Baker, "Passive coherent location radar systems. Part 1: Performance prediction", IEE Proceedings on

Radar, Sonar and Navigation, 152, 3 (June 2005), 153—159.

[Griffiths 2007] H.D. Griffiths, C.J. Baker, "The signal and interference environment in Passive Bistatic Radar", Information, Decision and Control Symposium, Adelaide, 12–14 February 2007.

[Guerci 2003] J. R: Guerci "Space-Time Adaptive Processing for Radar", 2003 ARTECH HOUSE.

[Guner 2003] A. Guner, M.A. Temple, R.L. Jr Claypoole, "Direct- path filtering of DAB waveform from PCL receiver target channel", Electron. Lett., 2003, 139, pp. 118–119.

[Howland 1999] P. Howland, "Target tracking using television-based bistatic radar," IEE Proc. Radar, Sonar Navig., vol. 146, no. 3, pp. 166–174, Jun. 1999.

[Howland 2005] P. Howland, "Editorial: Passive radar systems," IEE Proc. Radar, Sonar Navig., vol. 152, no. 3, pp. 105–106, Jun. 2005.

[Howland 2005_1] P. Howland, D Maksimiuk and G Reitsma "FM radio based bistatic radar", IEE Proceedings Radar Sonar and Navigation. Special issue: Passive Radar system, Volume 152, Number 3, June 2005, pp. 107-115.

[Klemm 2000] Klemm, R.; "Comparison between monostatic and bistatic antenna configurations for STAP," *Aerospace and Electronic Systems, IEEE Transactions on* , vol.36, no.2, pp.596-608, Apr 2000

[Klemm 2002] R. Klemm, "Principles of Space-Time Adaptive Processing", IET London 2002.

[Kubica 2006] M. Kubica, V. Kubica; X. Neyt; J. Raout, S. Roques, M. Acheroy, "Optimum target detection using illuminators of opportunity,", Radar 2006 IEEE Conference, pp. 8 pp., 24-27 April 2006.

[Kulpa 2005] K.S. Kulpa, Z. Czekala, "Masking effect and its removal in PCL radar", IEE Proc. Radar Sonar Navig., Vol. 152, Issue 3, June 2005, pp. 174-178.

[Kulpa 2011] K. Kulpa, M. Malanowski, P. Samczynski, B. Dawidowicz, "The concept of airborne passive radar," *Microwaves, Radar and Remote Sensing Symposium (MRRS), 2011*, pp.267-270, 25-27 Aug. 2011.

[Kulpa 2011_1] K. Kulpa, M. Malanowski, P. Samczynski, J. Misiurewicz, M. Smolarczyk, "On-board PCL systems for airborne platform protection," *Digital Communications - Enhanced Surveillance of Aircraft and Vehicles (TIWDC/ESAV), 2011 Tyrrhenian International Workshop on*,, pp.119-122, 12-14 Sept. 2011

[Kuschel 2008] H. Kuschel, J. Heckenbach, S. Mueller, and R. Appel, "On the potentials of passive, multistatic, low frequency radars to counter stealth and detect low flying targets," in Proc. IEEE Radar Conf., May 2008, pp.1443–1448.

[Kuschel 2010] H. Kuschel, D. O'Hagan, "Passive Radar from History to Future", "International Radar Symposium (IRS) 2010, 16-18 June, Vilnius Lithuania.

[Langellotti 2009]] D. Langellotti, F. Colone, C. Bongioanni, P. Lombardo, "Comparative study of Ambiguity Function evaluation algorithms for Passive Radar", International Radar Symposium IRS 2009, Hamburg, Germany, 9-11 September 2009, pp. 325-329.

[Langellotti 2010] D. Langellotti, C. Bongioanni, F. Colone, P. Lombardo, "Impact of Synchronization on the Ambiguity Function shape for PBR based on DVB-T signals", 11th International Radar Symposium IRS-2010, June 16-18, 2010, Vilnius, Lithuania.

[Lauri 2007] A. Lauri, R. Cardinali, F. Colone, P. Lombardo, "A geometrically based multipath channel model for passive radar", The IET International Radar Conference (Radar07), 15-18 October 2007, Edinburgh (UK).

[Liberti 1996] J. C. Liberti, T. S. Rappaport, "A geometrically based model for line-of-sight multipath radio channels", Vehicular Technology

Conference, 1996. “Mobile Technology for the Human Race”, IEEE 46th, Atlanta, USA.

[Malanowski 2008] M. Malanowski, K. Kulpa, “Digital Beamforming for Passive Coherent Location Radar”, Radar Conference 2008, Rome, 26-30 May 2008

[Malanowski 2006] M. Malanowski, "Comparison of Adaptive Methods for Clutter Removal in PCL Radar," *Radar Symposium, 2006. IRS 2006. International*, pp.1-4, 24-26 May 2006

[Manolakis 2005] D. G. Manolakis, "Statistical and Adaptive Signal Processing: Spectral Estimation, Signal Modeling, Adaptive Filtering and Array Processing", 2005 ARTECH HOUSE.

[Poullin 2005] D. Poullin, “Passive detection using broadcasters (DAB, DVB) with CODFM modulation”, IEE Proc., Radar Sonar Navig., 2005, 152, pp. 143–152.

[Poullin 2010] D. Poullin, “Passive Radar using COFDM (DAB or DVB-T) Broadcasters as Opportunistic Illuminators”, Chapter 11 in “Digital Video”, F. De Rango, In-Tech Publication February 2010.

[Raout 2006] Neyt, X.; Raout, J.; Kubica, M.; Kubica, V.; Roques, S.; Acheroy, M.; Verly, J.G.; , "Feasibility of STAP for passive GSM-based radar," Radar, 2006 IEEE Conference on, 24-27 April 2006.

[Raout 2007] Raout, J.; Neyt, X.; Rischette, P.; , "Bistatic STAP using DVB-T illuminators of opportunity," Radar Systems, 2007 IET International Conference on,, pp.1-5, 15-18 Oct. 2007.

[Raout 2008] Raout, J.; Preaux, J.-P.; , "Multi-target detection using noise-like signals," Radar Conference, 2008. RADAR '08. IEEE,, pp.1-5, 26-30 May 2008.

[Raout 2008_1] Raout, J.; , "Space-Time Adaptive Processing for noise-radar," Radar Conference, 2008. RADAR '08. IEEE , vol., no., pp.1-6, 26-30 May 2008.

[Raout 2008_2] Raout, J.; , "Sea target detection using passive DVB-T based radar," Radar, 2008 International Conference on, pp.695-700, 2-5 Sept. 2008.

[Raout 2009] Raout, J.; Santori, A.; , "Space-time clutter rejection using the APES method," Radar Conference, 2009. EuRAD 2009. European, pp.65-68, Sept. 30 2009-Oct. 2 2009

[Raout 2010] Raout, J.; Santori, A.; Moreau, E.; , "Passive bistatic noise radar using DVB-T signals," Radar, Sonar & Navigation, IET , vol.4, no.3, pp.403-411, June 2010.

[Raout 2010_1] Raout, J.; Santori, A.; Moreau, E.; , "Space-time clutter rejection and target passive detection using the APES method," Signal Processing, IET , vol.4, no.3, pp.298-304, June 2010.

[Reed 1974] S. Reed, J.D. Mallett, L.E. Brennan, “Rapid Convergence Rate in Adaptive Arrays”, November 1974, IEEE transaction on aerospace and electronic systems, Vol. 10, No 6.

[Saini 2005] R Saini, M.Cherniakov ‘DTV signal ambiguity function analysis for radar application’ Proceedings Radar Sonar and Navigation. Special issue: Passive Radar system Volume 152 Number 3, June 2005 pages 133-142.

[Tao 2010] R. Tao, H.Z. Wu, T. Shan, “Direct-path suppression by spatial filtering in digital television terrestrial broadcasting-based passiv radar”, IET Radar Sonar Navig., 2010, Vol. 4, Issue 6, pp. 791-805.

[Tsao 1997] T. Tsao, M. Slamani, P. Varshney, D. Weiner, H. Schwarzlander and S. Borek, “Ambiguity function for a bistatic radar”, IEEE Trans. Aerospace and Electronic Systems, Vol.33, No.3, pp1041–1051, July 1997.

[Van Trees 2002] Harry L. Van Trees, "Detection, Estimation, and Modulation Theory", Part IV, Optimum Array Processing, John Wiley & Sons, 2002.

[Van Veen 1998] B. D. Vann Veen, K. M. Buckley, “Beamforming: a versatile

approach to spatial filtering", IEEE ASSP Magazine, vol. 5, no. 2, pp. 4-24, April 1988.

[Villano 2009] M. Villano, F. Colone, P. Lombardo, "Adaptive Clutter Suppression in Passive Phased Array Radar", International Radar Symposium IRS 2009, Hamburg, Germany, 9-11 September 2009, pp. 343-347.

[Ward 1994] J. Ward, "Space Time Adaptive Processing for Airborne Radar". Technical Report 1015, Lincoln Laboratory, 13 Dec. 1994.

[Yardley 2007] H. Yardley, 'Bistatic radar based on DAB illuminators: the evolution of a practical system'. Proc. IEEE Conf. Radar 2007, Boston, 2007.

[Zemmari 2009]] R. Zemmari, U. Nickel, W.D. Wirth, "GSM passive radar for medium range surveillannce", Proceedings of European Radar Conference (EURAD 2009), Rome, Italy, 30 September-2 October 2009.

[Zemmari 2010] R. Zemmari, "Reference signal extraction for GSM passive coherent location ", Proceedings of International Radar Symposium (IRS 2010), Vilnius, Lithuania, 16-18 June 2010.